



Title	Studies on interaction between olfactory receptor and transient receptor potential vanilloid 1
Author(s)	森山, さくら
Citation	大阪大学, 2025, 博士論文
Version Type	VoR
URL	https://doi.org/10.18910/103173
rights	
Note	

The University of Osaka Institutional Knowledge Archive : OUKA

<https://ir.library.osaka-u.ac.jp/>

The University of Osaka

Studies on interaction between olfactory receptor and transient receptor potential vanilloid 1

嗅覚受容体と TRPV1 の相互作用に関する研究

Graduate School of Frontier Biosciences

The University of Osaka

大阪大学大学院 生命機能研究科 生命機能専攻

Department of Biomolecular Science and Reaction

SANKEN, The University of Osaka

大阪大学 産業科学研究所 生体反応科学研究分野

Sakura MORIYAMA

森山 さくら

2025年9月25日

Abstract

Olfaction is a critical sensory modality for detecting a diverse array of odorant molecules, influencing behavior and emotion. Olfactory receptors (ORs) are expressed in olfactory sensory neurons (OSNs) in the nasal cavities of humans. In the initial step of odor recognition, the binding of odorant molecules to ORs transduces signals in OSNs. However, it remains unclear whether OR signals alone contribute to the formation of brain-transmitting signals. Both transient receptor potential vanilloid 1 (TRPV1) and ORs are known to be expressed not only in OSNs but also in various other cell types, including prostate cancer cells. The present studies aimed to elucidate whether OR and TRPV1 can influence each other's intracellular signaling, employing HEK293T cells co-expressing the two receptors by transfecting expression plasmids. The findings of the studies revealed a bidirectional regulatory mechanism between ORs and TRPV1.

The initial study discovered that ORs play a role in regulating TRPV1 activation. Interestingly, the effects of ORs varied depending on the vanilloid ligands for TRPV1. For example, TRPV1 responses (Ca^{2+} influx) to capsaicin were potentiated upon OR activation, whereas those to eugenol were attenuated. This mechanism was as follows. Ligand-stimulated OR liberates GTP-Gs/olf, which activates adenylate cyclase, leading to the elevation of intracellular cAMP. Elevated cAMP activates protein kinase A, which promotes the phosphorylation of TRPV1. Consequently, ORs differentially regulate ligand-dependent TRPV1 activation through the phosphorylation of TRPV1. Furthermore, OR-induced changes in TRPV1 responses allowed vanilloid ligands for TRPV1 to be classified into three groups: the capsaicin type (enhancement), the eugenol type (suppression), and the 10-shogaol type (no significant change), each distinguished by unique chemical structures.

Subsequently, the effect of TRPV1 on cAMP production induced by ligand-activated OR was examined. TRPV1 activated by capsaicin suppressed cAMP production by ligand-stimulated OR51E1. This suppression was proven to be mediated by elevation of intracellular Ca^{2+} levels through TRPV1. Furthermore, it was found that GPCR kinase (GRK) activation by Ca^{2+} influx is involved in the suppression process. These results suggest that TRPV1 activation suppresses ligand-stimulated OR signal transduction by promoting desensitization of activated OR51E1 via Ca^{2+} influx and GRK activation.

In conclusion, these studies revealed the mechanisms that OR and TRPV1 mutually regulate each other's activation when expressed in HEK293T cells. Future research will be necessary to determine whether such mutual regulation occurs in OSNs or other cells that naturally express both receptors. Nevertheless, the findings of the present studies offer valuable insights into a potential mechanism through which signals generated by ORs (for example, critical for olfaction in OSNs) are dynamically regulated via multi-directional crosstalk between ORs and other receptors, including TRPV1.

Index

Abstract	2
Chapter I General Introduction	
Preface.....	6
Senses and Their Roles	6
Olfaction: Historical View	7
TRP Channels: Historical Views	9
Background of starting this study	10
References.....	12
Chapter II Divergent effects of ORs on TRPV1 activation by capsaicin and eugenol	
Introduction.....	14
Materials and Methods.....	17
Results.....	22
Discussion	33
References	38
Chapter III Role of phosphorylation and vanilloid ligand structure in ligand-dependent differential activations of TRPV1	
Introduction.....	41
Materials and Methods.....	44
Results.....	48
Discussion	59
References.....	65
Chapter IV Suppressive Effect of TRPV1 on ORs signal transduction	
Introduction.....	68
Materials and Methods.....	72
Results.....	77
Discussion	87
References.....	93
Chapter V Comprehensive Discussion	
Comprehensive Discussion.....	97

References	103
Acknowledgments	105
List of Publications	106
International and Domestic Academic Conferences	107
Awards, Grants and Fellowships	109

Chapter I General Introduction

1. Preface

In this study, I investigated the interaction between olfactory receptor (OR) and transient receptor potential vanilloid 1 (TRPV1). Despite the importance of these receptors for perception, their interactions remain largely unknown. Utilizing HEK293T cells co-expressing both receptors, I analyzed the effects of each receptor on the other. Through this study, I demonstrate that the two receptors regulate each other's signal transduction. Additionally, I delineate the molecular mechanisms underlying their interaction. In this dissertation, I introduce the background of the study, focusing on ORs and TRPV1 in Chapter I. In Chapters II, III, and IV, I describe three topics accompanied by experimental data demonstrating the interaction between ORs and TRPV1. Finally, I present the conclusions of this study in Chapter V.

2. Senses and Their Roles

In mammals, the senses are essential for recognizing and responding to the surrounding environment, playing a crucial role in survival and decision-making. The five primary senses (vision, hearing, touch, taste, and olfaction) each have distinct mechanisms for sensory reception. Vision, hearing, and touch rely on specific receptors that respond to physical stimuli, such as light, sound waves, and mechanical pressure, respectively. These senses are vital for organisms to properly address physical changes in the environment, enabling swift navigation and reaction.

In contrast, taste and olfaction are classified as chemical senses because they detect chemical substances. Among them, olfaction is intricately linked to taste and emotions and plays a key role in flavor perception (De Araujo *et al.* 2003). In the process of

olfaction, odors, which are frequently composed of a variety of molecules, are initially detected by ORs located in the nasal cavity (Buck and Axel 1991). When an odorant molecule binds to an OR, it triggers a signal transduction cascade that activates olfactory sensory neurons. Each mature olfactory sensory neuron expresses only one type of OR, and its axons converge at structures called glomeruli in the olfactory bulb. Each glomerulus integrates inputs from neurons expressing the same OR type, facilitating precise odor encoding. The olfactory bulb processes these signals and relays them to higher brain regions, allowing for the perception of smell (Matsunami and Buck 1997; Malnic *et al.* 2004; Sakano 2010). Recent studies have illustrated that the integration of sensory information from olfaction and other modalities is crucial for forming comprehensive perceptual experiences (Stevenson and Case 2005).

On the other hand, pain perception, while closely related to touch, is often considered an independent sensory modality that falls outside the traditional five senses. It serves as a vital signal that alerts individuals to potential dangers or internal abnormalities, prompting protective behaviors (Melzack and Wall 1965). This mechanism involves various receptors that detect different stimulus, leading to diverse experiences of acute and chronic pain. Additionally, pain perception is significantly influenced by emotional and psychological factors, resulting in individual variations (Dworkin *et al.* 2002; Pincus and Morley 2001). Thus, this complex interplay between physiological and psychological factors underscores the need for a holistic understanding of pain sensory systems.

3. Olfaction: Historical View

In ancient Greece and Rome, it was believed that olfaction occurred when odorants entered the nose through respiration; however, the mechanisms underlying this process remained unresolved for a long time. In the 19th century, physiologists such as Emil du

Bois-Reymond and Rudolf Virchow advanced the general understanding of the nervous system, laying the groundwork for later discoveries in sensory neuroscience. Nonetheless, the molecular mechanisms underlying olfaction remained largely unknown until the late 20th century.

The detailed mechanisms by which olfaction detects specific odor molecules and transmits this information to the brain remained a mystery for an extended period. A significant breakthrough in the study of OR occurred in 1991 when Buck and Axel made their groundbreaking discovery. They identified a gene family coding for human ORs and demonstrated that these receptors can specifically recognize odor molecules (Buck and Axel 1991). This discovery elucidated the fundamental mechanisms by which odor molecules are initially recognized in olfactory sensory neurons (OSNs) which signals are transmitted and processed in the brain. Buck and Axel's research was awarded the Nobel Prize in Physiology or Medicine in 2004, making a revolutionary contribution to my understanding of olfaction.

Subsequently, research has advanced in understanding how odors are linked to emotions and memory (Wilson and Sullivan 1994) and how olfaction interacts with other senses (Schoenbaum *et al.* 1998; Gottfried *et al.* 2004). For example, these odor-related emotional memories may influence not only affective states but also perceptions of physical discomfort or chronic pain, as cognitive and emotional factors are known to modulate pain experience (Turk 2003). The three-dimensional structures of ORs have also been elucidated (Billesbølle *et al.* 2021). To study the functions of ORs, using OSNs is not always suitable because of the difficulty of obtaining OSN preparations. Therefore, OR expression is often performed in ectopic cells such as HEK293T cell. However, this process is not always straightforward due to the complexities involved in ORs' functional

expression, including the difficulties of their accumulation in the endoplasmic reticulum. To resolve this issue, various approaches have been explored, for example, the use of chaperones and tags to facilitate proper folding and transport to the cell surface, ensuring effective signaling (Dey and Matsunami 2004: Sharma *et al.* 2017).

4. TRP Channels: Historical Views

The Transient Receptor Potential (TRP) family comprises of ion channel receptors that play a crucial role in pain perception and are involved in a wide range of sensory modalities, including temperature and chemical sensations. The initial discovery related to TRP channels emerged from studies of the visual system in *Drosophila* (Montell and Rubin 1989). This research demonstrated that a mutant exhibiting an anomalously brief response to light was associated with a phenomenon termed "Transient Receptor Potential," marking the inception of the TRP channel concept.

In the 1990s, TRP channels were also identified in mammals, revealing their significant roles in temperature sensation and pain perception. A particularly noteworthy discovery was the identification of the Transient Receptor Potential Vanilloid 1 (TRPV1) channel in 1997, which was shown to respond to capsaicin, the active component of chili peppers, and to mediate sensations related to thermal and chemical stimuli (Caterina *et al.* 1997). TRPV1 serves as a primary sensory receptor for pain induced by heat ($\geq 43^{\circ}\text{C}$) and chemical stimuli, and subsequent research has continued to establish the pivotal roles of TRP channels in pain and temperature sensations.

The TRP family comprises ion channel receptors with a structure that spans the cell membrane. These channels are primarily composed of subunits with six transmembrane domains, and four subunits assemble to form a single functional channel. In mammals, more than 28 types of TRP channels have been identified, and they are categorized into

seven subfamilies (TRPC, TRPV, TRPM, TRPA, TRPP, TRPML, and TRPN) based on differences in their functions and activation mechanisms. These subfamilies perform a wide range of physiological functions, including not only temperature sensing and chemical stimulus responses but also responses to osmotic pressure and mechanical stimuli. Transient Receptor Potential Melastatin8 (TRPM8), are activated by cold temperatures ($\leq 25^{\circ}\text{C}$) and menthol, contributing to the sensation of coolness. Similarly, Transient Receptor Potential Ankyrin 1 (TRPA1), responds to environmental irritants and noxious stimuli, including mustard oil and wasabi, and is involved in inflammatory pain responses (Clapham 2003).

Beyond pain and temperature perception, it has become evident that TRP channels play physiologically important roles in the cardiovascular, digestive, and respiratory systems. Furthermore, abnormalities in TRP channel function have been linked to neurological disorders, chronic pain, inflammatory diseases, and even cancer progression, prompting the development of new therapeutic strategies targeting TRP channels (Nilius and Owsianik 2011).

5. Background for starting this study

Before starting this study, I treated human embryonic kidney-derived HEK293T cells expressing the endothelin receptor type A (EDNRA), a G protein-coupled receptor (GPCR) related to blood pressure regulation, with various essential oils and examined changes in intracellular Ca^{2+} influx. During these preliminary experiments, I noticed that clove oil, a type of essential oil, significantly induced Ca^{2+} influx regardless of the presence of EDNRA. Clove oil, derived from the flower buds of the clove plant, contains approximately 70-80% (w/w) of eugenol as its fragrant component. HEK293T cells are known to endogenously express TRPV1, which has been presumed to respond to eugenol

(Jin *et al.* 2023. Retrieved from <https://www.proteinatlas.org/ENSG00000196689-TRPV1/cell+line> ; Xu *et al.* 2005). Therefore, I assumed that the Ca^{2+} influx observed in HEK293T cells upon exposure to clove oil was induced by eugenol acting through TRPV1.

On the other hand, the expression of certain TRP channels has been reported in OSNs (Ahmed *et al.* 2009 ; Nakashimo *et al.* 2010 ; Sakatani *et al.* 2023). Additionally, eugenol, an analog of vanilloids, is a common ligand for both ORs and TRPV1. Considering these shared characteristics, I considered the relationship between ORs and TRPV1 an intriguing theme. Preliminary co-expression of ORs and TRPV1 in HEK293T cells revealed suppression of TRPV1 activation. Since this phenomenon has not been previously reported, I decided to investigate the potential crosstalk between OR and TRPV1 as a research theme for the degree.

6. References

- Ahmed MK, *et al.* Expression of transient receptor potential vanilloid (TRPV) families 1, 2, 3 and 4 in the mouse olfactory epithelium. *Rhinology*. 2009; **47**: 242–247.
- Billesbølle CB, *et al.* Structural basis of odorant recognition by a human odorant receptor. *Nature*. 2023; **615**: 742–749.
- Buck L, Axel R. A novel multigene family may encode odorant receptors: A molecular basis for odor recognition. *Cell*. 1991; **65**: 175–187.
- Caterina MJ, *et al.* The capsaicin receptor: A heat-activated ion channel in the pain pathway. *Nature*. 1997; **389**: 816–824.
- Clapham DE. TRP channels as cellular sensors. *Nature*. 2003; **426**: 517–524.
- De Araujo IE, *et al.* Orosensory and homeostatic functions of the insular taste cortex. *Chem Percept*. 2012; **5**: 64–79.
- Dey RA, Matsunami H. Endoplasmic reticulum degradation impedes olfactory G-protein coupled receptor functional expression. *BMC Mol Cell Biol*. 2004; **5**: 34.
- Dworkin RH, *et al.* Core outcome measures for chronic pain clinical trials: IMMPACT recommendations. *Pain*. 2005; **106**: 337–345.
- Gottfried JA, *et al.* Remembrance of odors past: Human olfactory cortex in cross-modal recognition memory. *Neuron*. 2004; **42**: 687–695.
- Jin H, *et al.* Systematic transcriptional analysis of human cell lines for gene expression landscape and tumor representation. *Nat Commun*. 2023; **14**: 5417.
<https://doi.org/10.1038/s41467-023-41132-w>
- Koivisto AP, *et al.* Advances in TRP channel drug discovery: from target validation to clinical studies. *Nat Rev Drug Discov*. 2022; **21**: 41–59.
- Malnic B, *et al.* The human olfactory receptor gene family. *Proc Natl Acad Sci USA*. 2004; **101**: 2584–2589.
- Matsunami H, Buck L. A multigene family encoding a diverse array of putative pheromone receptors in mammals. *Cell*. 1997; **90**: 775–784.
- Melzack R, Wall PD. Pain mechanisms: A new theory. *Science*. 1965; **150**: 971–979.
- Montell C, Rubin GM. Molecular characterization of the *Drosophila* trp locus: A putative integral membrane protein required for phototransduction. *Neuron*. 1989; **2**: 1313–1323.
- Nakashimo Y, *et al.* Expression of transient receptor potential channel vanilloid (TRPV) 1–4, melastatin (TRPM) 5 and 8, and ankyrin (TRPA1) in the normal and methimazole-treated mouse olfactory epithelium. *Acta Otolaryngol*. 2010; **130**: 1278–1286.

- Nilius B, Owsianik G. The transient receptor potential family of ion channels. *Genome Biol*. 2011; **12**: 218.
- Pincus T, Morley S. Cognitive-processing bias in chronic pain: A review and integration. *Psychol Bull*. 2001; **127**: 599–617.
- Sakano H. Neural map formation in the mouse olfactory system. *Neuron*. 2010; **67**: 530–542.
- Sakatani H, et al. The roles of transient receptor potential vanilloid 1 and 4 in olfactory regeneration. *Lab Invest*. 2023; **103**: 100051.
- Schoenbaum G, et al. Orbitofrontal cortex and basolateral amygdala encode expected outcomes during learning. *Nat Neurosci*. 1998; **1**: 155–159.
- Sharma R, et al. Olfactory receptor accessory proteins play crucial roles in receptor function and gene choice. *eLife*. 2017; **6**: e21895.
- Stevenson RJ, Case TI. Olfactory imagery: a review. *Psychon Bull Rev*. 2005; **12**: 244–264.
- Turk DC. Cognitive-behavioral approach to the treatment of chronic pain patients. *Reg Anesth Pain Med*. 2003; **28**: 573–579.
- Wilson DA, Sullivan RM. Neurobiology of associative learning in the neonate: Early olfactory learning. *Behav Neural Biol*. 1994; **61**: 1–18.
- Xu H, et al. Camphor activates and strongly desensitizes the transient receptor potential vanilloid subtype 1 channel in a vanilloid-independent mechanism. *J Neurosci*. 2005; **25**: 8924–8937.

Chapter II Divergent effects of ORs on TRPV1 activation by capsaicin and eugenol

1. Introduction

Human olfactory receptors (ORs) belong to the G protein-coupled receptor (GPCR) family, characterized by seven transmembrane structures. The human genome contains nearly 400 OR genes (Jimenez *et al.* 2021). These ORs are primarily expressed in olfactory sensory neurons (OSNs) and play a crucial role in odorant recognition (Lankford *et al.* 2020). In the process of olfaction, many odors and their combinations are believed to be distinguished through the pattern recognition of ORs (Malnic *et al.* 1999). When odors stimulate ORs, it triggers a signal transduction cascade (Sklar *et al.* 1986; Mombaerts *et al.* 1996; Nakamura and Geoffrey 1987). Odor molecules bind to ORs, which activate G protein heterotrimers composed of GNAL (G α olf), G β , and G γ . Resultant GNAL-GTP then stimulates adenylate cyclase (AC), leading to cAMP synthesis. The increase in intracellular cAMP in OSNs opens cyclic nucleotide-gated (CNG) channels, mediating the influx of Ca²⁺ and Na⁺ ions. The cationic ion influx subsequently activates Cl⁻ channels, causing Cl⁻ efflux and amplifying depolarization from the cilia to the axon of an OSN. Finally, these signals are integrated and processed in the brain to generate the sensation of smell.

OR51E1 and OR51E2 exhibit about 60% amino acid identity, which surpasses that of other ORs, where the identity is around 30%. OR51E1 responds to short-chain to medium-chain carboxylic acids (C3-C9) but it does not respond to acetic acid. While OR51E2 responds to acetic and propionic acids, it does not react to a longer chain carboxylic acids. The stimulation of OR51E1 and OR51E2 by these ligands leads to an increase in intracellular cAMP levels (Mainland *et al.* 2015; Pronin *et al.* 2021). Both

receptors are expressed not only in OSNs but also in ectopic locations, such as prostate cancer cells (Pronin *et al.* 2021).

On the other hand, the transient receptor potential (TRP) family comprises 28 members, all of which are nonselective cation channels. This family is further divided into subfamilies, one of which is the transient receptor potential vanilloid (TRPV) subfamily. The TRPV subfamily includes TRPV1 through TRPV6, which are characterized by their six transmembrane structures and can be activated by vanilloid compounds (Samanta *et al.* 2018). TRPV1 was discovered as a receptor for capsaicin, a pungent ingredient of hot chili peppers. TRPV1 is highly expressed in the nervous system, and it plays a vital role in pain perception (Koivisto *et al.* 2022). TRPV1 expression is also detected in non-neuronal tissues, suggesting that it plays regulatory roles in non-neuronal cells and neurons, including immune cells (Bujak *et al.* 2019). The TRPV1 channel, which allows Ca^{2+} to pass through its pore, is formed by a homologous tetramer of TRPV1 molecules. Various factors can affect the structure and functions of TRPV1, including phosphorylation. TRPV1 can be activated by binding ligands including capsaicin, eugenol, camphor, and resiniferatoxin (Xu *et al.* 2005; Yang *et al.* 2003; Yelshanskaya *et al.* 2022). Activation of the TRPV1 channel induces Ca^{2+} influx, which could trigger various cellular events (Peyravian *et al.* 2020).

Both ORs and TRPV1 are expressed in OSNs (Ahmed *et al.* 2009; Nakashimo *et al.*; O'Hanlon *et al.* 2007; Olender *et al.* 2016; Seki *et al.* 2006). Furthermore, previous studies have shown that TRPV1 plays an important role in the regeneration of OSNs (Sakatani *et al.* 2023). Notably, ORs and TRPV1 share common properties: (1) ligand stimulation of both receptors results in a Ca^{2+} influx in neurons; (2) some ligands, such as eugenol and camphor, can stimulate both receptors. At least several ORs, i.e., OR5D18 (OR73),

OR4Q3, and OR10G7, have been reported to respond to eugenol (Malnic *et al.* 2003; Mainland *et al.* 2015). On the other hand, the modulation of TRPV1 activation by some GPCRs has been studied, particularly in nociceptive regulation. The following processes have been elucidated: prostaglandin E2-stimulated EP3C and EP4 receptors coupling to G α s activate a cAMP production pathway and protein kinase A (PKA) phosphorylates TRPV1, which is implicated in the regulation of TRPV1 desensitization and the development of thermal hyperplasia (Moriyama *et al.* 2005). An AC activator, FSK, can replace the prostaglandin receptor activation to initiate the processes of TRPV1 phosphorylation. In contrast, stimulation of the μ opioid receptor (MOR) coupling to G α i suppresses FSK-induced potentiation of TRPV1-mediated Ca²⁺ influx (Vetter I *et al.*, 2008; Melkes *et al.* 2020). In addition, previous reports indicate that various other GPCRs, i.e., receptors coupling with G α q/11, G α s, and G α i/o, influence TRPV1 activation through regulation of its phosphorylation (Salzer I *et al.* 2019). However, the molecular mechanisms of the interactions between ORs and TRPV1 remain largely unknown. In this study, I examined using HEK293T cells co-expressing OR and TRPV1 whether ORs exhibit modulatory activities for TRPV1 activation similarly to the previously reported other GPCRs.

2. Materials and methods

2.1. Plasmids

A plasmid to express human TRPV1 tagged with a C-terminal flag (DYKDDDK) (catalog number: OHu22257D) was purchased from Genscript (Piscataway, NJ, USA). We obtained a human sodium taurocholate cotransporting peptide (NTCP) expression plasmid (catalog number: HG16027-UT) from Sino Biological Inc. (Kawasaki, Kanagawa, Japan). An empty vector plasmid (catalog number: 3240) was purchased from Takara Bio Inc. (Kusatsu, Shiga, Japan). We acquired OR51E1 and OR51E2 expression plasmids from Thermo Fisher Scientific (Waltham, MA, USA). Synthetic DNA fragments encoding OR51E1 (NCBI accession No. NM_152430.4) and OR51E2 (NCBI accession No. NM_030774.3), along with DNA encoding the N-terminal Lucy and Rho tag, were inserted downstream of the CMV promoter in the pcDNA5 vector. The green fluorescence protein (GFP) expression plasmid was prepared as previously described (Fujita *et al.* 2021). We purchased pGloSensor 22F cAMP plasmid (catalog number: E2301) from Promega (Madison, WI, USA).

2.2. Cell Culture

HEK293T cells were obtained from RIKEN BRC (Tsukuba, Ibaraki, Japan). They were maintained in RPMI 1640 medium containing 10% heat-inactivated fetal bovine serum and antibiotics and then used for experiments as described previously (Fujita *et al.* 2019).

2.3. Reagents

Eugenol (catalog number: A0232; TCI chemicals, Tokyo, Japan), N-arachidonoyl dopamine (NADA; catalog number: AB120099-5; Abcam, Cambridge, United Kingdom), capsaicin (catalog number: 034-11351; Fujifilm Wako Pure Chemical Corp., Osaka, Japan), piperine (catalog number: 162-17241; Fujifilm Wako Pure Chemical Corp.), and

FSK (catalog number: 067-02191; Fujifilm Wako Pure Chemical Corp.) were initially dissolved in ethanol and subsequently diluted to the necessary concentrations with Hanks' Balanced Salt Solution (HBSS; catalog number: 084-08965; Fujifilm Wako Pure Chemical Co.). Propionic acid (catalog number 194-03012; Fujifilm Wako Pure Chemical Corp.) was dissolved in HBSS and 3-isobutyl-1-methylxanthine (IBMX; catalog number: I5879; Sigma-Aldrich, St. Louis, MO, USA) was dissolved in dimethyl sulfoxide (catalog number: 046-21981; Fujifilm Wako Pure Chemical Corp.). Then, they were diluted to appropriate concentrations with HBSS.

2.4. Flow cytometric analysis

Transfection of plasmids into HEK293T cells was performed as described previously (Hinuma *et al.* 2022). After being cultured for 24 h, cells were harvested with trypsinization. They were washed twice with phosphate-buffered saline (PBS) at 4 °C by centrifugation and then pelleted in a tube. Fixation and permeabilization of cells were performed using Leucoperm (catalog number: BFU09; Bio-Rad, Hercules, CA, USA) according to the manufacturer's instructions. To detect OR51E1, I used mouse monoclonal anti-Rho antibody (catalog number: 200-301-G36; Rockland, Limerick, PA, USA) as a 1st antibody in a dilution of 1:200 and Alexa Fluor 647-conjugated goat polyclonal anti-mouse IgG (H+L) F(ab')2 fragment (catalog number: 4410; Cell Signaling Technology, Carlsbad, CA, USA) as a 2nd antibody in a dilution of 1:500. To detect TRPV1, I used rabbit polyclonal anti-Flag antibody (catalog number: 20543-1-AP; Proteintech, Tokyo, Japan) as a 1st antibody in a dilution of 1:200 and Alexa Fluor 488-conjugated goat polyclonal anti-rabbit IgG (H+L) F(ab')2 fragment (catalog number: 20543-1-AP-150; Cell Signaling Technology) as a 2nd antibody in a dilution of 1:500. Cells were incubated with these antibodies at 4 °C for 1 h. After the incubation with antibodies, they were

washed twice with PBS. Then, they were subjected to flow cytometry. The fluorescence intensities (FIs) of 1×10^4 cells were analyzed using the FITC and APC channels of a FACSCant™ II (BD Biosciences, Franklin Lakes, NJ, USA). Geometric mean values were analyzed using software (FlowJoTM 7.6.5, BD Biosciences). To obtain histograms, measurements were taken from 3×10^4 cells.

2.5. Detection of cAMP production

HEK293T cells were cultured in a 96-well white plate (catalog number: 236105; Thermo Fisher Scientific) coated with poly-L-lysine (catalog number: VBH-SPL01; Cosmo Bio, Tokyo, Japan). We then seeded cells at a density of 4×10^5 cells/mL in 50 μ L/well of culture medium. These cells were cultured for 24 h at 37°C in a humidified atmosphere containing 5% CO₂. We transfected the cells with expression plasmids, i.e., GloSensor 22F, GFP, empty vector, and OR51E1 to be 300 ng in a serum free Opti-MEM (catalog number: 31985062; Thermo Fisher) per well in total using PolyMagNeo, and then fresh medium (100 μ L) was added to each well. Following a 24h culture period, I used a Synergy 2 plate reader (BioTek, Winooski, VT, USA) to determine the FI of GFP in each well. We then replaced the supernatant with 75 μ L/well of HBSS containing a 2% GloSensor cAMP reagent (catalog number: E1290; Promega) and allowed the cells to incubate for 2 h at room temperature. Afterward, I added an aliquot (25 μ L) of HBSS containing both ligands and IBMX (with a final concentration of 0.5 mM) to each well. Immediately following this, I measured the change in luminescence at 2 min intervals for 20 min. We obtained normalized relative luminescence unit (RLU) using the following calculations. (1) We calculated FI of GFP in each well using the formula: (FI in a well with GFP expression plasmid transfection) - (that without GFP expression plasmid transfection). (2) We determined a coefficient value (Co) to normalize RLU in each well

based on GFP plasmid transfection efficacy using the formula: (FI of GFP in a well with receptor expression plasmid transfection) / (that with empty vector plasmid transfection).

(3) We calculated RLU using the formula: (maximal luminescence in a well with receptor expression plasmid transfection after addition of HBSS with or without a ligand) / (that with empty vector plasmid transfection after addition of HBSS without a ligand). (4) We obtained normalized RLU from the formula: RLU/Co. We performed assays in triplicate and expressed data as mean values (n = 3) and SD.

2.6. Detection of intracellular Ca^{2+} influx

We initiated my experiment by coating a 96 well black/clear bottom Plate (catalog number: 165305; Thermo Fisher Scientific) with poly-L-lysine. We then seeded cells at a density of 4×10^5 cells/mL in 50 μL /well of culture medium. These cells were cultured for 24 h at 37°C in a humidified atmosphere containing 5% CO₂. We transfected the cells with plasmids (300 ng/well in total) using PolyMagNeo as described above. Then fresh medium (100 μL) was added to each well. The transfected cells were cultured for an additional 24 h. After removing the culture medium, I incubated the cells in HBSS (50 μL /well) containing a dye loading buffer supplied with a Calcium 6 Assay Explorer Kit (catalog number: OZB-PG60200-200-200; OZ Biosciences, Marseille, France). The incubation was carried out for 2 h at 37°C in a humidified atmosphere containing 5% CO₂. Subsequently, I added HBSS with or without a ligand (50 μL /well) and measured changes in FI using a FLIPR tetra (Molecular Devices; San Jose, CA, USA). When treatment with FSK (20 μM) was required, it was added to the cells 15 min before measuring changes in FI by ligand stimulation. Finally, I measured FI changes (%) induced by the addition of ligands every second for 3 min. Specific responses of cells to

ligands, which were caused by the transfection of TRPV1 expression plasmid, were calculated by subtracting the FI changes in control cells, which were not transfected with the TRPV1 expression plasmid, from the FI changes in cells that were transfected with the TRPV1 expression plasmid.

3. Results

Functional expression of OR51E1 and TRPV1 in HEK293T cells. In this study, I utilized ORs tagged with a secretory peptide tag, Lucy-Rho, at their N-termini. This tag is reported to enhance the functional expression of ORs when they are introduced into heterologous cells, such as HEK293T cells (Shepard *et al.* 2013). To express TRPV1 in HEK293T cells, I used an expression plasmid for TRPV1 with a C-terminal Flag tag. The protein expressions of OR51E1 and TRPV1 were confirmed using flow cytometric analyses when plasmids to express the two receptors were transfected into HEK293T cells. For flow cytometry, transfected cells were fixed and permeabilized, and then they were stained using 1st and 2nd antibodies. To detect OR51E1, I used 1st antibody against Rho. While TRPV1 was detected using 1st antibody against the Flag. As shown in Figure 1a (histogram) and Figure 1b (geometric values of FI), OR51E1 protein expression was detected in HEK293T cells, both when transfected with OR51E1 alone and when co-transfected with TRPV1 expression plasmids. Although OR51E1 protein expression patterns in cells appeared to differ between the transfection of OR51E1 alone (Figure 1a) and the co-transfection of OR51E1 and TRPV1 (as depicted - in Figure 1a), OR51E1 expression in cells co-transfected with the two receptors increased 1.1 times more than that in cells transfected OR51E1 alone (Figure 1b). On the other hand, evident TRPV1 protein expression was detected in cells transfected with TRPV1 alone and those co-transfected with OR51E1 and TRPV1 expression plasmids (Figure 1c and Figure 1d). In histograms, TRPV1 protein expression patterns in cells were similar between the transfection of TRPV1 alone (as depicted - in Figure 1c) and the co-transfection of OR51E1 and TRPV1 (as depicted - in Figure 1c), TRPV1 expression in cells co-transfected with the two receptors increased 1.1 times more than that in cells transfected

TRPV1 alone (Figure 1d). These results demonstrate that OR51E1 and TRPV1 proteins are produced when these expression plasmids are transfected into HEK293T cells. In addition, the protein expression levels of TRPV1 were comparable between the transfection of TRPV1 expression plasmid alone and the co-transfection of TRPV1 and OR51E1 expression plasmids. These results indicate that OR51E1 and TRPV1 do not drastically affect each other regarding their protein expression levels in HEK293T cells.

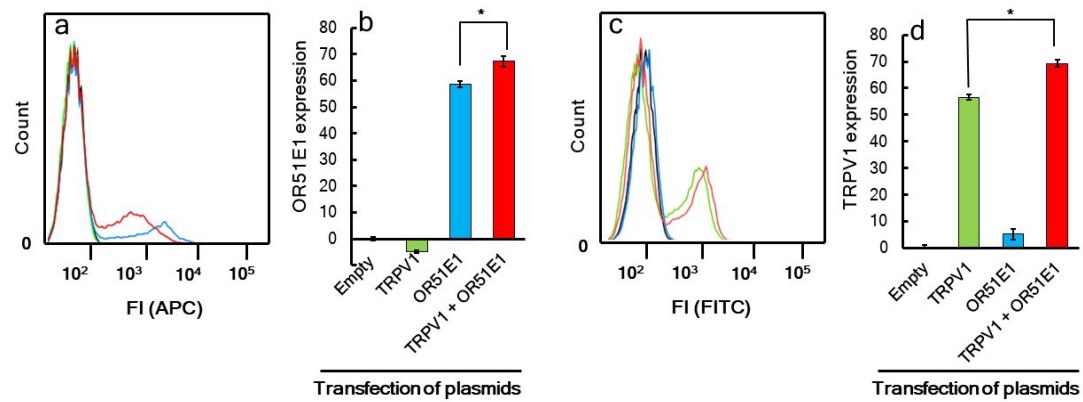


Figure 1. Flow cytometric analyses of OR51E1 and TRPV1 protein expressions in HEK293T cells. Plasmids (a total of 800 ng plasmid DNA /well) used for transfection were as follows. Empty (■): 800 ng of empty vector plasmid; TRPV1 (■): 720 μ g of TRPV1 expression plasmid and 80 ng of empty vector plasmid; OR51E1 (■): 720 μ g of empty vector plasmid and 80 ng of OR51E1 expression plasmid; TRPV1 + OR51E1 (■): 720 ng of TRPV1 expression plasmid and 80 ng of OR51E1 expression plasmid. After plasmid-transfected cells were fixed and permeabilized, they were stained with the following antibody combinations. Panels (a) and (b): 1st mouse anti-Rho antibody and 2nd Alexa Flour 647-conjugated goat anti-mouse IgG antibody. Panels (c) and (d): 1st rabbit anti-Flag antibody and 2nd Alexa Flour 488-conjugated goat anti-rabbit IgG antibody. (a) and (c) display histograms, while (b) and (d) depict OR51E1 and TRPV1 protein expression levels (geometric means of FIs) determined from the histograms of (a) and (c), respectively. Geometric means were obtained from triplicate assays. OR51E1 and TRPV1 expressions were estimated from geometric mean values calculated by subtracting the geometric mean values of the 'Empty' from the geometric mean values of 'TRPV1' and 'OR51E1' transfection. Data were expressed as geometric means ($n = 3$) \pm SD (vertical bars). Statistical analysis was performed using Tukey test. *: $p < 0.05$.

It is well-established that ORs activated by their ligands enhance intracellular cAMP production (Sklar *et al.* 1986; Mombaerts *et al.* 1996; Nakamura and Geoffrey 1987). We

examined the responses of cells expressing OR51E1 to isovaleric and propionic acids in cAMP production assays. HEK293T cells expressing OR51E1 dose dependently responded to isovaleric acid (Figure 2a). While OR51E1's response to propionic acid was considerably lower than that to isovaleric acid (Figure 2b). Under the conditions employed here, increasing amounts of OR expression plasmids in transfection strengthened the responses of OR51E1 to isovaleric acid. The ligand specificity of OR51E1 was well consistent with that reported elsewhere (Pronin *et al.* 2021). Notably, under the conditions without ligand stimulation, the intracellular cAMP level of cells transfected with OR51E1 expression plasmid was greater than that of cells transfected with empty vector plasmid (Figure 2c). In the absence of ligands, transfection of OR51E1 dose dependently enhance cAMP production. These findings indicate that the expression of OR51E1 in HEK293T cells may inherently trigger the cAMP production pathway to some degree, even without ligand stimulation. However, the activation level was significantly lower compared to when the ligands stimulated it. Furthermore, I investigated how OR51E1 responds to capsaicin and eugenol, which were utilized as ligands to activate TRPV1 in subsequent experiments. Figure 2d indicates that neither capsaicin nor eugenol induced cAMP in cells. This was observed in both the cells transfected with OR51E1 (as depicted in the right section of Figure 1d) and those without the transfection (shown in the left section of Figure 1d). In contrast, isovaleric acid induced cAMP production in cells transfected with OR51E1 as depicted in the right section of Figure 1d. These results demonstrate that capsaicin and eugenol do not activate OR51E1 as agonistic ligands.

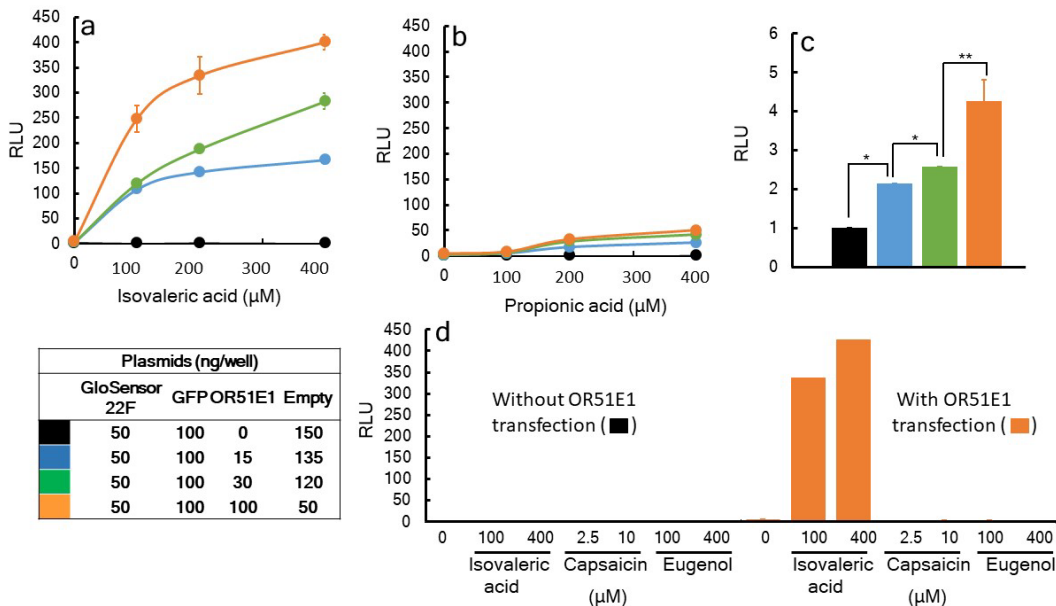


Figure 2. cAMP production in HEK293T cells expressing OR51E1 with or without ligand stimulation. HEK293T cells were transfected with the indicated combinations of plasmids (total 300 ng/well) in a 96-well microplate. The amount of each plasmid used for transfection is shown in the table under (a) and the color code used here corresponds to lines and bars in (a) - (c). FI of GFP was utilized to normalize the RLU in each well, considering the transfection efficacy. Cells were treated with indicated concentrations of isovaleric acid (a) or propionic acid (b) in the presence of IBMX. After ligands were added to the wells, luminescence in each well was measured every 2 min for a total of 20 min, and the maximum value was used to calculate the RLU. Assays were performed in triplicate, and data are presented as mean values ($n = 3$) of normalized RLU \pm SD (vertical bars). (c), a part of the panel (a), i.e., in the absence of the ligand, is enlarged and shown as a bar graph with a differential vertical scale. Statistical analysis was performed using Tukey test. *: $p < 0.05$; **: $p < 0.01$.

To examine the responsiveness of TRPV1, I measured Ca^{2+} influx, which was detected as changes in FI, in HEK293T cells transfected with empty vector plasmid or TRPV1 expression plasmid after stimulation with TRPV1 ligands. As these ligands, I chose capsaicin and eugenol because capsaicin is a typical TRPV1 agonist while eugenol, an analog of capsaicin, is known not only as a TRPV1 ligand but also as a low molecular weight odorant molecule. As shown in Figure 3a and Figure 3c, capsaicin or eugenol caused greater dose dependent responses in cells transfected with TRPV1 expression plasmid than those transfected with empty vector plasmid. However, control cells that

were transfected with the empty vector plasmid also exhibited responses to capsaicin or eugenol, although these were significantly less pronounced compared to the responses of the TRPV1 expression plasmid transfected cells. There is a possibility that the low levels of responses in control cells to these ligands are due to the expression of endogenous TRPV1. Publicly available RNA-seq data, ARCHS4, indicates that a certain level of TRPV1 is expressed in a variety of cells including HEK293T cells (<https://maayanlab.cloud/archs4/gene/TRPV1>). However, I could not definitively exclude the possibility that the presence of other receptors for these ligands or a combination of endogenous TRPV1 and other receptors contributes to the response of control cells to these ligands. Therefore, in this study, I defined specific TRPV1 responses to capsaicin or eugenol, which were attributable to the transfected TRPV1 as IF changes, i.e., response/baseline (%), in TRPV1 transfected cells subtracting those in control cells (Figure 3b and Figure 3d). The dose-response curve of eugenol differed from that of capsaicin, particularly in terms of effective doses, maximal responses, and curve patterns. Under the experimental conditions employed in this study, cell viability remained relatively stable even at high concentrations of capsaicin and eugenol during short-term measurements. These results suggest that the way in which these two ligands interact with TRPV1, is not the same. However, both capsaicin and eugenol are vanilloid compounds and a previous report indicates that they bind to a similar pocket on TRPV1 (Harb *et al.* 2019). Considering them, it's likely that there are both common and unique aspects in the interactions between TRPV1 and these two ligands. Similar to the case with capsaicin, control cells exhibited a response to eugenol. However, these response levels were significantly lower compared to those observed in TRPV1-transfected cells. Therefore, the specific response of TRPV1 to eugenol was also determined by subtracting the

responses of control cells from those of TRPV1-transfected cells (Figure 3d).

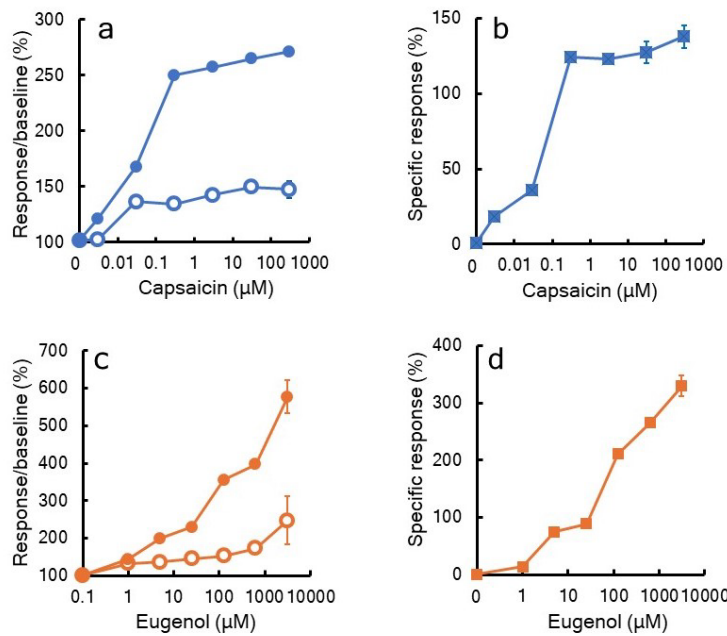


Figure 3. Ca^{2+} influx induced in HEK293T cells transfected with TRPV1 expression plasmid or empty vector plasmid after stimulation with capsaicin or eugenol. HEK293T cells were transfected with the following plasmids (total 300 ng/well) in a 96-well microplate. In (a) and (c), filled circles (● and ○): 270 ng of TRPV1 expression plasmid and 30 ng of empty vector plasmid; blank circles (○ and ○): 300 ng of empty vector plasmid. After the addition of the indicated concentration of capsaicin (a) or eugenol (c) dissolved in HBSS, Ca^{2+} influx in cells was measured through changes in FI every second for 3 min using a FLIPR. The assays were performed in triplicate. The data, represented by the maximal FI values in each measurement, were shown as mean values ($n = 3$) with standard SD (vertical bars). The specific TRPV1 responses (■ and ■) to capsaicin (b) and eugenol (d) were determined respectively by subtracting the responses of control cells to the indicated ligands from those of the TRPV1-transfected cells.

Modulatory effects of OR51E1 on TRPV1 responses to capsaicin and eugenol. We investigated whether ORs could alter TRPV1 responses to capsaicin or eugenol, using HEK293T cells co-transfected with OR51E1 and TRPV1 expression plasmids. As shown in Figure 4a, the addition of HBSS without TRPV1 ligands did not induce Ca^{2+} influx in HEK293T cells transfected with any plasmids. On the other hand, the addition of capsaicin extensively induced Ca^{2+} influx in cells transfected with TRPV1 (Figure 4b). Co-expression of OR51E1 with TRPV1 enhanced capsaicin-induced Ca^{2+} influx. As

explained in Figure 3, capsaicin could induce a low level of Ca^{2+} influx in cells transfected with empty vector plasmid (control). To obtain a transfected TRPV1-dependent response, I calculated a specific TRPV1 response to capsaicin (Figure 4c). When the dose of OR51E1 expression plasmid in transfection was doubled from 15 to 30 ng per well, the capsaicin-induced specific response of TRPV1 was enhanced by 1.3 and 1.8 times in maximal responses, respectively. In these experiments, I refrained from stimulating OR51E1 with its ligand. Despite this, the co-expression of OR51E1 modified the TRPV1 response to capsaicin. As shown in Figure 2c, the transfection of OR51E1 could trigger the cAMP production pathway, even in the absence of ligand stimulation. Taking all these results into account, my results suggest that the signaling dependent on OR51E1, i.e., eliciting cAMP production, amplified the TRPV1 response to capsaicin. In contrast to the effect of OR51E1 on TRPV1 response to capsaicin, TRPV1-mediated Ca^{2+} influx by stimulation with eugenol was decreased by the co-expression of OR51E1 (Figure 4d). When the OR51E1 expression plasmid was co-transfected at doses of 15 to 30 ng per well, the specific response of TRPV1 to eugenol was respectively reduced to 0.4 and 0.3 times its original level in maximal responses (Figure 4e). Our results indicate that OR51E1 can differentially modulate TRPV1 activation in response to stimulation by capsaicin and eugenol.

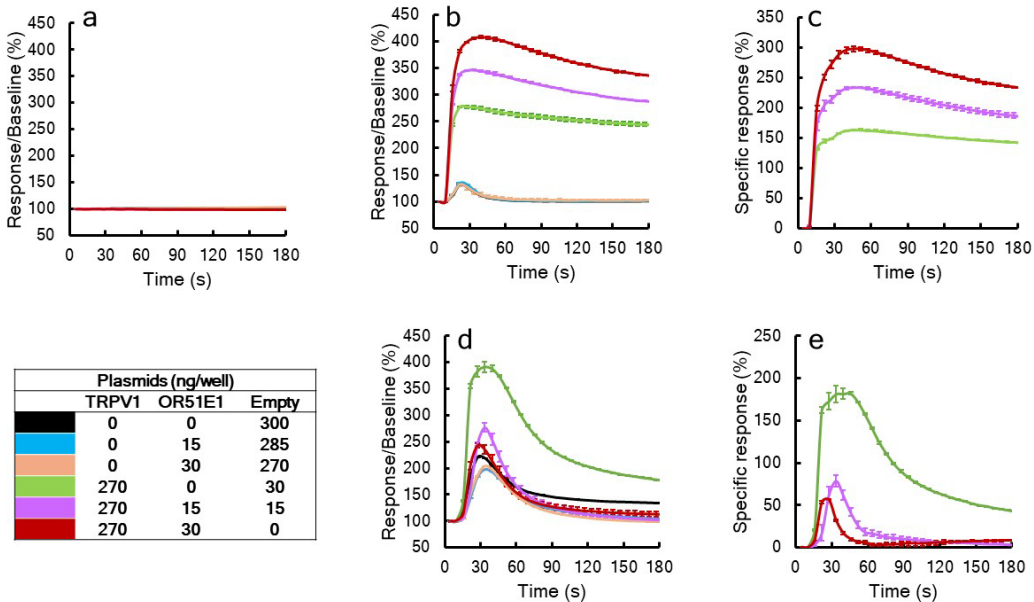


Figure 4. Modulatory effects of OR51E1 on TRPV1-mediated Ca^{2+} influx in response to capsaicin or eugenol. HEK293T cells were transfected with combinations of plasmids (total 300 ng/well) in a 96-well microplate. The amount of each plasmid used for transfection is shown in the table under (a) and the color code used here corresponds to lines in (a) - (e). Using a FLIPR, the influx of Ca^{2+} in cells was measured through changes in FI every second for 3 min. This was done after the addition of HBSS without ligands for TRPV1 (a), HBSS containing 10 μM of capsaicin (b), or HBSS containing 400 μM of eugenol (d). The assays were performed in triplicate. The data showed as mean values ($n = 3$) with standard SD (vertical bars). The specific responses of TRPV1 to capsaicin (c) and eugenol (e) were determined by subtracting the responses to capsaicin or eugenol in cells without TRPV1 expression plasmid from those in cells with TRPV1 expression plasmid transfection.

Amplification of modulatory activities of OR51E1 by stimulation with isovaleric acid. We verified if stimulation of OR51E1 with its ligand, i.e., isovaleric acid, could intensify its modulatory activities for the responsiveness of TRPV1 to capsaicin and eugenol. The addition of isovaleric acid to cells transfected with the TRPV1 expression plasmid, without the co-transfection of OR51E1 expression plasmid, did not affect the Ca^{2+} influx via TRPV1 in response to either capsaicin or eugenol as indicated by ■ and □ in Figure 5a and Figure 5b. Conversely, the same treatment with isovaleric acid intensified the enhancing effect of OR51E1 on the TRPV1 response to capsaicin, as well as the inhibitory effect of OR51E1 on the TRPV1 response to eugenol (■ and □ in

Figure 5a and Figure 5b). These results suggest that the cAMP production pathway triggered by activated OR51E1 plays a vital role in the modulatory effects of ORs on TRPV1 in responses to both capsaicin and eugenol, despite the effects appearing to be divergent between TRPV1 responses to these two ligands.

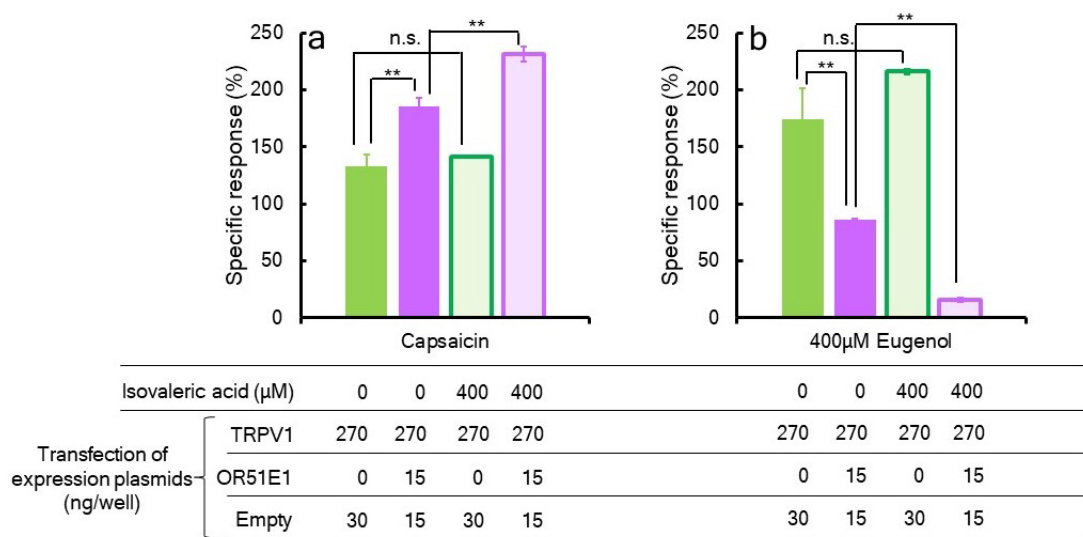


Figure 5. Intensified modulations of TRPV1 responses to capsaicin and eugenol in HEK293T cells co-expressing TRPV1 and OR51E1 by ligand stimulation of OR51E1. Indicated expression plasmids were transfected into HEK293T cells cultured in a 96-well plate, totaling 300 ng/well. After 24-h culture, the cells were stimulated with either capsaicin (a) or eugenol (b), in the presence or absence of isovaleric acid. FI changes in the cells following the addition of capsaicin or eugenol were measured. Assays were performed in triplicate. Data were presented as mean values of maximal TRPV1-specific responses ($n = 3$) with SD (horizontal bars). Statistical analysis was performed using Tukey test. *: $p < 0.05$; **: $p < 0.01$; n.s.: not significant.

Modulatory effects of OR51E2 but not NTCP on TRPV1 responses. As shown in Figure 4 and Figure 5, the co-expression of OR51E1 influenced TRPV1 responses to ligands, although its effects differed between eugenol and capsaicin. We further examined whether another OR, i.e., OR51E2, could exhibit similar modulatory effects. The co-expression of OR51E2 enhanced the specific response of TRPV1 to capsaicin while suppressing that to eugenol (Figure 6a). However, the co-expression of NTCP, which is

not a GPCR, did not exhibit such modulatory effects on TRPV1 responses (Figure 6b). These results suggest that the modulatory effects of OR51E1 and OR51E2 on the ligand responses of TRPV1 are closely tied to OR functions.

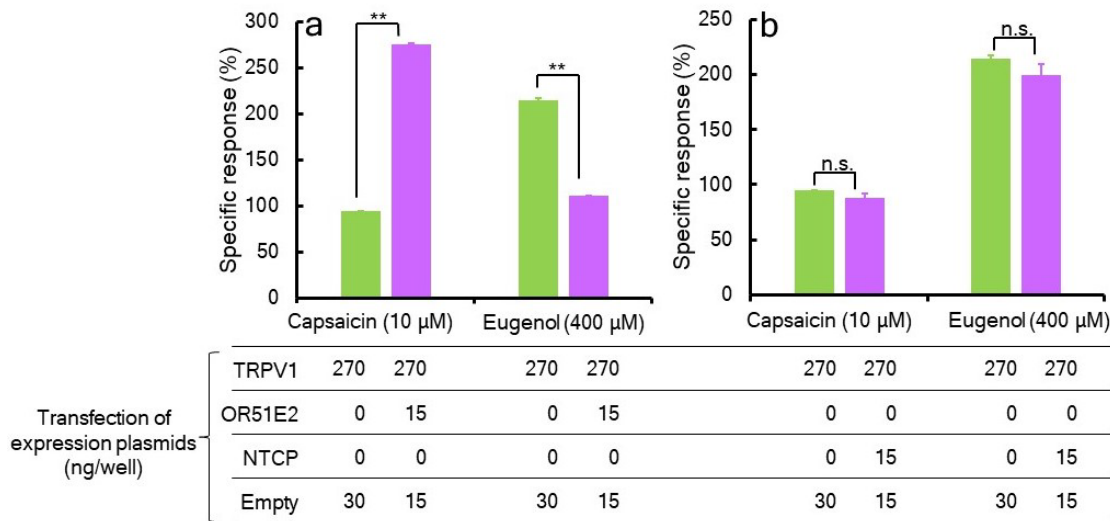


Figure 6. Effects of OR51E2 and NTCP on TRPV1-mediated Ca^{2+} influx in response to capsaicin and eugenol in HEK293T cells. Indicated expression plasmids were transfected into HEK293T cells cultured in a 96-well plate, totaling 300 ng/well. After 24 h culture, the cells were stimulated with either capsaicin (a) or eugenol (b). FI changes in the cells following the addition of capsaicin or eugenol were measured. Assays were performed in triplicate. Data were presented as mean values of maximal TRPV1-specific responses ($n = 3$) with SD (horizontal bars). Statistical analysis was performed using Student's t-test. *: $p < 0.05$; **: $p < 0.01$; n.s.: not significant.

Modulatory effects of FSK on TRPV1 responses to various TRPV1 ligands.

Considering that stimulation of ORs promotes cAMP production, I hypothesized that the activation of AC, which catalyzes the conversion of ATP to cAMP, could be involved in this process. We examined whether FSK, an AC activator, could mimic the effects of OR on the ligand responses of TRPV1. As shown in Figure 7a, compared to untreated (■), FSK treatment (■) significantly enhanced the capsaicin-induced TRPV1 response. Conversely, the eugenol-induced TRPV1 response was reduced by FSK (Figure 7b). These results indicate that FSK can replicate the effects of ORs on the ligand responses

of TRPV1 and that AC activation plays a crucial role in OR-dependent modulations. Furthermore, I evaluated the effects of FSK on the responsiveness of TRPV1 to other compounds, NADA and piperine, which are known as TRPV1 ligands (Ferreira *et al.* 2009; McNamara *et al.* 2005). FSK increased the TRPV1 response to NADA (Figure 7a), whereas it diminished the response to piperine (Figure 7b). It has been reported that FSK treatment augments the TRPV1 response to capsaicin (Melkes *et al.* 2020). Regarding the effect of FSK on capsaicin-induced TRPV1 response, these results were consistent with the previous report. However, my findings indicate that FSK or ORs can modulate TRPV1 responses in different manners that are dependent on the TRPV1 ligands. Depending on whether FSK and OR enhance or inhibit TRPV1 activation, it seems that TRPV1 ligands can be classified into two categories: those like capsaicin (i.e., capsaicin-type ligands as shown in Figure 7a) and those like eugenol (i.e., eugenol-type ligands as shown in Figure 7b).

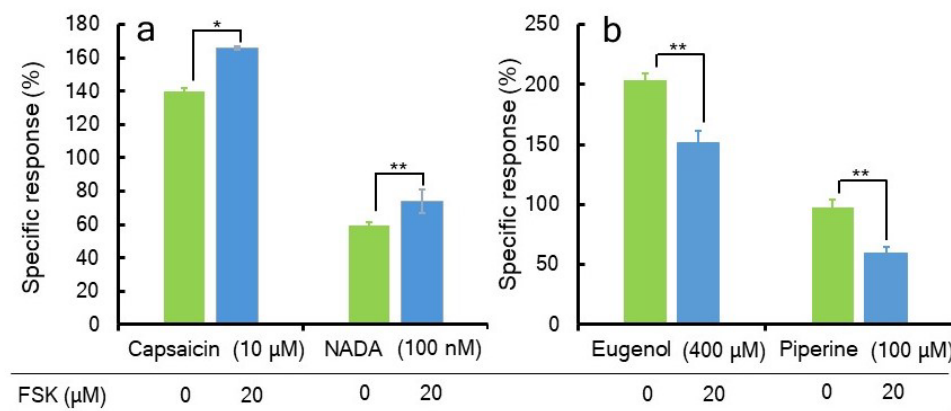


Figure 7. Effects of FSK on TRPV1-mediated Ca^{2+} influx in response to various TRPV1 ligands. TRPV1 expression plasmid (270 ng/well) and empty vector plasmid (30 ng/well) were transfected into HEK293T cells. FSK treatment was performed 15 min before indicated TRPV1 ligands were added. FI changes in the cells following the addition of ligands were measured. Assays were performed in triplicate. Data were presented as mean values of maximal TRPV1-specific responses ($n = 3$) with SD (horizontal bars). Statistical analysis was performed using Student's *t* test. *: $p < 0.05$; **: $p < 0.01$.

4. Discussion

Both ORs and TRPV1 are expressed in OSNs and these two types of receptors share identical ligands at least a portion of their ligands, such as eugenol and camphor. However, the mechanism of their interaction remains largely unknown. In this study, I analyzed the effects of ORs on the ligand responsiveness of TRPV1 using HEK293T cells that co-express both receptors. In OSNs, activation of ORs increases intracellular cAMP, opening CNG channels and leading to Ca^{2+} influx (Sklar *et al.* 1986; Mombaerts *et al.* 1996; Nakamura and Geoffrey 1987). Conversely, TRPV1, being a cationic ion channel, can directly elicit Ca^{2+} influx when stimulated by TRPV1 ligands. Since HEK293T cells do not express CNG channels, they are useful for analyzing the influence of ORs on TRPV1-mediated Ca^{2+} influx.

Our results indicate that ORs can modulate the ligand responsiveness of TRPV1 by activating the cAMP production pathway. Regulatory roles of GPCRs other than ORs in TRPV1 activation have been reported, especially about nociception. Ligand-stimulated prostaglandin receptors activate the cAMP production pathway, and PKA promotes the phosphorylation of TRPV1 (Moriyama *et al.* 2005). This phosphorylation lowers the threshold of TRPV1 response to capsaicin. In addition, various other GPCRs except for ORs have been reported to regulate TRPV1 activation through its phosphorylation (Salzer *et al.* 2019). Therefore, it is suggested that ORs induce the phosphorylation of TRPV1, which in turn makes TRPV1 more susceptible to capsaicin, although this presumption must be confirmed by future studies.

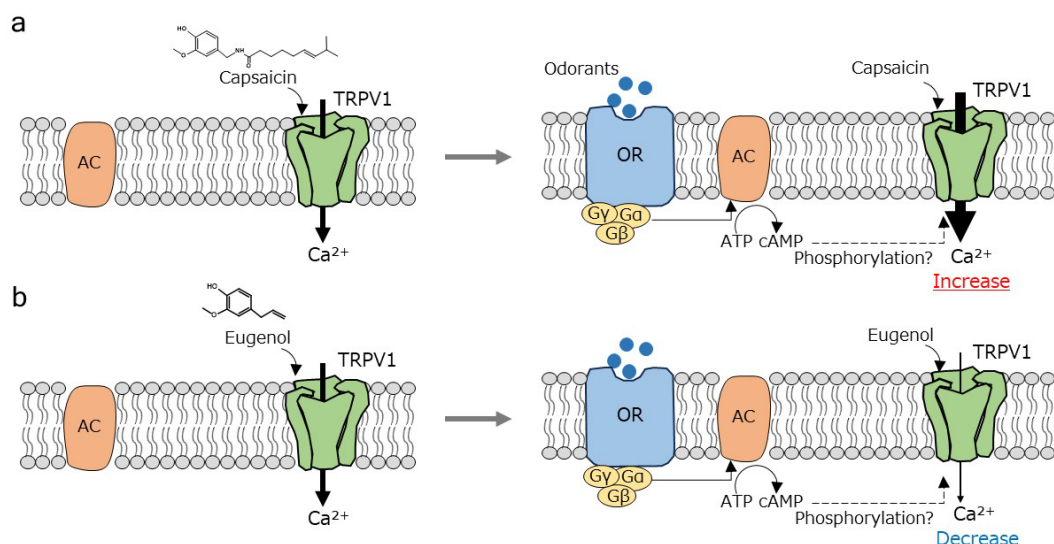
However, the effects of ORs or FSK on Ca^{2+} influx were opposite in response to the between capsaicin and eugenol. Phosphorylation would make TRPV1 insusceptible to eugenol, which is opposite to capsaicin. Generally, odors are composed of smaller

molecules rather than capsaicin (molecular weight of 305.4), and eugenol (molecular weight of 164.2) is a representative odorant molecule. Our results suggest that the way TRPV1 interacts with small molecules such as odors is distinct from its interaction with capsaicin. We found that the ligands of TRPV1 can be divided into two categories (i.e., capsaicin-type and eugenol-type ligands) based on the modulation of TRPV1 responses to these ligands by ORs or FSK. Future studies need to clarify which structural properties in compounds determine the two types of TRPV1 ligands.

TRPV1, a multimodal receptor, can bind various substances, leading to changes in its function and structure (Kwon *et al.* 2021; Sun *et al.* 2022; Zhang *et al.* 2021). The existence of a binding pocket in TRPV1 for capsaicin has been unveiled through the analysis of 3D structures using cryo-electron microscopy and computational modeling (Yang *et al.* 2015; Yang *et al.* 2018; Vu *et al.* 2020; Li *et al.* 2023). This pocket has been reported to be surrounded by S3-S6 in six transmembrane segments in TRPV1 (Yelshanskaya *et al.* 2022). The components of capsaicin, referred to as the head (vanillyl group), neck (amide bond), and tail (aliphatic chain) respectively, interact with different positions within the binding pocket (Yang *et al.* 2015). Capsaicin is presumed to bind the pocket in a ‘tail-up and head-down’ configuration (Kwon *et al.* 2021; Sun *et al.* 2022; Zhang *et al.* 2021; Yang *et al.* 2015; Yang *et al.* 2018; Vu *et al.* 2020; Li *et al.* 2023). Previous reports suggest that longer aliphatic tails enhance the affinities of capsaicin analogs through their interaction with TRPV1 via van der Waals force (Yang *et al.* 2015). On the other hand, computational ligand docking studies suggest that eugenol attaches to a site adjacent to the TRPV1 pocket where the vanillyl group of capsaicin forms hydrogen bonds with TRPV1 amino acid residues (Harb *et al.* 2019; Yang *et al.* 2015). It is hypothesized that ORs and FSK modify TRPV1 configuration to interact with capsaicin

or eugenol, possibly through phosphorylation, resulting in an increased affinity and/or channel opening capability of TRPV1 for capsaicin, while decreasing those for eugenol.

In this study, I demonstrated that the regulation of TRPV1 activation by ORs can vary depending on the specific TRPV1 ligands when both OR and TRPV1 were expressed in HEK293T cells. As future studies, it will be necessary to investigate whether such an interaction between ORs and TRPV1 exists in OSNs as well as HEK293T cells. It is also intriguing to investigate whether TRPV1 signaling influences the activation of ORs.



Graphical abstract. The effects of OR on TRPV1 activation vary depending on whether TRPV1 is stimulated with capsaicin (a) or eugenol (b).

Data availability

The datasets used and/or analyzed during the current study are available from the corresponding author upon reasonable request.

Author contribution

S.M., conceptualization, methodology, validation, formal analysis, investigation, data curation, writing—original, draft preparation, writing—review and editing, and funding; Y.T.; methodology and writing—review and editing; S.H., conceptualization, methodology, validation, formal analysis, investigation, data curation, writing—original, draft preparation, writing—review and editing, and supervision; and S.K., investigation, writing—review & editing, resources, funding, and supervision.

Funding

The following entities have provided support for this work: Japan Science and Technology Agency (JST), the establishment of university fellowships toward the creation of science technology innovation, Grant Number JPMJFS2125 (to S.M.); KAKENHI (Grant-in-Aid for Challenging Research (Pioneering) from Japan Society for the Promotion of Science (JSPS) Grant Number 18H05359 (20K20370), 22K18343 (to S.K.); and Adaptable and Seamless Technology Transfer Program through Target-driven R&D (A-STEP) from JST Grant Number JPMJTR194C; a project JPNP 23200460, commissioned by the New Energy and Industrial Technology Development Organization (NEDO) (to S.K.).

Disclosure statement

No potential conflict of interest was reported by the authors.

Acknowledgments

We thank Dr. Norikazu Tamura for his advice on chemical compounds and Komi-Hakko Corporation for their help with FLIPR.

5. References

- Ahmed MK, *et al.* Expression of transient receptor potential vanilloid (TRPV) families 1, 2, 3 and 4 in the mouse olfactory epithelium. *Rhinology*. 2009; **47**: 242–247.
- Bujak JK, *et al.* Inflammation, cancer and immunity-implication of TRPV1 channel. *Front Oncol*. 2019; **9**: 1087.
- Ferreira SG, *et al.* N-acyldopamines control striatal input terminals via novel ligand-gated cation channels. *Neuropharmacology*. 2009; **56**: 676–683.
- Fujita K, *et al.* A regulatory role of scavenger receptor class B type 1 in endocytosis and lipid droplet formation induced by liposomes containing phosphatidylethanolamine in HEK293T cells. *Biochim Biophys Acta Mol Cell Res*. 2021; **1868**: 118859.
- Fujita K, *et al.* Induction of lipid droplets in non-macrophage cells as well as macrophages by liposomes and exosomes. *Biochem Biophys Res Commun*. 2019; **510**: 184–190.
- Harb AA, *et al.* Eugenol reduces LDL cholesterol and hepatic steatosis in hypercholesterolemic rats by modulating TRPV1 receptor. *Sci Rep*. 2019; **9**: 14003.
- Hinuma S, *et al.* Specific binding and endocytosis of liposomes to HEK293T cells via myristoylated pre-S1 peptide bound to sodium taurocholate cotransporting polypeptide. *Vaccines (Basel)*. 2022; **10**: 2050.
- Jimenez RC, *et al.* The mutational landscape of human olfactory G protein-coupled receptors. *BMC Biol*. 2021; **19**: 21.
- Koivisto AP, *et al.* Advances in TRP channel drug discovery: from target validation to clinical studies. *Nat Rev Drug Discov*. 2022; **21**: 41–59.
- Kwon DH, *et al.* Heat-dependent opening of TRPV1 in the presence of capsaicin. *Nat Struct Mol Biol*. 2021; **28**: 554–563.
- Lankford CK, *et al.* A comparison of the primary sensory neurons used in olfaction and vision. *Front Cell Neurosci*. 2020; **14**: 595523.
- Li S, Jie Z. The capsaicin binding affinity of wildtype and mutant TRPV1 ion channels. *J Biol Chem*. 2023; **299**: 105268.
- Mainland JD, *et al.* Human olfactory receptor responses to odorants. *Sci Data*. 2015; **2**: 150002.
- Malnic B, *et al.* Combinatorial receptor codes for odors. *Cell*. 1999; **96**: 713–723.
- Malnic B, *et al.* The human olfactory receptor gene family. *Proc Natl Acad Sci U S A*. 2003; **101**: 2583–2589.

- McNamara FN, *et al.* Effects of piperine, the pungent component of black pepper, at the human vanilloid receptor (TRPV1). *Br J Pharmacol.* 2005; **144**: 781–790.
- Melkes B, *et al.* β -arrestin 2 and ERK1/2 are important mediators engaged in close cooperation between TRPV1 and μ -opioid receptors in the plasma membrane. *Int J Mol Sci.* 2020; **21**: 4626.
- Mombaerts P, *et al.* Visualizing an olfactory sensory map. *Cell.* 1996; **87**: 675–686.
- Moriyama T, *et al.* Sensitization of TRPV1 by EP1 and IP reveals peripheral nociceptive mechanism of prostaglandins. *Mol Pain.* 2005; **1**: 3.
- Nakamura T, Geoffrey HG. A cyclic nucleotide-gated conductance in olfactory receptor cilia. *Nature.* 1987; **325**: 442–444.
- Nakashimo Y, *et al.* Expression of transient receptor potential channel vanilloid (TRPV) 1–4, melastatin (TRPM) 5 and 8, and ankyrin (TRPA1) in the normal and methimazole-treated mouse olfactory epithelium. *Acta Otolaryngol.* 2010; **130**: 1278–1286.
- O'Hanlon S, *et al.* Neuronal markers in allergic rhinitis: expression and correlation with sensory testing. *Laryngoscope.* 2007; **117**: 1519–1527.
- Olander T, *et al.* The human olfactory transcriptome. *BMC Genomics.* 2016; **17**: 619.
- Peyravian P, *et al.* Cannabidiol as a novel therapeutic for immune modulation. *Immunotargets Ther.* 2020; **9**: 131–140.
- Pronin A, Slepak VZ. Ectopically expressed olfactory receptors OR51E1 and OR51E2 suppress proliferation and promote cell death in a prostate cancer cell line. *J Biol Chem.* 2021; **296**: 100475.
- Sakatani H, *et al.* The roles of transient receptor potential vanilloid 1 and 4 in olfactory regeneration. *Lab Invest.* 2023; **103**: 100051.
- Salzer I, *et al.* Nociceptor signalling through ion channel regulation via GPCRs. *Int J Mol Sci.* 2019; **20**: 2488.
- Samanta A, *et al.* Transient receptor potential (TRP) channels. *Subcell Biochem.* 2018; **87**: 141–165.
- Seki N, *et al.* Expression and localization of TRPV1 in human nasal mucosa. *Rhinology.* 2006; **44**: 128–134.
- Shepard BD, *et al.* A cleavable N-terminal signal peptide promotes widespread olfactory receptor surface expression in HEK293T cells. *PLoS One.* 2013; **8**: e68758.
- Sklar PB, *et al.* The odorant-sensitive adenylate cyclase of olfactory receptor cells: differential stimulation by distinct classes of odorants. *J Biol Chem.* 1986; **261**: 15538–15543.

- Sun MY, *et al.* Vanilloid agonist-mediated activation of TRPV1 channels requires coordinated movement of the S1–S4 bundle rather than a quiescent state. *Sci Bull (Beijing)*. 2022; **67**: 1062–1076.
- Vetter I, *et al.* Rapid, opioid-sensitive mechanisms involved in transient receptor potential vanilloid 1 sensitization. *J Biol Chem*. 2008; **283**: 19540–19550.
- Vu S, *et al.* New capsaicin analogs as molecular rulers to define the permissive conformation of the mouse TRPV1 ligand-binding pocket. *eLife*. 2020; **9**: e62039.
- Xu H, *et al.* Camphor activates and strongly desensitizes the transient receptor potential vanilloid subtype 1 channel in a vanilloid-independent mechanism. *J Neurosci*. 2005; **25**: 8924–8937.
- Yang BH, *et al.* Activation of vanilloid receptor 1 (VR1) by eugenol. *J Dent Res*. 2003; **82**: 781–785.
- Yang F, *et al.* Structural mechanism underlying capsaicin binding and activation of the TRPV1 ion channel. *Nat Chem Biol*. 2015; **11**: 518–524.
- Yang F, *et al.* The conformational wave in capsaicin activation of transient receptor potential vanilloid 1 ion channel. *Nat Commun*. 2018; **9**: 2879.
- Yelshanskaya MV, Sobolevsky AI. Ligand-binding sites in vanilloid-subtype TRP channels. *Front Pharmacol*. 2022; **13**: 900623.
- Zhang K, *et al.* Structural snapshots of TRPV1 reveal mechanism of polymodal functionality. *Cell*. 2021; **184**: 5138–5150.

Chapter III Role of phosphorylation and vanilloid ligand structure in ligand-dependent differential activations of TRPV1

1. Introduction

Since transient receptor potential (TRP) channels were first discovered in *Drosophila* in 1969, their functions as sensors for various physiological and environmental stimuli such as chemicals, temperature, and mechanical stress have been extensively studied (Zhang *et al.* 2023). Mammalian TRP channels form a super family of 28 (27 in human) distinct cation-selective ion channels, which are categorized into 6 subfamilies based on amino acid sequence homology: 6 TRPV (vanilloid), 7 TRPC (canonical), 8 TRPM (melastatin-related), 1 TRPA (ankyrin), 3 TRPP (polycystic), and 3 TRPML (mucolipin) (Samanta *et al.* 2018; Yelshanskaya and Sobolevsky 2022; Zhang *et al.* 2023). Since TRP subfamilies were not classified based on their functions, the members of each subfamily do not always share common functional characteristics (e.g. TRPM2 functions as a sensor for redox in macrophages, TRPM7 is involved in intestinal Mg^{2+} uptake, and TRPM8 regulates epithelial growth) (Koivisto *et al.* 2022). TRPV1 was first discovered as a receptor for capsaicin, the spicy component of hot chili peppers, and the first cloned TRP channels in mammals (Caterina *et al.* 1997). TRPV1-4 functions as nonselective cationic ion channels, while TRPV5 and TRPV6 are selective for calcium ions. Although all TRPV members were initially thought to be sensitive to temperature like TRPV1, recent studies including those using knockout mice have shown that TRPV2-6, which have more than 50% amino acid identity, are not always sensitive to temperature stimuli (Samanta *et al.* 2018). The TRPV1 monomer includes an intracellular N-terminal region with 6 ankyrin repeats, transmembrane domains (S1-S6) that form a pore for cationic ions (Ca^{2+} and

Na^+) to pass through, and an intracellular C-terminal region. A functional TRPV1 is composed of a homotetramer. TRPV1 is abundantly expressed in the nervous system and is involved in the detection of external noxious stimuli, mucosal protection, and wound healing (Abdel-Salam *et al.* 1996 ; Caterina *et al.* 1997 ; Schuligoi *et al.* 1998 ; Ward *et al.* 2003). TRPV1 expression is also detected in non-neuronal tissues, suggesting that it plays regulatory roles in non-neuronal cells as well as neurons (Bujak *et al.* 2019). Various stimuli including chemical compounds (e.g. capsaicin, resiniferatoxin, oxytocin, rinvanil, and arvanil), temperatures above 43 °C, and acids can alter the structure and functions of TRPV1. These stimuli evoke TRPV1-mediated $\text{Na}^+/\text{Ca}^{2+}$ influx in cells, changing the membrane potential (Kwon *et al.* 2021; Yang *et al.* 2003; Yelshanskaya and Sobolevsky 2022). Olfactory receptors (ORs) and several TRP channels, including TRPV1, TRPV4, and TRPM5, have been reported as being expressed in olfactory sensory neurons (OSNs) (Lin *et al.* 2007; Nakashimo *et al.* 2010; Sakatani *et al.* 2023). However, there has been controversy regarding which types of TRP channels are expressed in mature OSNs (Pyrski *et al.* 2017; Sakatani *et al.* 2023). On the other hand, OR51E1 and OR51E2 are found to be expressed in not only OSNs but also in prostatic cells along with a variety of TRP channels, including TRPV1, TRPV2, TRPV6, TRPM8, TRPM2, and TRPC6 (Chen *et al.* 2014; Pronin *et al.* 2021). Therefore, it is inferred that ORs and TRP channels including TRPV1, are co-expressed in certain cellular contexts. However, the potential interaction between ORs and TRP channels including TRPV1 remained largely unexplored. Previous reports indicate that some G protein-coupled receptors (GPCRs) (in which ORs are not involved) alter TRPV1 activation through the phosphorylation of TRPV1, consequently influencing nociception (Salzer *et al.* 2019). In my previous report, I co-expressed OR51E1 or OR51E2 and TRPV1 in HEK293T cells and then analyzed the

effect of OR51E1 on TRPV1 activation induced by vanilloid compounds. As a result, I found a unique aspect of OR regulation on TRPV1 activation: these ORs enhanced the response of TRPV1 to capsaicin while attenuating that to eugenol (Moriyama *et al.* 2024). The two ORs have the potential to trigger an increase in cAMP levels. Our results indicated that the effects produced by these ORs could be replicated using a forskolin (FSK) known as an adenylate cyclase (AC) activator. Therefore, it was suggested that ORs or FSK can stimulate the cAMP production pathway, which consequently phosphorylates TRPV1. In this study, I further confirmed this presumption using a protein kinase A (PKA) inhibitor and TRPV1 mutants that FSK induces phosphorylation, which results in ligand-dependent TRPV1 activation. In my previous report, I demonstrated that the ligands of TRPV1 could be divided into two categories, namely capsaicin and eugenol. This classification was based on the varying susceptibility of ligand-activated TRPV1 to modulation by ORs or FSK. However, the molecular characteristics that distinguish the two types of ligands remained elusive. In this study, I sought to clarify the roles of chemical groups in vanilloid compounds, leading me to categorize them into distinct types. During these analyses, I found a third type of TRPV1 ligand 10-shogaol. The activation of TRPV1 by 10-shogaol was unaffected by treatment with FSK.

2. Materials and methods

2.1. Cell culture

HEK293T and COS-7 cells were obtained from RIKEN BRC (Tsukuba, Ibaraki, Japan). These cells were cultured in RPMI 1640 medium supplemented with 10% heat-inactivated fetal bovine serum and antibiotics (Fujita *et al.* 2019).

2.2. Plasmids and transfection

A human TRPV1 expression plasmid (pcDNA3.1⁺ /C-(K)-DYK- TRPV1; catalog number: OHu22257D) was purchased from Genscript (Piscataway, NJ, USA), while an empty vector plasmid (pBApo-CMV Neo; catalog number: 3240) from Takara Bio Inc. (Kusatsu, Shiga, Japan). We also obtained TRPV1 mutant expression plasmids from GenScript, which included substitutions of S502A, T370A, or T144A in the TRPV1 ORF in the pcDNA3.1⁺ vector. Transfection of plasmids into HEK293T and COS-7 cells was performed using PolyMag Neo (catalog number: PG60100; OZ Biosciences, Marseille, France) as described previously (Moriyama *et al.* 2024).

2.3. Reagents

Eugenol (catalog number: A0232; TCI chemicals, Tokyo, Japan), N-arachidonoyl dopamine (NADA; catalog number: AB120099-5; Abcam, Cambridge, UK), zingerone (catalog number: ASB-00026600-250; ChromaDex, Inc. LA, USA), vanillin (catalog number: h0264; TCI chemicals), capsaicin (catalog number: 034-11351; Fujifilm Wako Pure Chemical Corp., Osaka, Japan), piperine (catalog number: 162-17241; Fujifilm Wako Pure Chemical Corp.), FSK (catalog number: 067-02191; Fujifilm Wako Pure Chemical Corp.), and H-89 (hydrochloride) (catalog number: CAY-10010556-5; Cayman

Chemical, Ann Arbor, MI, USA) were dissolved in ethanol and then diluted to the necessary concentrations with Hanks' balanced salts solution (HBSS) (catalog number: 084-08965; Fujifilm Wako Pure Chemical Co.). The following reagents were directly resolved in HBSS: Vanillyl alcohol (catalog number: 320-29932; Fujifilm Wako Pure Chemical Corp.), coniferyl alcohol (catalog number: 034-20163; Fujifilm Wako Pure Chemical Corp.), 4-(Ethoxy methyl)-2-methoxyphenol (vanillyl ethyl ether; catalog number: E1028-5G; TCI chemicals), vanillyl butyl ether (catalog number: V0161-25G; Fujifilm Wako Pure Chemical Corp.), nordihydrocapsaicin (catalog number: CAY33407-1; Cayman Chemical), olvanil (catalog number: CAY90262-5; Cayman Chemical), and 6-shogaol (catalog number: CAY-11901-1; Cayman Chemical), 10-shogaol (catalog number: HY-N2434; MedchemExpress. NJ, USA), and capsiate (catalog number: SCB-SC-506004-10; Santa Cruz Biotechnology, Dallas, TX, USA).

2.4. Measurement of intracellular Ca^{2+} influx

Ca^{2+} influx in cells was detected as described previously (Moriyama *et al.* 2024). Briefly, plasmid transfected cells were cultured in a 96-well black/clear bottom plate (catalog number: 165305; Thermo Fisher Scientific) coated with poly-L-lysine for 24 h at 37 °C in a humidified atmosphere containing 5% CO_2 . After removing the culture medium, I incubated the cells in HBSS (50 μL /well) containing a dye loading buffer supplied with a Calcium 6 Assay Explorer Kit (catalog number: OZB-PG60200-200-200; OZ Biosciences) for 2 h at 37 °C. Then, I added HBSS containing a sample (50 μL /well) and measured fluorescence using a Fluorometric imaging plate reader (FLIPR) tetra from Molecular Devices (San Jose, CA, USA). When treatments with reagents FSK and H-89 were required for cells, these were added to the cells 15 and 10 min before applying

FLIPR, respectively. We measured changes (%) in fluorescence intensity (FI) every second for 3 min in triplicate assays. The data were expressed as mean values and standard deviation. Specific responses of cells to ligands, resulting from transfection with the TRPV1 expression plasmid, were calculated by subtracting FI changes in control cells (not transfected with TRPV1 expression plasmid) from FI changes in cells transfected with TRPV1 expression plasmids (Moriyama *et al.* 2024).

2.5. Western blot analyses

We seeded COS-7 cells in 24-well culture plates (catalog number: 3526; Corning, NY, USA) at 4.0×10^5 cells/mL in 500 μ L/well. These cells were cultured at 37 °C for 24 h in a humidified atmosphere containing 5% CO₂. Then the cells were transfected with 0.8 μ g per well of plasmid DNA using PolyMag Neo. After adding fresh culture medium (1 mL/well), they were cultured for 24 h. Following this, they were washed with PBS, and cell lysates were prepared using a RIPA buffer containing a protease inhibitor cocktail (catalog number 25955-11; Nacalai Tesque, Inc., Kyoto, Japan). SDS-PAGE and Western blot procedures were conducted as described previously (Hinuma, Fujita and Kuroda. 2022). To detect TRPV1, I treated the samples with the first antibody (monoclonal mouse anti-TRPV1; catalog number ab6166; Abcam, Cambridge, UK) at a dilution of 1:2000 at room temperature for 1 h. This was followed by treatment with a horseradish peroxidase (HRP)-conjugated second antibody (goat anti-mouse IgG (H + L) antibody, HRP conjugate 1; catalog number: SA00001-1; Proteintech, Tokyo, Japan) diluted to 1:4000 at room temperature for 1 h. The FLAG tag (DYKDDDDK) located at the C-terminus of both wild-type and mutant TRPV1 was identified using an HRP-conjugated anti-FLAG mouse monoclonal antibody (catalog number: 015-22391; Fujifilm Wako Pure Chemical

Co.). The antibody treatment at a dilution of 1:5000 was carried out at room temperature for 30 min. To detect glyceraldehyde-3-phosphate dehydrogenase (GAPDH) as an internal standard protein, I used an HRP-conjugated anti-GAPDH mouse monoclonal antibody (catalog number: 015-25473; Fujifilm Wako Pure Chemical Co.) at a dilution of 1:10 000. We performed antibody treatment at room temperature for 1 h. Finally, I visualized the antibody-bound protein bands on the membrane by enhanced chemiluminescence using Luminograph II (Atto, Tokyo, Japan).

3. Results

Suppression of FSK's modulatory effects on capsaicin and eugenol-induced TRPV1 activation by H-89 In my prior study, I hypothesized that the modulatory mechanisms of OR and FSK for TRPV1 activation, triggered by capsaicin or eugenol stimulation, could be attributed to the phosphorylation of TRPV1 (Moriyama *et al.* 2024). As shown in Figure 1, FSK could substitute the divergent effects of OR on TRPV1 activation induced by either capsaicin or eugenol. FSK treatment amplified the capsaicin-induced Ca^{2+} influx in HEK293T cells transfected with TRPV1 (Figure 1a). Conversely, TRPV1 activation induced by eugenol was diminished under identical treatment conditions (Figure 1b). As I explained in the previous study, control cells, transfected with the empty vector plasmid, also responded to capsaicin or eugenol. Because I could not exclude the possibility that the endogenous TRPV1 and other receptors contribute to the responses of control cells to these ligands, I calculated here specific TRPV1 responses to capsaicin (Figure 1c) and eugenol (Figure 1d), which were attributable to the transfected TRPV1 as FI changes, that is response/baseline (%), in TRPV1-transfected cells subtracting those in control cells.

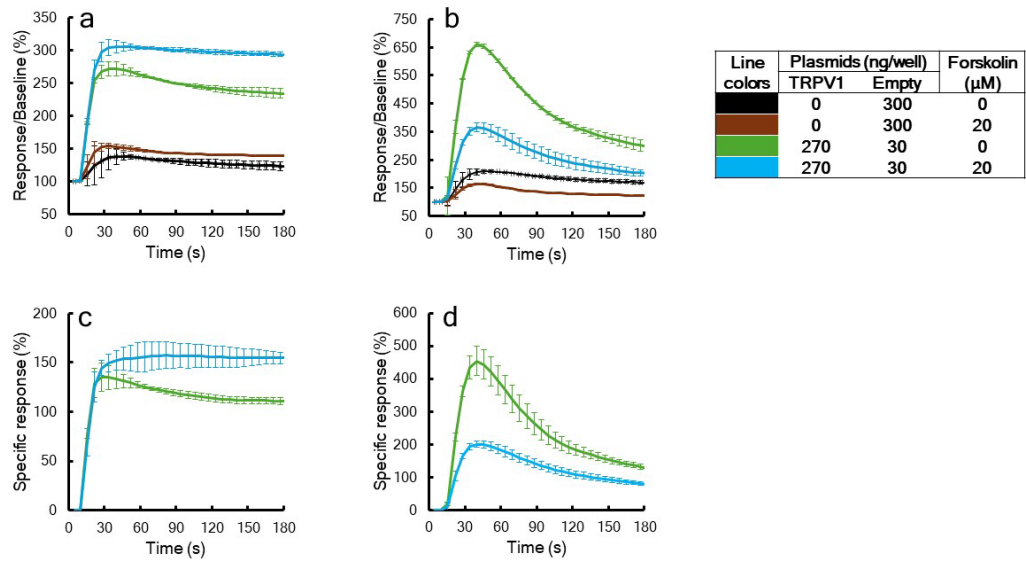


Figure 1. Modulatory effects of FSK on TRPV1-mediated Ca^{2+} influx in response to capsaicin or eugenol. HEK293T cells, cultured in a 96-well microplate, were transfected with plasmids. The table adjacent to graph (b) displays the quantity of each plasmid utilized for transfection, as well as the color codes that correspond to the lines in graphs (a) through (d). The transfected cells were cultured for 24 h. After adding HBSS containing 10 μM of capsaicin (a), or HBSS containing 400 μM of eugenol (b), the influx of Ca^{2+} within cells was tracked by detecting changes in FI every second for 3 min using a FLIPR. The data are shown as mean values ($n = 3$) with standard deviations (vertical bars). The specific responses of TRPV1 to capsaicin (c) and eugenol (d) were determined by subtracting the FIs of cells transfected with the empty vector from those of cells transfected with the TRPV1 expression plasmid.

In the regulatory mechanism of GPCRs (except for ORs) for TRPV1 activation, previous studies have shown that a rise in cAMP levels sequentially induces the activation of PKA and the phosphorylation of TRPV1. These events significantly enhance the activation of TRPV1 induced by capsaicin (Moriyama *et al.* 2005; Vetter *et al.* 2008; Jeske *et al.* 2008; Melkes *et al.* 2020). To validate whether a similar mechanism underlies the divergent effects of ORs or FSK on TRPV1 responses to vanilloid ligands, I examined if H-89, a PKA inhibitor, could alleviate the effects of FSK on capsaicin and eugenol-induced TRPV1 activation. As shown in Figure 2a, FSK treatment did not evoke Ca^{2+} influx in TRPV1-transfected HEK293T cells without ligand stimulation, even with the addition of

H-89. On the other hand, FSK amplified the capsaicin-induced Ca^{2+} influx by a factor of 1.7. This amplification was dose-dependently diminished by H-89, reaching a factor of 1.25 in the presence of 50 μM H-89 (Figure 2b). Unlike the case with capsaicin, FSK treatment decreased eugenol-induced TRPV1-mediated Ca^{2+} influx to 0.2-fold, but this reduction was partially reversed to 0.5 fold by 50 μM H-89 (Figure 2c). These findings strongly suggest that PKA-mediated phosphorylation of TRPV1 plays a crucial role in the modulatory effects of FSK on TRPV1 responses to both capsaicin and eugenol.

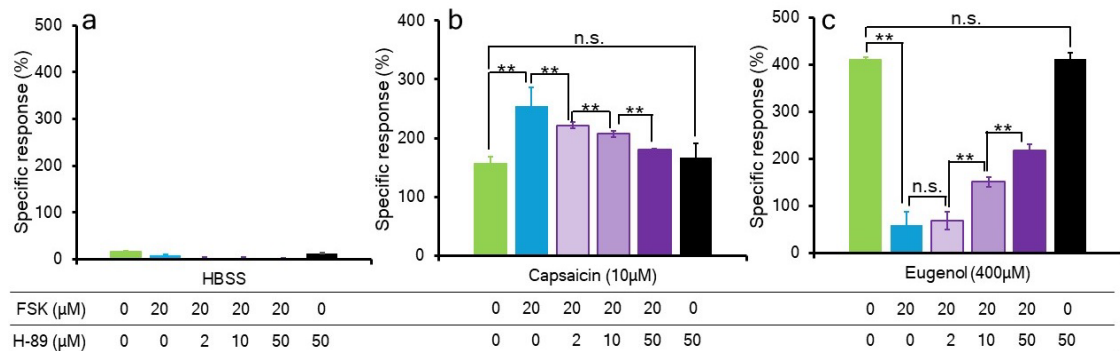


Figure 2. Suppression of FSK modulatory effects on TRPV1 responses to capsaicin and eugenol by H-89. HEK293T cells, cultured in a 96-well plate, were transfected with 300 ng per well of the empty vector plasmid alone (a), and co-transfection with 30 ng per well of the empty vector plasmid and 270 ng per well of the TRPV1 expression plasmid (b and c). After transfection, the cells were cultured for 24 h. The influx of Ca^{2+} in the cells was monitored by observing changes in FI every second for 3 min using a FLIPR. Ligand stimulation of TRPV1 was carried out by adding HBSS without ligands (a), HBSS containing 10 μM of capsaicin (b), or HBSS containing 400 μM of eugenol (d). FSK and H-89 were administered at the concentrations below the Figure, 15 and 10 min before applying the ligands. Data were presented as mean values of maximal TRPV1-specific responses ($n = 3$) with standard deviation (horizontal bars). The specific responses of TRPV1 to capsaicin (b) and eugenol (c) were determined by subtracting the responses to capsaicin or eugenol in cells without TRPV1 expression plasmid from those in cells with TRPV1 expression plasmid transfection. Statistical analysis was performed using the Tukey test.* $P < .05$; ** $P < .01$; n.s.: not significant.

Effects of FSK on TRPV1 mutants stimulated with capsaicin and eugenol To confirm my presumption, that is FSK's divergent effects on ligand-induced TRPV1 activation are exhibited via the phosphorylation of TRPV1, I examined whether FSK

could alter the ligand responsiveness of TRPV1 mutants, in which possible PKA phosphorylation sites of threonine and serine were replaced with alanine (T145A, T371A, and S502A) (Rathee *et al.* 2002 ; Mohapatra and Nau 2003 ; Schnizler *et al.* 2008). For the analysis of TRPV1 mutants, I employed COS-7 cells instead of HEK293T cells to avoid the potential interference of endogenous TRPV1 expression. As shown in Figure 3 a and c, the influx of Ca^{2+} triggered by capsaicin was less pronounced in COS-7 cells than in HEK293T cells. We used zingerone as a eugenol-type ligand instead of eugenol because control COS-7 cells without transfection of TRPV1 expression plasmid showed minimal response to zingerone under my experimental conditions (Figure 3 b and d).

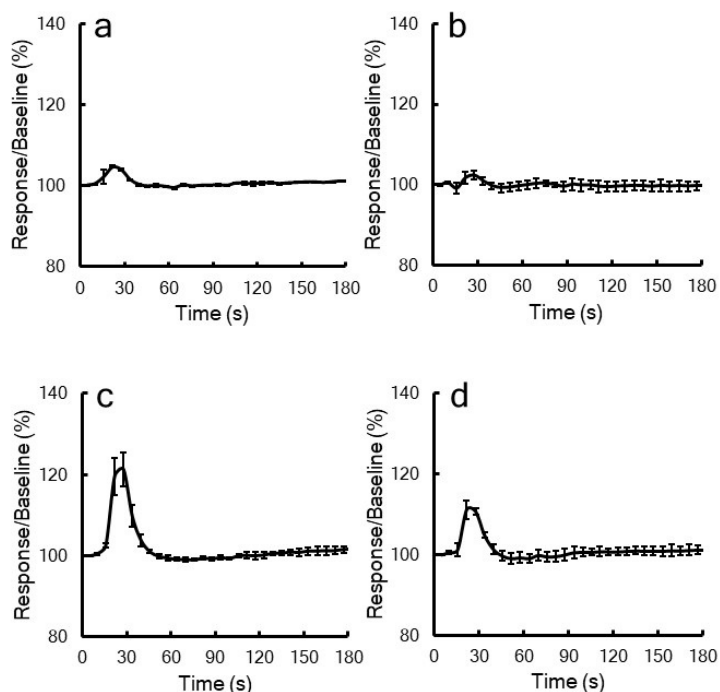


Figure 3. Ca^{2+} influx in COS-7 and HEK293T cells stimulated with capsaicin and zingerone. COS-7 (a, b) and HEK293T (c, d) cells, cultured in a 96-well plate for 48 h without transfection of TRPV1 expression plasmid, were applied to assays to detect Ca^{2+} influx. Changes in FI in cells were measured using a FLIPR every second for 3 min after 10 μM capsaicin (a, c) or 100 μM zingerone (b, d) was added to cells. Assays and data processing were conducted as described in Figure 1 .

The existence of TRPV1 proteins in COS-7 cells, which were transfected either with or without expression plasmids for wildtype TRPV1 and mutated TRPV1, was confirmed through Western blot analyses. The levels of TRPV1 protein expression in these cells were almost identical (Figure 4).

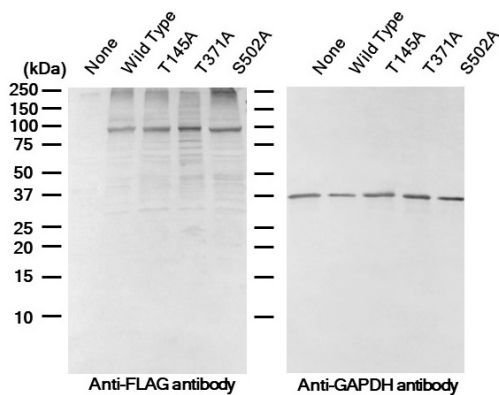


Figure 4. Western blot analyses of TRPV1 mutant proteins expressed in COS-7 cells. COS-7 cells, cultured in a 24-well plate, were transfected with or without wild-type TRPV1 and TRPV1 mutant (ie T145A, T371A, and S502A) expression plasmids. After cells were cultured for 24 h, proteins were extracted from these cells. SDS-PAGE was performed with 10 μ g of protein in each lane under reducing conditions. The bands on the membrane were identified using the specific antibody indicated beneath each image. TRPV1 protein was detected as major bands (approximately at 92 kDa) in the left image. GAPDH protein expression levels are shown in the right image.

Figure 5 illustrates that FSK amplified the response of wildtype TRPV1 to capsaicin. However, this effect was absent in TRPV1 mutants (T145A, T371A, and S502A). The absence of FSK's amplification of capsaicin-induced Ca^{2+} influx in these mutants was consistent with prior research reporting that the FSK's enhancing effect on the capsaicin-induced current responses of TRPV1 expressed in HEK293T cells is negated by the same mutation (Rathee *et al.* 2002). Similarly, the inhibitory effect of FSK on the response of wildtype TRPV1 to zingerone was also missing in the TRPV1 mutants, as shown in Figure 5b. The findings from Figures 2 and 5 collectively indicate that FSK modulates

the responses of TRPV1 to both capsaicin and eugenol-type ligands via TRPV1 phosphorylation.

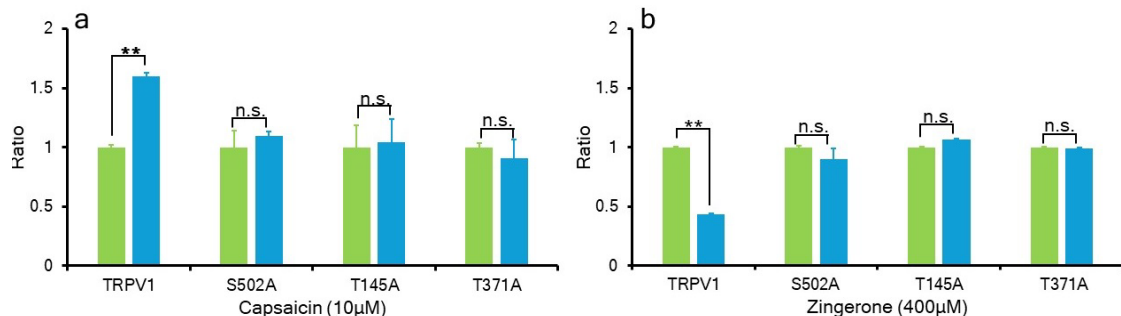


Figure 5. Effects of FSK on the responsiveness of TRPV1 mutants to capsaicin and zingerone. COS-7 cells, cultured in a 96-well plate, were transfected with a combination of the empty vector (0.03 μ g/well) and expression plasmids for wild-type TRPV1 and TRPV1 mutants (0.27 μ g/well), in which specific threonine or serine residues were substituted with alanine as shown in the Figure. Following a 24-h culture period, cells were either untreated (left bars in each pair) or treated (right bars in each pair) with 20 μ M FSK. Changes in FIs in cells were measured using a FLIPR after adding 10 μ M capsaicin (a) or 100 μ M zingerone (b). The specific responses of TRPV1 to capsaicin and zingerone were determined by subtracting the responses to capsaicin or zingerone in cells without the transfection of expression plasmids from those in cells with the transfection of wild-type TRPV1 and TRPV1 expression plasmids. The vertical axis represents ratios calculated using the following formula: (the maximal FI change in cells expressing wild type or TRPV1 mutant after stimulation with the indicated TRPV1 ligand in the presence of FSK)/(that after stimulation with the indicated TRPV1 ligand in the absence of FSK). Assays, data processing, and statistical analysis were conducted as described in Figure 2.

Modulatory effects of FSK on the responsiveness of HEK293T cells stimulated with various vanilloid analogs In the previous study, I demonstrated that TRPV1 ligands could be categorized into two types, exhibiting capsaicin-like or eugenol-like actions on TRPV1 concerning OR and FSK treatment (Moriyama *et al.* 2024). Furthermore, eugenol is predicted to bind near the capsaicin binding pocket in TRPV1 (Harb *et al.* 2019). To elucidate the structural traits of vanilloid compounds that distinguish between these two types of TRPV1 ligands, I analyzed the structure-activity relationship of TRPV1 responses to 13 vanilloid compounds in FSK-treated HEK293T cells. In these

experiments, I evaluated the dose responses of TRPV1 to each ligand, both with and without FSK treatment, across 3 different doses. As demonstrated in my previous report, the dose-response curves of TRPV1 to vanilloid compounds do not always follow the typical sigmoid pattern. Additionally, the maximal responses varied among the vanilloid compounds. To obtain essential data demonstrating the modulatory effects of FSK on each vanilloid compound-induced TRPV1 activation, I sought appropriate doses of the compounds to discern these effects, then repeated experiments several times to confirm the FSK's effects. Representative data are shown in Figure 6 . FSK treatment enhanced TRPV1 responses to vanillyl ethyl ether, vanillyl butyl ether, nordihydrocapsaicin, capsiate, capsaicin, and olvanil. Because these vanilloid ligands activated TRPV1 expressed in HEK293T cells, which was strengthened by FSK treatment, I defined these compounds as capsaicin-type ligands.

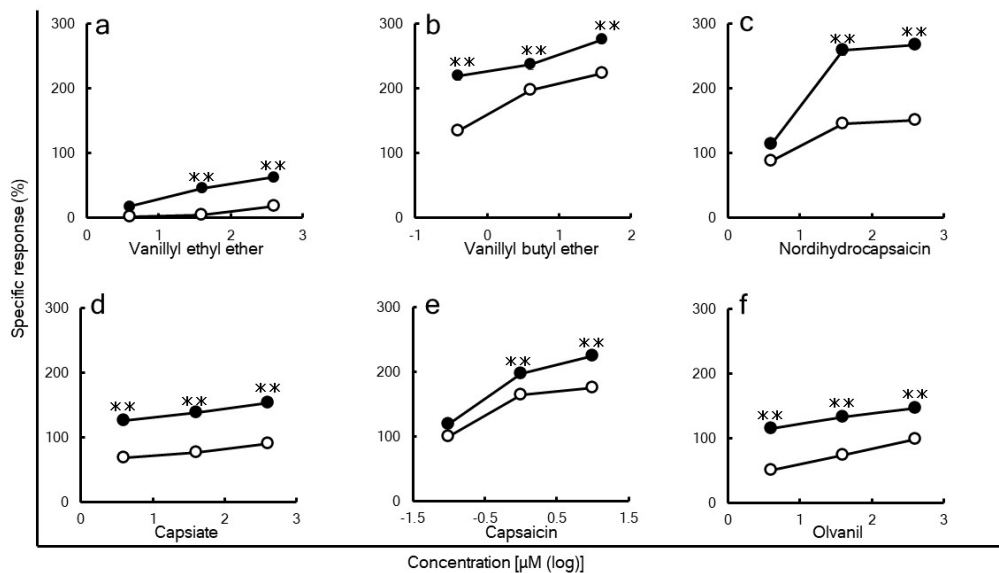


Figure 6. Vanilloid compounds inducible enhancement of Ca^{2+} influx in HEK293T cells treated with FSK. HEK293T cells were transfected with the empty vector and TRPV1 expression plasmids following the identical protocol described in Figure 2 . After transfected cells were cultured for 24 h, changes in FIs in the cells were measured following the addition of the indicated vanillyl compounds. The markers, either blank or filled, represent FI changes in cells that were either untreated or treated

with FSK, respectively. FI changes were measured following the addition of vanillyl ethyl ether (a), vanillyl butyl ether (b), nordihydrocapsaicin (c), capsiate (d), capsaicin (e), and olvanil (f). Because the data were gathered from separate experiments, we normalized them based on the response to capsaicin in each respective experiment. Except for data normalization, the assays and data processing followed the procedure depicted in Figure 2 . Statistical analysis ($n = 3$) was performed using the Tukey test.* $P < .05$; ** $P < .01$. Due to the small size of the error bars, they are often not visible within the symbols.

In contrast, FSK treatment reduced the responsiveness of HEK293T cells expressing TRPV1 to vanillin, vanillyl alcohol, eugenol, coniferyl alcohol, zingerone, and 6-shogaol (Figure 7). Therefore, I designated these vanilloid analogs as eugenol-type ligands. During these analyses, I found that TRPV1 activation by 10-shogaol was not affected by the treatment with FSK (Figure 8). Therefore, I named this novel ligand type unaffected by FSK as a 10-shogaol-type ligand.

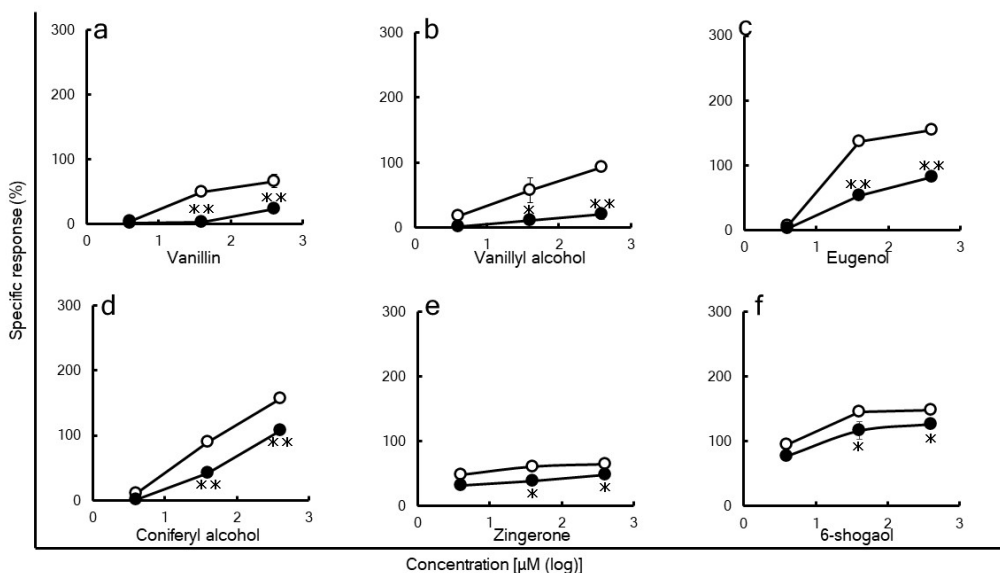


Figure 7. Vanilloid compounds inducible reduction of Ca^{2+} influx in HEK293T cells treated with FSK. Experimental conditions, data processing, and statistical analysis are the same as described in Figure 6 . The markers, either blank or filled, represent FI changes in cells that were either untreated or treated with FSK, respectively. FI changes were measured following the addition of vanillin (a), vanillyl alcohol (b), eugenol (c), coniferyl alcohol (d), zingerone (e), and 6-shogaol (f). Due to the small size of the error bars, they are often not visible within the symbols.

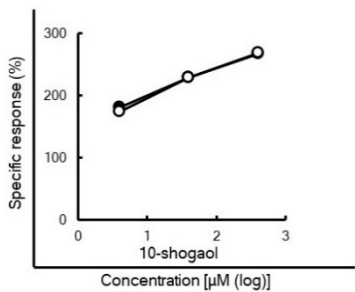


Figure 8. No change in 10-shogaol-induced TRPV1 activation by FSK treatment. The experimental conditions, data processing, and statistical analysis methods are identical to those described in Figure 6. The empty or filled markers denote the changes in FI in cells that were either untreated or treated with FSK, respectively. The changes in FI were measured after the introduction of 10-shogaol. Due to the small size of the error bars, they are often not visible within the symbols.

Previous reports have suggested that the dose responses of TRPV1 to ligands, measured using the patch clamp method to monitor electrical changes in the membrane, are influenced by the ligand's affinity for TRPV1 and its ability to induce conformational changes gating the pore formed by TRPV1 tetramers (Yang *et al.* 2015). These changes are closely associated with TRPV1-mediated Ca^{2+} influx (Yang *et al.* 2003; Samanta *et al.* 2018; Yelshanskaya and Sobolevsky 2022; Vu *et al.* 2020). Therefore, capsaicin-type ligands would enhance the affinity and/or gating efficacy for phosphorylated TRPV1 (Figure 6), whereas eugenol-type ligands would decrease them (Figure 7).

Structural characteristics of capsaicin and eugenol-type vanilloid ligands

Regarding the binding of capsaicin to TRPV1, it has been reported that the structure of capsaicin can be functionally divided into 3 parts: the head (vanillyl group), neck (amide bond), and tail (aliphatic chain) (Yang *et al.* 2015). Additionally, I designated here the positions of the amino group and carbonyl group within the amide bond as neck 1 and neck 2, respectively (Figure 9). Our findings indicate that the structure of the neck is pivotal in differentiating between capsaicin and eugenol-type ligands, as all compounds

that have an ether bond, ester, and amide bond at the position of neck 1 were identified as capsaicin-type ligands. For example, despite having similar side chain lengths, zingerone and vanillyl ethyl ether were classified into eugenol-type ligands. Therefore, the polarity of the functional group at the neck 1 position is likely to be essential. Conversely, a carbonyl group at neck 2 is unlikely to be indispensable. Because the carbonyl group at neck 2 was found in both capsaicin and eugenol-type compounds. In the binding process of capsaicin to the TRPV1 binding pocket, the tail is presumed to provide support through Van der Waals (VDW) forces between the tail and TRPV1 amino acid residues (Yang *et al.* 2015). Despite 6-shogaol possessing a longer aliphatic tail than vanillyl ethyl ether and vanillyl butyl ether, it behaved as a eugenol-type ligand, while the latter two compounds exhibited capsaicin-type behavior. This suggests that the functional groups at the neck are more crucial for capsaicin-type ligands than the lengths of the aliphatic tail. However, vanillin and vanillyl alcohol, which have short side chains extending from the vanillyl group and terminate with the oxygen atom and hydroxyl group at the position of neck 1, were classified as eugenol-type ligands. These results indicate that capsaicin-type ligands necessitate a polar neck 1 and side chains extending beyond the neck, regardless of the length. Previously, I hypothesized that vanillyl compounds with lower molecular weights would be classified as eugenol-type ligands, and molecules with relatively higher molecular weights would fall under the capsaicin-type category. However, this hypothesis should be reconsidered. Because of having a molecular weight greater than vanillyl ethyl ether and vanillyl butyl ether of capsaicin-type compounds, 6-shogaol was identified as a eugenol-type ligand. Furthermore, 6-shogaol exhibited characteristics like the eugenol-type ligand when treated with FSK, while 10-shogaol was not susceptible. The primary difference between 6-shogaol and 10-shogaol is the length of the aliphatic side chain. This

suggests the tail length plays a significant role in distinguishing between eugenol-type ligands and 10-shogaol-type ligands.

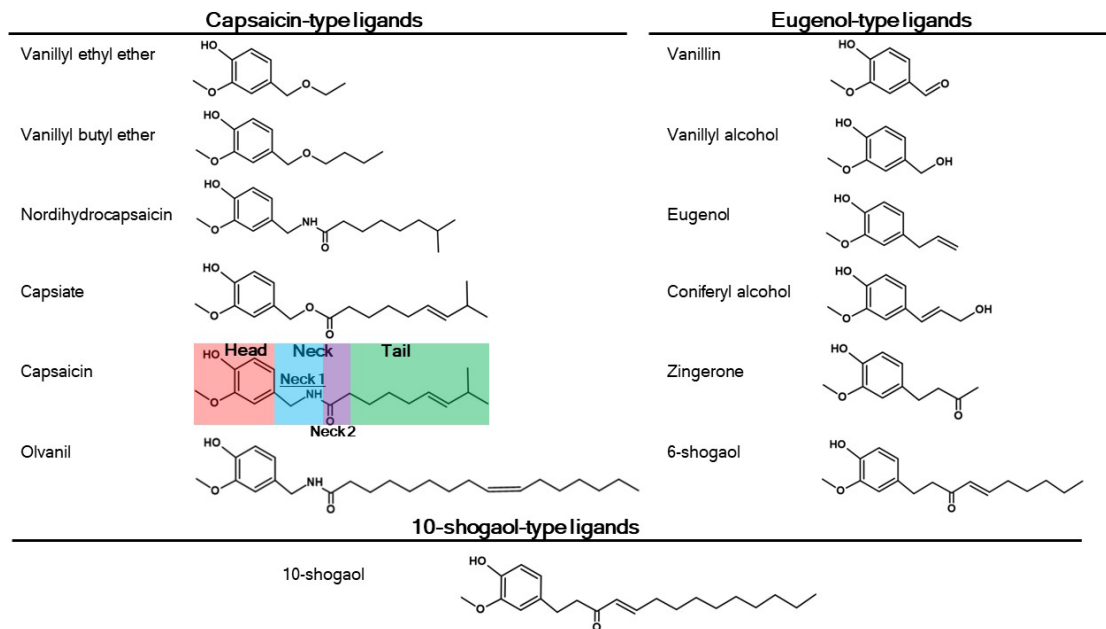


Figure 9. Classification of tested vanillyl compounds into capsaicin-type, eugenol-type, and 10-shogaol-type TRPV1 ligands. Based on the experiments in Figures 6, 7 and 8, tested vanillyl compounds were classified into capsaicin-type, eugenol-type, and 10-shogaol-type categories. The structural components of capsaicin are divided as follows: the head contains a vanillyl group, the neck 1 includes an amino group, the neck 2 includes a carbonyl group, and the tail represents an aliphatic chain.

4. Discussion

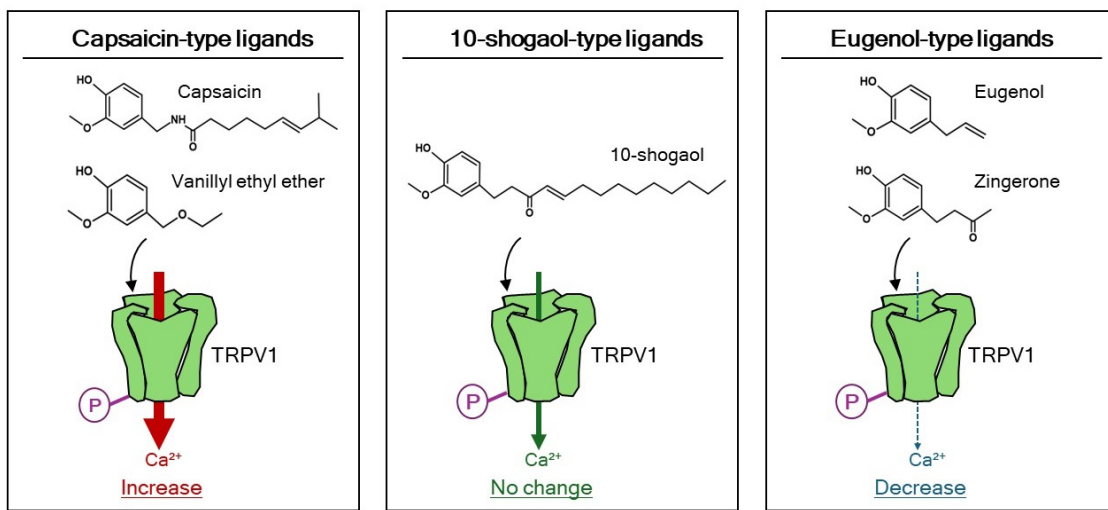
In the previous report, I demonstrated that ORs regulate TRPV1 activation in a ligand-dependent manner. Because the regulatory functions of these ORs could be substituted with an AC activator FSK, in this study, I intended to confirm the following hypothesis using HEK293T cells expressing TRPV1. Treatment with FSK elevates cAMP levels, which triggers PKA activation. The activated PKA in turn catalyzes the phosphorylation of TRPV1. Utilizing a PKA inhibitor (H-89) and TRPV1 mutants, I secured results that corroborate my hypothesis. Furthermore, it has been reported that GPCRs, excluding ORs, and FSK regulate TRPV1 activation through the phosphorylation of TRPV1 (Rathee *et al.* 2002 ; Mohapatra and Nau 2003 ; Schnizler *et al.* 2008 ; Vetter *et al.* 2008 ; Salzer *et al.* 2019 ; Melkes *et al.* 2020). Our results related to phosphorylated TRPV1 activation by capsaicin were consistent with those reported previously. However, it should be noted that little is known about the suppressive effects of FSK on TRPV1 responses to eugenol-type vanilloid ligands. In this study, I showed that FSK's enhancing and suppressing effects on TRPV1 responses to capsaicin and eugenol-type ligands are manifested similarly through the phosphorylation of TRPV1.

Furthermore, I investigated using 13 vanilloid compounds to determine the key structural characteristics that categorize these compounds into two types. Capsaicin-type ligands included vanillyl ethyl ether, vanillyl butyl ether, nordihydrocapsaicin, capsiate, capsaicin, and olvanil. On the other hand, vanillin, vanillyl alcohol, eugenol, coniferyl alcohol, zingerone, and 6-shogaol were classified as eugenol-type ligands. In addition, in this study, I found a third type of TRPV1 ligand, that is 10-shogaol type by which activation of TRPV1 is unaffected by FSK. Structural analyses of TRPV1 using cryo-electron microscopy and computational modeling reveal TRPV1 binding pocket for

capsaicin (Yang *et al.* 2015 ; Yang *et al.* 2018 ; Vu *et al.* 2020 ; Li *et al.* 2023). In the binding model of capsaicin and TRPV1, capsaicin adopts a “tail-up and head-down” configuration within the TRPV1 ligand-binding pocket, assembled by the S3-S6 transmembrane segments. The hydroxyl group of the capsaicin’s head forms a hydrogen bond with a specific amino acid residue of TRPV1 (Yang *et al.* 2018). Furthermore, it has been reported that at least the vanillyl group in eugenol and 6-shogaol binds near the TRPV1 binding pocket for capsaicin (Ohbuchi *et al.* 2016 ; Harb *et al.* 2019). We postulate that the binding mode of the head (vanillyl group) among the compounds tested to TRPV1 would be nearly identical. Our structure-activity relationship analyses indicate that possessing a head-neck-tail structure is vital for capsaicin-type ligands. In addition, the polarity of neck 1 (ie amide, ether, ester) appears crucial for capsaicin-type ligands. In the capsaicin binding to unphosphorylated TRPV1, the oxygen atom at the neck 2 position forms a hydrogen bond with a specific amino acid residue of TRPV1. Therefore, the functional group at the neck 2 position has been presumed more critical than that at the neck 1 position in the capsaicin binding to unphosphorylated TRPV1. However, the functional group at the neck 1 position seems to influence more than that at neck 2 in the interaction between the neck and phosphorylated TRPV1. Capsiate, a capsaicin analog in which the amide group of capsaicin is replaced with an ester, exhibits a considerably reduced ability to activate TRPV1 (Yang *et al.* 2015). Therefore, neck 1 of the amido bond in capsaicin has been supposed to function as an anchor for TRPV1. Despite the reduced ability of capsiate to activate TRPV, this compound behaved as a capsaicin-type ligand. There is a possibility that the functional group of neck 1 may have an unknown important role in the interaction of vanilloid compounds with TRPV1. Interestingly, 6-shogaol triggered TRPV1 activation like eugenol, which was diminished by FSK

treatment. In contrast, 10- shogaol-induced TRPV1 activation was not affected by the same treatment. In the case of capsaicin, it is hypothesized that the tail structure enhances the affinities of capsaicin analogs through their interaction with TRPV1 via VDW forces (Yang *et al.* 2015). Our results suggest that the extended aliphatic tail of 10-shogaol interacts with a site on TRPV1, a configuration that remains unaffected by the phosphorylation of TRPV1. Several hypotheses have been proposed to elucidate why FSK treatment or phosphorylation of TRPV1 could modify its responsiveness to capsaicin: (1) FSK may facilitate the formation of a functional TRPV1 multimer in the plasma membrane, thereby enhancing TRPV1's response to capsaicin; (2) phosphorylation could add an increased negative charge to certain TRPV1 amino acid residues, thus enhancing TRPV1's binding affinity for capsaicin; (3) FSK-induced phosphorylation might influence a downstream signal transduction process, independent of capsaicin binding and gate opening (Vetter *et al.* 2008 ; Studer *et al.* 2010 ; Yang *et al.* 2015). As these hypotheses are grounded in data obtained using capsaicin, they may not be necessarily applicable for explaining FSK's effects on TRPV1 activation induced by eugenol-type and 10- shogaol-type ligands. In addition, experiments using TRPV1 mutants indicate that amino acid substitutions at phosphorylation candidate sites, which are not adjacent to the capsaicin-binding pocket, abolish the effects of FSK treatment. It has been reported that TRPV1 alters its configuration in the gate-opening process after ligand binding to allow cationic ions to permeate (Kwon *et al.* 2021 ; Sun *et al.* 2022 ; Zhang *et al.* 2023). It is hypothesized that mutations distant from the binding pocket influence the configuration of the binding pocket or the structural alteration process leading to gate opening. Furthermore, the possibility that the indirect actions of vanilloid compounds in cells influence their differential interactions with phosphorylated TRPV1

cannot be ruled out. As information about the conformational changes associated with the phosphorylation of TRPV is not currently enough, it is anticipated that future studies will elucidate the manner and structure of ligand-binding phosphorylated TRPV1 to understand our findings.



Graphical abstract. Ligand-dependent activation of phosphorylated TRPV1.

Data availability

The datasets used and/or analyzed during the current study are available from the corresponding author upon reasonable request.

Author contribution

S.M., conceptualization, methodology, validation, formal analysis, investigation, data curation, writing—original, draft preparation, writing—review and editing, and funding; K.T.; methodology and writing—review and editing; S.H., conceptualization, methodology, validation, formal analysis, investigation, data curation, writing—original, draft preparation, writing—review and editing, and supervision; and S.K., investigation, writing—review & editing, resources, funding, and supervision.

Disclosure statement

No potential conflict of interest.

Funding

The following entities have provided support for this work: Japan Science and Technology Agency (JST), the establishment of university fellowships toward the creation of science technology innovation, Grant Number JPMJFS2125 (to S.M.); KAKENHI (Grant-in-Aid for Challenging Research (Pioneering) from Japan Society for the Promotion of Science (JSPS) Grant Number 18H05359 (20K20370), 22K18343 (to S.K.); and Adaptable and 534 Seamless Technology Transfer Program through Target-driven 535 R&D (A-STEP) from JST Grant Number JPMJTR194C; a project JPNP 536

23200460, commissioned by the New Energy and Industrial Technology Development Organization (NEDO) (to S.K.).

Acknowledgments

We thank Mr. Yoshihiro Sugihara and Dr. Norikazu Tamura for their suggestions on chemical compounds and Komi-Hakko Corporation's help with FLIPR.

5. References

- Abdel-Salam O, *et al.* Effect of capsaicin and resiniferatoxin on gastrointestinal blood flow in rats. *Eur. J. Pharmacol* 1996; **305** : 127-136.
- Bujak JK, *et al.* Inflammation, cancer and immunity-implication of TRPV1 channel. *Front Oncol* 2019; **9**: 1087.
- Caterina MJ, *et al.* The capsaicin receptor: a heat-activated ion channel in the pain pathway. *Nature* 1997; **389**: 816-824.
- Chen J, *et al.* Transient receptor potential (TRP) channels, promising potential diagnostic and therapeutic tools for cancer. *Biosci Trends*. 2014; **8**:1-10.
- Fujita K, *et al.* Induction of lipid droplets in non-macrophage cells as well as macrophages by liposomes and exosomes. *Biochem Biophys Res Commun* 2019 ; **510** : 184-190.
- Harb AA, *et al.* Eugenol Reduces LDL Cholesterol and Hepatic Steatosis in Hypercholesterolemic Rats by Modulating TRPV1 Receptor. *Sci Rep* 2019 ; **9** : 14003.
- Hinuma S, *et al.* Specific binding and endocytosis of liposomes to HEK293T cells via myrisoylated pre-S1 peptide bound to sodium taurocholate cotransporting polypeptide. *Vaccines (Basel)* 2022 ; **10** : 2050.
- Jeske NA, *et al.* A-kinase anchoring protein mediates TRPV1 thermal hyperalgesia through PKA phosphorylation of TRPV1. *Pain* 2008 ; **138** : 604-616.
- Jimenez RC, *et al.* The mutational landscape of human olfactory G protein-coupled receptors. *BMC Biology* 2021; **19** : 21.
- Kwon DH, *et al.* Heat-dependent opening of TRPV1 in the presence of capsaicin. *Nat Struct Mol Biol* 2021 ; **28** : 554-563.
- Lankford CK, *et al.* A comparison of the primary sensory neurons used in olfaction and vision. *Front Cell Neurosci* 2020 ; **14** : 595523.
- Li DS, *et al.* Role of calcitonin gene-related peptide in gastric hyperemic response to intragastric capsaicin. *Am. J. Physiol* 1991 ; **261** : G657-661.
- Li S, Jie Z. The capsaicin binding affinity of wildtype and mutant TRPV1 ion channels. *J Biol Chem* 2023 ; **299** : 105268.
- Lin W, *et al.* Olfactory neurons expressing transient receptor potential channel M5 (TRPM5) are involved in sensing semiochemicals. *Proc Natl Acad Sci U S A*. 2007; **104**: 2471-6.
- Malnic B, *et al.* Combinatorial receptor codes for odors. *Cell* 1999 ; **96** : 713-723.
- Melkes B, *et al.* β -arrestin 2 and ERK1/2 are important mediators engaged in close cooperation between TRPV1 and μ -opioid receptors in the plasma membrane. *Int J*

Mol Sci 2020; 21 :4626.

- Mohapatra DP, Nau C. Desensitization of capsaicin-activated currents in the vanilloid receptor TRPV1 is decreased by the cyclic AMP-dependent protein kinase pathway. *J Biol Chem* 2003 ; **278** : 50080-50090.
- Mombaerts P, *et al.* Visualizing an olfactory sensory map. *Cell* 1996 ; **87** : 675-686.
- Moriyama S, *et al.* Divergent effects of olfactory receptors on transient receptor potential vanilloid 1 activation by capsaicin and eugenol. *Biosci. Biotechnol. Biochem* 2024 ; zbae060.
- Moriyama T, *et al.* Sensitization of TRPV1 by EP1 and IP reveals peripheral nociceptive mechanism of prostaglandins. *Mol Pain* 2005; 1 :3-9.
- Nakamura T, Geoffrey HG. A cyclic nucleotide-gated conductance in olfactory receptor cilia. *Nature* 1987; **325**: 442-444.
- Nakashimo Y, *et al.* Expression of transient receptor potential channel vanilloid (TRPV) 1–4, melastatin (TRPM) 5 and 8, and ankyrin (TRPA1) in the normal and methimazole-treated mouse olfactory epithelium. *Acta Otolaryngol*. 2010; **130**:1278-86.
- Ohbuchi K, *et al.* Detailed Analysis of the Binding Mode of Vanilloids to Transient Receptor Potential Vanilloid Type I (TRPV1) by a Mutational and Computational Study. *PLoS One* 2016 ; **11** : e0162543.
- Persuy MA, *et al.* Mammalian olfactory receptors: molecular mechanisms of odorant detection, 3D-modeling, and structure-activity relationships. *Prog Mol Biol Transl Sci*. 2015; **130**: 1-36.
- Pronin A, Slepak V. Ectopically expressed olfactory receptors OR51E1 and OR51E2 suppress proliferation and promote cell death in a prostate cancer cell line. *J Biol Chem* 2021; 296 :100475.
- Pyrski M, *et al.* Trpm5 expression in the olfactory epithelium. *Mol Cell Neurosci*. 2017; **80**:75-88.
- Sakatani H, *et al.* The Roles of Transient Receptor Potential Vanilloid 1 and 4 in Olfactory Regeneration. *Lab Invest*. 2023; **103**:100051.
- Samanta A, *et al.* Transient receptor potential (TRP) channels. *Subcell Biochem* 2018 ; **87** : 141-165.
- Schuligoj R, *et al.* Gastric acid-evoked c-fos messenger RNA expression in rat brainstem is signaled by capsaicin-resistant vagal afferents. *Gastroenterology* 1998 ; **115** : 649-660.
- Sklar PB, *et al.* The odorant-sensitive adenylate cyclase of olfactory receptor cells. differential stimulation by distinct classes of odorants. *J Biol Chem*. 1986 ; **261** :

15538-15543.

- Schnizler K, *et al.* Protein kinase A anchoring via AKAP150 is essential for TRPV1 modulation by forskolin and prostaglandin E2 in mouse sensory neurons. *J Neurosci* 2008 ; **28** : 4904-4917.
- Studer M, McNaughton PA. Modulation of single-channel properties of TRPV1 by phosphorylation. *J Physiol* 2010 ; **588** : 3743-56.
- Rathee PK, *et al.* PKA/AKAP/VR-1 module: A common link of Gs-mediated signaling to thermal hyperalgesia. *J Neurosci* 2002 ; **22** : 4740-4745.
- Vetter I, *et al.* Rapid, opioid-sensitive mechanisms involved in transient receptor potential vanilloid 1 sensitization. *J Biol Chem.* 2008 ; **283** :19540-50.
- Vu S, *et al.* New capsaicin analogs as molecular rulers to define the permissive conformation of the mouse TRPV1 ligand-binding pocket. *eLife* 2020 ; **9** : e62039.
- Ward SM, *et al.* Distribution of the vanilloid receptor (VR1) in the gastrointestinal tract. *J Comp Neurol* 2003 ; **465** : 121-135.
- Yang B, *et al.* Activation of vanilloid receptor 1 (VR1) by eugenol. *J Dent Res* 2003 ; **82** : 781-785.
- Yang F, *et al.* Structural mechanism underlying capsaicin binding and activation of the TRPV1 ion channel. *Nat Chem Biol.* 2015 ; **11** : 518-524.
- Yang F, *et al.* The conformational wave in capsaicin activation of transient receptor potential vanilloid 1 ion channel. *Nat Commun.* 2018 ; **9** : 2879.
- Yelshanskaya MV, Sobolevsky AI. Ligand-binding sites in vanilloid-subtype TRP channels. *Front Pharmacol* 2022 ; **13** : 900623.
- Zhang M, *et al.* TRP (transient receptor potential) ion channel family: structures, biological functions and therapeutic interventions for diseases. *Signal Transduct Target Ther.* 2023; **8**: 261.

Chapter IV Suppressive Effect of TRPV1 on ORs signal transduction

1. Introduction

Olfactory receptors (ORs), members of the G protein-coupled receptor (GPCR) family, play a pivotal role in the initial detection of odorant molecules. Approximately 400 functional ORs are coded in the human genome. ORs are primarily expressed on the cilia of olfactory sensory neurons (OSNs) of the olfactory epithelium in the nasal cavity (Persaud and Dodd, 1982; Buck and Axel, 1991; Jimenez *et al.*, 2021). In the first step of odor perception, odorant molecules bind ORs, which causes conformational changes in ORs, leading to signal transduction in OSNs. Various combinatorial signal patterns arise from ORs stimulated by differential sets of odorants. Olfaction is generated by transmitting this information to the brain (Malnic *et al.*, 1999). Upon odorant binding, ORs activate the olfactory-specific G protein, $\text{G}_{\alpha\text{olf}}$, which subsequently stimulates adenylate cyclase, leading to the production of cAMP (Lowe, Nakamura and Gold, 1989; Pace *et al.*, 1985; Mainland *et al.*, 2014; Pronin *et al.*, 2021). Elevated intracellular cAMP triggers the opening of cyclic nucleotide-gated ion channels, permitting Na^+ and Ca^{2+} influx, which leads to the depolarization of OSN (Nakamura and Gold 1987; Mombaerts *et al.*, 2004).

When expressing ORs in heterologous cells, their cell surface and functional expressions are frequently insufficient. (Saito *et al.*, 2004). To overcome this issue, various strategies have been developed to enhance cell surface and functional OR expression. The N-terminal modification of ORs by adding N-terminal tags such as Rho tag (a non-cleavable signal sequence derived from rhodopsin) and Lucy tag (a cleavable signal peptide derived from LRRC32) is an effective approach to promote the surface

expression of ORs (Krautwurst *et al.*, 1998; Shepard *et al.*, 2013). We have previously reported that OR51E1 modified with Lucy-Rho at the N-terminus is functionally expressed in HEK293T cells (Moriyama *et al.*, 2024a).

Gene expressions of transient receptor potential (TRP) channels, including TRPV1, have been identified in OSNs (Nakashimo *et al.*, 2010; Sakatani *et al.*, 2023; Lin *et al.*, 2007). These channels may contribute to olfactory perception, particularly in response to spice-derived compounds (Yang *et al.*, 2003 ; Caterina *et al.*, 1997 ; McNamara *et al.*, 2005). TRPV1, originally identified as the capsaicin receptor, is a nonselective cation channel implicated in nociception, mucosal protection, and wound healing (Ward *et al.*, 2003; Abdel-Salam *et al.*, 1996; Schuligoi *et al.*, 1998). TRPV1 is an ion channel consisting of a homotetramer that permits Na^+ and Ca^{2+} influx in response to vanilloid compounds, noxious heat ($>43^\circ\text{C}$), and acidic conditions (Hardie and Minke 1993; Kwon *et al.*, 2012; Yelshanskaya and Sobolevsky, 2022).

ORs and TRPV1 have been detected in OSNs (Verbeurg *et al.*, 2014; Nakashimo *et al.*, 2010; Sakatani *et al.*, 2023; Lin *et al.*, 2007). However, the stage of differentiation in OSNs at which TRPV1 is expressed remains a subject of debate (Sakatani *et al.*, 2023; Pyrski *et al.*, 2017). On the other hand, OR51E1 and OR51E2 are found not only in OSNs but also in prostatic cells, alongside various TRP channels such as TRPV1, TRPV2, TRPV6, TRPM8, TRPM2, and TRPC6 (Pronin *et al.*, 2021; Chen *et al.*, 2014). In the LNCaP prostate cancer cell line, stimulation of OR51E1 and OR51E2 with their ligands, short- to medium-chain fatty acids (C3–C9), led to inhibited cell proliferation (Maßberg *et al.*, 2016; Pronin *et al.*, 2021). This suggests a potential co-expression of ORs and TRP channels, including TRPV1, in specific cellular environments. However, the nature of

interactions between ORs and TRP channels, particularly TRPV1, remains largely unexamined.

Various studies on the interaction between TRPV1 and GPCRs, except for ORs, have been reported. For instance, activation of the prostaglandin E2 receptors (EP3C and EP4), which couple to G_αs, induces cAMP production and protein kinase A (PKA) activation, leading to TRPV1 phosphorylation and subsequent desensitization or sensitization in nociceptive pathways (Moriyama *et al.*, 2005). GPCRs coupling to G_αq/11, and G_αi/o, have also been reported to modulate TRPV1 activation via phosphorylation-dependent mechanisms (Salzer *et al.*, 2019). Although numerous studies have investigated the modulatory effects of GPCRs on TRPV1, the influence of TRPV1 on the activation of GPCRs, including ORs, remains largely unknown.

Based on DNA sequences, ORs are classified as I and II. Class I ORs are predominantly found in aquatic animals, such as fish, and are supposed to respond primarily to water-soluble odorant molecules. Class II ORs are more common in terrestrial animals and are presumed to be activated by relatively hydrophobic molecules. OR51E1 belongs to Class I ORs. As mentioned earlier, expressing functional ORs in heterologous cells is frequently challenging. Among human ORs, OR51E1 is a well-characterized receptor regarding its signal transduction pathway and cell surface expression (Maßberg *et al.*, 2016; Pronin *et al.*, 2021). Thus, OR51E1 was chosen to investigate the influence of TRPV1 in this study as well as in our previous study (Moriyama *et al.*, 2024a).

In the previous studies, we demonstrated that ORs, including OR51E1, could regulate ligand-stimulated TRPV1 activation. Interestingly, the regulatory role of OR51E1 on TRPV1 activation diverged depending on the ligands used for stimulating TRPV1. When OR51E1 and TRPV1 were co-expressed in HEK293T cells, TRPV1 activation

(intracellular Ca^{2+} influx) by capsaicin was enhanced by OR51E1 co-expression. This enhancement was strengthened by the stimulation of OR with a ligand. In contrast, TRPV1 activation by eugenol was suppressed by OR51E1 co-expression and its stimulation with a ligand (Moriyama *et al.*, 2024a). We have demonstrated the following mechanism for the modulatory effects of OR51E1 on TRPV1 activation. Ligand-stimulated OR51E1 increases intracellular cAMP concentration, leading to the activation of protein kinase A (PKA), which subsequently phosphorylates TRPV1. Phosphorylated TRPV1 exhibits differential susceptibility to vanilloid compounds in its activation. Based on the differential susceptibility of phosphorylated TRPV1 to ligands, we found that vanilloid compounds are classified into three types: capsaicin type (enhancement), 10-shogaol type (no change), and eugenol type (suppression) (Moriyama *et al.*, 2024b). Although we have shown the effects of ORs on TRPV1 activation, it remains unclear whether TRPV1 has a regulatory role in OR activation. In this study, we investigated whether and how TRPV1 influences OR51E1 response to a ligand.

2. Materials and methods

2.1. Cell culture

HEK293T was obtained from RIKEN BRC (Tsukuba, Ibaraki, Japan). These cells were cultured in RPMI 1640 medium supplemented with 10% heat-inactivated fetal bovine serum and antibiotics (Fujita *et al.*, 2019).

2.2. Plasmids

Expression plasmids encoding TRPV1, OR51E1 (fused with Lucy-Rho at the N-terminus), green fluorescent protein (GFP), pGloSensor 22, and the empty vector were prepared as previously described by Moriyama *et al.*, 2024a.

2.3. Reagents

Capsaicin (catalog number: 034-11351 from Fujifilm Wako Pure Chemical Corp., Osaka, Japan), A23187 (catalog number: C7522-1MG from Sigma-Aldrich, St. Louis, MO, USA), CCG21022 (catalog number: S6621-1MG from Selleck Chemicals, Houston, TX, USA), Staurosporine (catalog number: S1421-2MG from Selleck Chemicals), and H-89 (catalog number: CAY-10010556-5 from Cayman Chemical, Ann Arbor, MI, USA) were dissolved in ethanol and diluted with Hanks' balanced salts solution (+) (HBSS(+); catalog number: 084-08965 from Fujifilm Wako Pure Chemical Co.) or Hanks' balanced salt solution (-) (HBSS(-); catalog number: 085-09355 from Fujifilm Wako Pure Chemical Corp.). Ethylenediaminetetraacetic acid (EDTA; catalog number: 15105-35 from Nacalaitesque, Kyoto, Japan) was dissolved in water and then diluted with HBSS (-). 3-isobutyl-1-methylxanthine (IBMX; catalog number: I5879 from Sigma-Aldrich, St. Louis, MO, USA) was initially dissolved in dimethyl sulfoxide (catalog number: 046-

21981 from Fujifilm Wako Pure Chemical Corp.) before being added to HBSS. Isovaleric acid (catalog number: M0182 from TCI chemicals, Tokyo, Japan) was first dissolved in Opti-MEM (catalog number: 31985062 from Thermo Fisher Scientific, Waltham, MA, USA) and then further diluted with HBSS containing IBMX.

2.4. Detection of cAMP production

Intracellular cAMP levels were measured as described previously (Moriyama *et al.*, 2024a). HEK293T cells were cultured in a 96-well white plate (catalog number: 236105 from Thermo Fisher Scientific) pre-coated with poly-L-lysine (catalog number: VBH-SPL01 from Cosmo Bio, Tokyo, Japan). The cells were seeded at a density of 4×10^5 cells/mL in 50 μ L of culture medium per well and cultured at 37°C in a humidified atmosphere containing 5% CO₂ for 24 h. Transfection of plasmids was performed using PolyMagNeoTM (catalog number: PG60100 from OZbioscience, Marseille, France) with a total of 300 ng of DNA per well, including GloSensor 22F, GFP, empty vector, and OR51E1 expression plasmids, in serum-free Opti-MEM. Then, 100 μ L of fresh culture medium was added to each well, and the cells were cultured for 24 h. The fluorescence intensity (FI) of GFP was measured using a Synergy 2 plate reader (BioTek, Winooski, VT, USA). Subsequently, the culture medium was replaced with 75 μ L of HBSS containing 2% GloSensor cAMP reagent (catalog number: E1290 from Promega, Madison, WI, USA), and the cells were incubated at room temperature for 2 h. Thereafter, 25 μ L of HBSS containing both ligands and IBMX (final concentration: 0.5 mM) were added to each well. Luminescence changes were recorded immediately at 2-min intervals for a total duration of 20 min. The inhibitors were added 15 min before the assay, while A23187 was co-administered at the time of the ligand stimulation.

Afterward, the assay was performed using a Synergy 2 plate reader. Normalized relative luminescence units (RLU) were calculated using the following procedure: (1) FI of GFP for each well was determined as the difference between FI in wells transfected with GFP expression plasmid and those without its transfection. (2) A normalization coefficient (Co) was calculated to account for transfection efficiency, using the formula: (FI of GFP in wells transfected with the receptor expression plasmid) / (FI of GFP in wells transfected with the empty vector). (3) RLU was determined as follows: (maximal luminescence in wells transfected with the receptor expression plasmid after HBSS addition, with or without a ligand) / (maximal luminescence in wells transfected with the empty vector after HBSS addition without a ligand). (4) Finally, normalized RLU was obtained using the formula: RLU / Co. All assays were performed in triplicate, and data were expressed as mean ($n = 3$) \pm standard deviation (SD).

2.5. Treatment with siRNA

Silencer® Select siRNA (catalog number: 31985062) and TRPV1 siRNA (catalog number: 4392420) were purchased from Thermo Fisher Scientific. HEK293T cells were seeded at a density of 4×10^4 cells/mL in 50 μ L of RPMI 1640 per well in a 96-well white-bottom plate coated with poly-L-lysine. Transfection was performed using PolyMagNeo™. A mixture containing siRNA (1 pmol), 50 ng of GloSensor 22F, 100 ng of GFP, and 50 ng of OR51E1 expression plasmids was prepared in 50 μ L of Opti-MEM. This mixture was added to each well, followed by magnetic treatment at room temperature for 30 minutes. The transfected cells were then cultured for 48 h. Treatment with a ligand, measurements of fluorescence and luminescence, and data processing were conducted in the same manner outlined in the preceding section.

2.6. Reverse-transcription quantitative polymerase chain reaction (RT-qPCR)

To investigate the effect of siRNA treatment on TRPV1 expression levels in HEK293T cells, we conducted RT-qPCR following the method previously described by Fujita *et al.*, 2019. HEK293T cells (4×10^4 cells/mL) were plated in 500 μ L per well in a 24-well tissue culture microplate (catalog number: 3526, Corning Japan, Tokyo, Japan) and cultured at 37°C with 5% CO₂ for 24 h. The siRNA transfection process involved adding a mixture of siRNA (1 pmol) and 0.5 μ L PolyMagNeo in Opti-MEM (50 μ L) to each well, followed by a 30-minute magnetic treatment at room temperature. Subsequently, 1.5 mL of fresh medium was added to each well, and the cells were cultured for an additional 48 h. Total RNA was extracted from treated HEK293T cells using a NucleoSpin® RNA kit and quantified with a DS-11 spectrophotometer (DeNovix). To determine mRNA expression levels of TRPV1 and glyceraldehyde-3-phosphate dehydrogenase (GAPDH), reverse transcription was performed using 1.2 μ g of total RNA as a template, along with PrimeScript™ RT Master Mix (TaKaRa). Reverse-transcribed RNA (6.4 ng) was amplified with oligonucleotides specific for TRPV1 () and GAPDH (5'-GAGACCCTGGTGGACATC-3' and 5'-TTCTTGGTCTGCATTC-3') under the following conditions: initial denaturation at 95 °C for 30 seconds, followed by 45 cycles at 95 °C for 10 seconds and 60 °C for 1 minute. The amplification process utilized TB Green® Premix EX Taq™ II (TaKaRa) on the MyGo Pro Real-Time PCR system (IT-IS Life Science).

The suppressive effects of siRNAs were assessed by comparing the relative mRNA expression levels. Expression levels from cells treated with negative control siRNA (control) were set to 100%, while expression levels following treatment with TRPV1

siRNAs were presented as relative values. All samples were tested in triplicate. TRPV1 mRNA expression levels were normalized to GAPDH expression levels. Relative mRNA expression levels were expressed as means \pm standard errors (vertical bars). Statistical significance was analyzed using t-test, with * indicating $p < 0.05$ and ** indicating $p < 0.01$.

2.7. Detection of intracellular Ca^{2+} influx

We measured Ca^{2+} influx as described previously (Moriyama *et al.*, 2004ab). Briefly, HEK293T cells were cultured in a 96-well black/clear bottom Plate (catalog number: 165305 from Thermo Fisher Scientific) coated with poly-L-lysine. We then seeded cells at a density of 4×10^5 cells/mL in 50 μL /well of culture medium. After these cells were cultured for 24 h, we transfected the cells with plasmids (300 ng/well in total) using PolyMagNeo. The transfected cells were cultured for an additional 24 h. After removing the culture medium, we incubated the cells in HBSS (+) (50 μL /well) containing a dye loading buffer supplied with a Calcium 6 Assay Explorer Kit (catalog number: OZB-PG60200-200-200 from OZ Biosciences, Marseille, France). The cells were incubated for 2 h at 37°C. Subsequently, we added HBSS (+) (50 μL /well) without a ligand and then measured changes in FI (%) every second for 3 min using a FLIPR tetra (Molecular Devices; San Jose, CA, USA).

3. Results

Suppressive effect of TRPV1 on cAMP production induced by ligand-stimulated OR51E1 We investigated whether TRPV1 alters OR51E1 response to isovaleric acid using HEK293T cells co-expressing OR51E1 and TRPV1. OR51E1 was modified with a Lucy-Rho tag to improve its cell surface expression (Krautwurst *et al.*, 1998; Shepard *et al.*, 2013). In the previous study, we confirmed that OR51E1 co-expression with TRPV1 in HEK293T cells does not significantly affect the expression levels of either protein (Moriyama *et al.*, 2024a). Figure 1 (the left graph) shows that adding a ligand (ivaleric acid) did not induce significant cAMP production in cells transfected with empty vector plasmid. In contrast, the addition of isovaleric acid markedly induced cAMP production in cells expressing OR51E1 (Figure 1, the stripped bar in the middle graph). The cAMP production induced by ligand-stimulated OR51E1, which were not co-transfected with TRPV1 expression plasmid, was suppressed dose-dependently to 77.3 and 48.9% by 0.04 and 0.2 μ M capsaicin, respectively (Figure 1, the filled bars in the middle graph). These results suggest that this suppressive effect of capsaicin is mediated via an endogenous capsaicin receptor TRPV1. On the other hand, the co-expression of TRPV1 significantly suppressed the cAMP production of cells expressing OR51E1 to isovaleric acid (Figure 1, the right graph). Notably, cAMP production induced by ligand-stimulated OR51E1 in the absence of capsaicin was reduced to 66.6% by the transfection of TRPV1 expression plasmid (Figure 1, the stripped bars in the middle and right graphs). These results indicated that TRPV1 expression alone could affect the activation of OR51E1. Furthermore, when capsaicin was simultaneously applied with isovaleric acid, OR51E1-mediated cAMP production was more profoundly suppressed dose-dependently by capsaicin in HEK293T cells co-expressing OR51E1 and TRPV1 (Figure 2, the filled bars

in the right graph). These results suggest that TRPV1 activation suppresses the cAMP production mediated by ligand-stimulated OR51E1 in HEK293T cells.

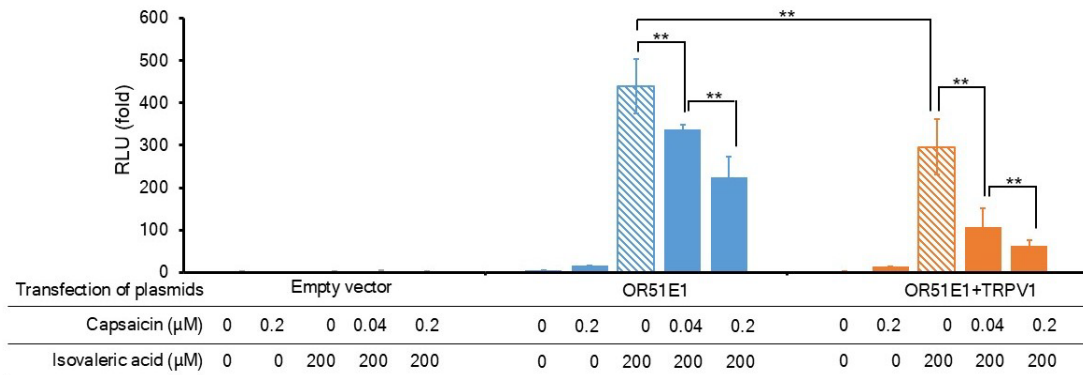


Figure 1. Suppressive effects of TRPV1 co-expression and capsaicin on cAMP production induced by ligand-stimulated OR51E1. HEK293T cells, cultured in a 96-well microplate, were transfected with plasmid combinations that included 50 ng of GloSensor 22F expression plasmid, 100 ng of GFP expression plasmid, and additional plasmids, totaling 300 ng per well. The additional plasmids: (the left bar graph) 150 ng of empty vector plasmid; (the middle bar graph) 100 ng of OR51E1 expression plasmid combined with 50 ng of empty vector plasmid; (the light bar graph) 100 ng of OR51E1 expression plasmid, 25 ng of TRPV1 plasmid, and 25 ng of empty vector plasmid. Ligands (i.e., capsaicin for TRPV1 and isovaleric acid for OR51E1) with IBMX in HBSS were applied at the doses as indicated in the table under the bar graphs. After ligand addition, luminescence was measured every 2 minutes for 20 minutes, and the maximum value was used to calculate the RLU. Assays were performed in triplicate, and data (normalized RLU) are presented as the mean values ($n = 3$) \pm SD (error bars). Statistical analysis was performed using the Tukey test. *: $p < 0.05$; **: $p < 0.01$.

Offsetting capsaicin-induced suppression of OR51E1 response to isovaleric acid in HEK293T cells by TRPV1 siRNA As shown in Figure 1 (the middle graph), capsaicin suppressed cAMP elevation in HEK293T cells expressing OR51E1 despite the absence of transfecting TRPV1 expression plasmid. There is a possibility that the endogenous TRPV1 mediates this suppression because TRPV1 is known to be expressed in various tissues and cells (Retrieved from <https://www.proteinatlas.org/ENSG00000196689-TRPV1/cell+line>; Jin *et al.*, 2023.). We examined this presumption using siRNA for

TRPV1. We transfected the OR51E1 expression plasmid in HEK293T cells with or without siRNA treatment, and these cells were stimulated with isovaleric acid, both individually and in combination with capsaicin (Figure 2). When the cAMP production of HEK293T cells expressing OR51E1 stimulated with isovaleric acid alone was set as 100% (Figure 2 (a), the stripped bar), stimulation with the combination of capsaicin at the dose of 0.2 μ M and isovaleric acid decreased the response to 48.0% without siRNA treatment (Figure 2 (a), the filled bar). A similar level of reduction in the response to isovaleric acid (55.3%) was observed in OR51E1-expressing cells treated with negative control siRNA (Figure 2 (b), the filled bar). In contrast, by treatment with siRNA for TRPV1, the suppressive effect of capsaicin was almost completely abolished (Figure 2 (c), the filled bar). At the capsaicin dose of 5 μ M, nearly identical outcomes were observed, although its suppressive effects were slightly more pronounced than those seen with 0.2 μ M, as shown in Figure 2 (d), (e), and (f). The suppressive effects of capsaicin between doses of 0.2 and 5 μ M appeared largely similar. It may be because the effective dose reaches a plateau at approximately 0.2 μ M. These results suggest that the suppression of ligand-stimulated OR51E1 activation by capsaicin in OR51E1-expressing HEK293T cells, which were not transfected with TRPV1 expression plasmid, is attributable to the endogenous TRPV1.

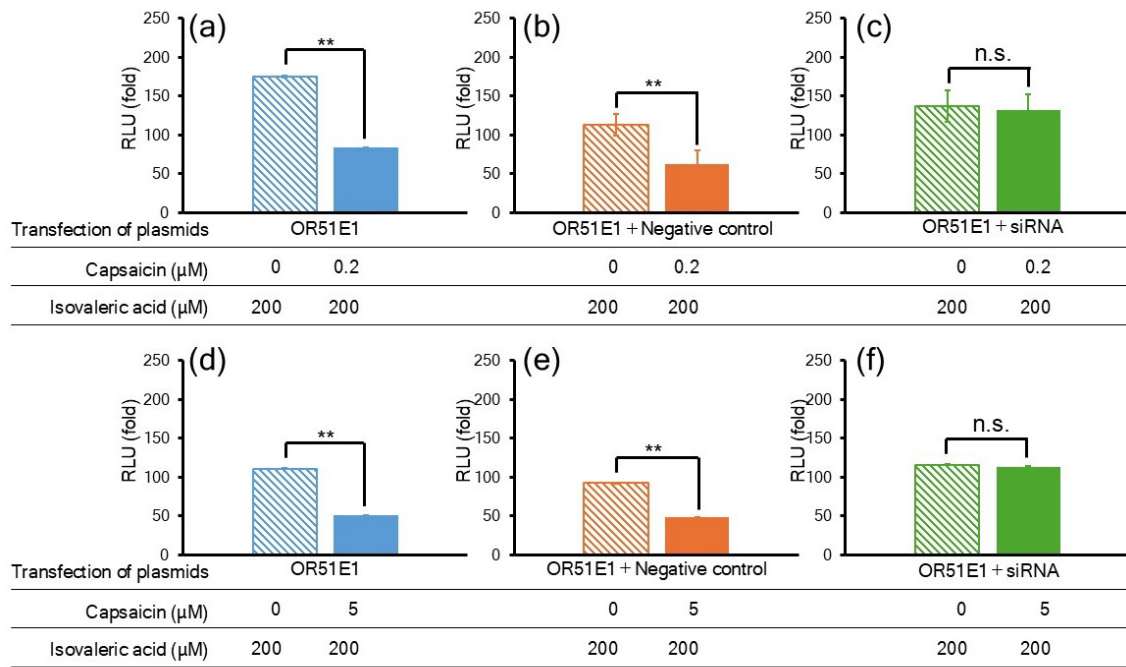


Figure 2. Offsetting suppressive effect of capsaicin on ligand-stimulated OR signal transduction in HEK293T cells by siRNA for TRPV1. HEK293T cells, cultured in a 96-well microplate, were transfected with plasmid combinations that included 50 ng of GloSensor 22F expression plasmid, 100 ng of GFP expression plasmid, 50 ng of OR51E1, and siRNA (1 pmol). Treatment with siRNAs. (a) and (d): none; (b) and (e): negative control siRNA; (c) and (f): siRNA for TRPV1. Panels (a)–(c) represent the results of treatment with 0.2 μM capsaicin, while panels (d)–(f) represent those with 5 μM capsaicin. Ligands (i.e., capsaicin for TRPV1 and isovaleric acid for OR51E1) with IBMX in HBSS were applied at the doses indicated in the table under the bar graphs. Data acquisition was carried out as described in Figure 1. Statistical analysis was performed using Student's t-test. *: $p < 0.05$; **: $p < 0.01$.

Role of Ca^{2+} influx in TRPV1-induced suppression of OR51E1 activation The results obtained from Figures 1 and 2 suggested that the activation of TRPV1 influences the cAMP signaling of ligand-stimulated OR51E1. Therefore, we investigated whether Ca^{2+} influx from extracellular fluid is involved in the suppression of OR51E1 activation by TRPV1 stimulated with capsaicin. HEK293T cells were co-transfected with OR51E1 and TRPV1 expression plasmids and then stimulated with ligands in either HBSS (+), containing Ca^{2+} , or HBSS (-), which lacked Ca^{2+} and included the Ca^{2+} chelator EDTA. When cAMP production in HEK293T cells expressing OR51E1 in response to isovaleric

acid in HBSS (+) was set at 100% (Figure 3 (a), the stripped bar in the middle graph), co-stimulation with isovaleric acid and capsaicin reduced the response to 58.1% (Figure 3 (a), the filled bar in the middle graph). In HEK293T cells co-expressed OR51E1 with TRPV1, the cAMP production decreased to 14.5% without capsaicin stimulation (Figure 3 (a), the stripped bar in the right graph). Furthermore, this reduction was strengthened by the addition of capsaicin. When cAMP production in HEK293T cells co-expressing OR51E1 and TRPV1 in response to isovaleric acid in HBSS (-) was set at 100% (Figure 3 (a), the stripped bar in the right graph), co-stimulation of these cells with isovaleric acid and capsaicin in HBSS (+) reduced the cAMP production to 51.7% (Figure 3 (a), the filled bar in the right graph). These results were principally consistent with those in Figure 1.

HEK293T cells expressing OR51E1 exhibited almost the same level of cAMP production in response to isovaleric acid in both HBSS (+) and HBSS (-) (Figure 3 (a), the stripped bar in the middle graph and Figure 3 (b), the stripped bar in the middle graph). However, a significant decrease in cAMP production was not observed in HEK293T cells expressing OR51E1 stimulated with capsaicin in HBSS (-) (Figure 3 (b), the filled bar in the middle graph), suggesting that the suppression of cAMP production depending on endogenous TRPV1 was abolished in HBSS (-). Additionally, the reduction of cAMP production by co-expression of TRPV1 with OR51E1 was retained within 73.8% in HBSS (-) (Figure 3 (b), the stripped bar in the right graph), which did not show a significant decrease by treatment with capsaicin (the filled bar in the right graph). These results indicated that the TRPV1-induced suppression of OR51E1-mediated cAMP production is primarily due to the Ca^{2+} influx through TRPV1 from extracellular Ca^{2+} .

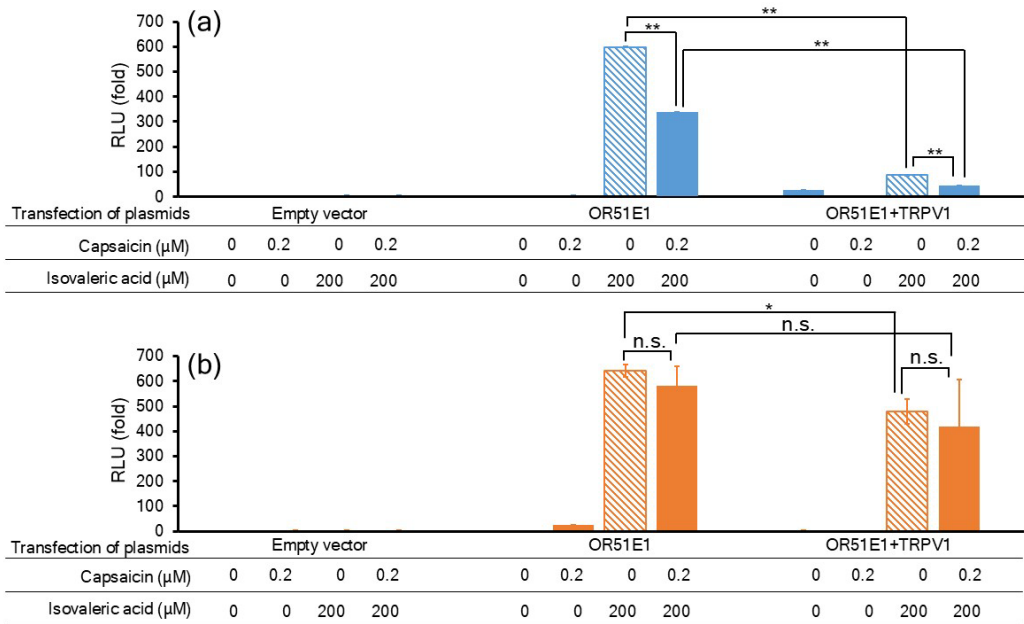


Figure 3. Offsetting suppressive effects of TRPV1 and capsaicin on OR51E1 activation by extracellular Ca²⁺ depletion. Transfection of plasmids into HEK293T cells was performed as described in Figure 1. Capsaicin and isovaleric acid administrations at the doses indicated in the table under the bar graphs were carried out using HBSS (+), which contained 140 mg/L of Ca²⁺ (a), or HBSS (-), which contained 5 mM EDTA to ensure Ca²⁺ depletion without supplementing Ca²⁺ (b). Data acquisition and statistical analysis were performed as described in Figure 3.

Suppression of OR51E1-mediated cAMP production was observed upon co-expression of TRPV1, even without capsaicin stimulation (Figures 1 and 3). Our previous reports indicate that transfection with OR expression plasmids leads to a noticeable but moderate increase in cAMP levels in HEK293T cells (Moriyama *et al.*, 2024a). In the present study, we investigated whether a significant Ca²⁺ influx was induced in HEK293T cells by TRPV1 expression plasmid transfection alone without capsaicin stimulation. As shown in Figure 4, a small but significant increase in Ca²⁺ influx was detected in HEK293T cells (Figure 4, the black bar) without capsaicin treatment by the transfection of TRPV1 expression plasmid compared to the control group (Figure 4, the gray bar). These results suggest that under the conditions employed here, even without capsaicin stimulation, transfection of TRPV1 expression plasmid can induce a slight Ca²⁺ influx in HEK293T

cells.

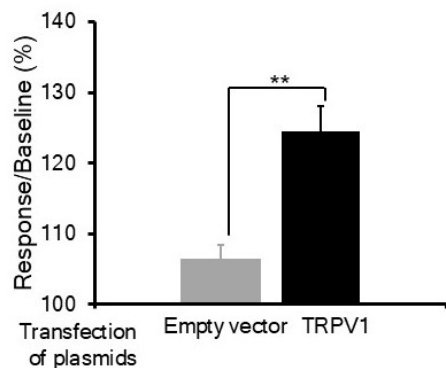


Figure 4. Increase of intracellular Ca^{2+} in HEK293T cells transfected with TRPV1 expression plasmid without capsaicin. HEK293T cells, cultured in a 96-well plate, were transfected with 300 ng per well of the empty vector plasmid alone, and co-transfection with 30 ng per well of the empty vector plasmid and 270 ng per well of the TRPV1 expression plasmid. After the transfection, the cells were cultured for 24 h. In the presence of Calcium 6, Ca^{2+} influx in the cells was monitored by detecting changes in FI every second for 3 min using a FLIPR. Immediately after adding HBSS (+) in the absence of capsaicin, FI in each well was measured. Data were presented as mean values of maximal FI increases ($n = 3$) with SD (vertical bars). Statistical analysis was performed using Student's t-test. **: $p < 0.01$.

Furthermore, to confirm that the suppressive effect of TRPV1 on OR51E1 activation is mediated by intracellular Ca^{2+} elevation, we examined whether a calcium ionophore, A23187, can be replaced with TRPV1. A23187 is a compound that can cross the lipid bilayer of the cell membrane and selectively induce the influx of Ca^{2+} from the extracellular fluid Ca^{2+} into cells. HEK293T cells expressing OR51E1 were treated with isovaleric acid and simultaneously with A23187. The suppression of the cAMP production induced by ligand-stimulated OR51E1 was detected dose-dependently after adding A23187 (Figure 5). A23187 exhibited a suppressive effect (decrease to 71.0% in cAMP production) on OR activation at the dose of 1 - 2 μM , which is comparable to the effect of capsaicin at the dose of 0.2 μM , i.e., suppression to 73.1% in cAMP production (Figure 5). The results of Figures 3, 4, and 5 demonstrated that Ca^{2+} influx via TRPV1 causes the suppression of cAMP production induced by ligand-stimulated OR51E1.

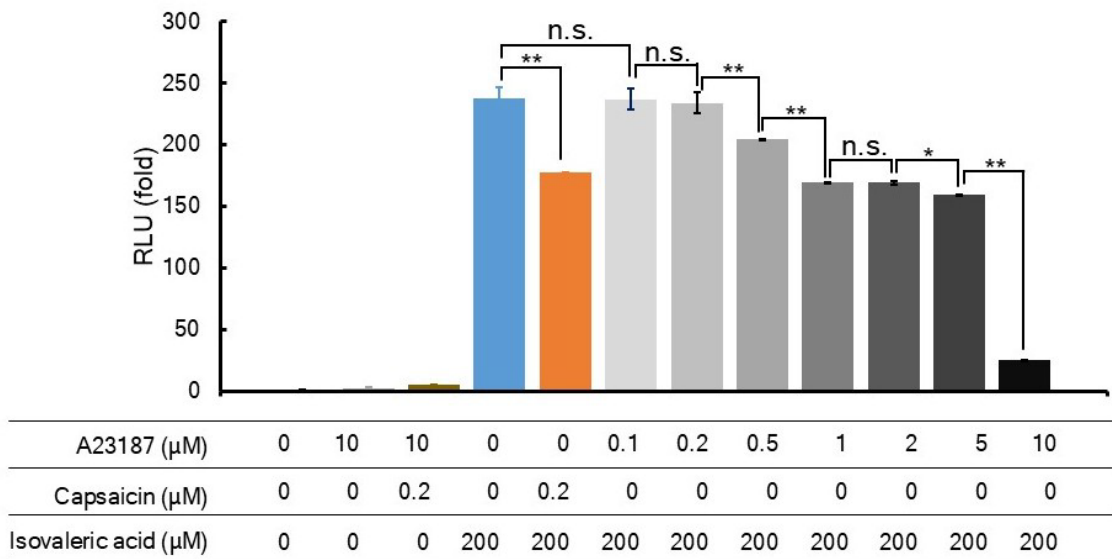


Figure 5. Suppressive effect of A23187 on cAMP production induced by ligand-stimulated OR51E1. Transfection of plasmids into HEK293T cells was performed as described in Figure 1. The calcium ionophore (A23187) was applied simultaneously with ligand administrations (capsaicin and isovaleric acid) at the concentrations indicated in the table under the bar graph. Data were obtained as described in Figure 1. Statistical analysis was performed using the Tukey test. *: $p < 0.05$; **: $p < 0.01$.

Inhibition of A13287-induced suppression of OR51E1 activation by a G protein-coupled receptor kinase (GRK) inhibitor In the regulatory mechanism of GPCR activation, the desensitization process occurs following ligand-induced activation. In desensitization, phosphorylation of intracellular domains in GPCRs plays a key role (Benovic *et al.*, 1986). GPCRs are phosphorylated by GRKs, promoting β -arrestin binding, which inhibits G protein interaction with GPCRs and suppresses the signaling of activated GPCRs. We hence investigated whether Ca^{2+} influx influences this process in cAMP production mediated by ligand-stimulated OR51E1. We used various phosphorylation inhibitors, i.e., GRK, PKA, and protein kinase C (PKC) inhibitors, to examine their effects on the A23187-induced suppression of OR51E1 activation. The concentrations of a GRK inhibitor (CCG215022), PKA inhibitor (H-89), and PKC

inhibitor (Staurosporine) were selected based on prior studies demonstrating their efficacy (Homan *et al.*, 2015; Chijiwa *et al.*, 1990; Yao *et al.*, 2005). As shown in Figure 6 (a), CCG21052, H-89, and Staurosporine did not induce cAMP production in HEK293T cells. Additionally, when OR51E1-expressing cells were treated with isovaleric acid and each inhibitor, no inhibitory effect was observed on the cAMP production induced by ligand-stimulated OR51E1. Adding A23187 reduced the cAMP production of ligand-stimulated OR51E1 (Figure 6 panels (b) – (d)). The GRK inhibitor CCG215022 blocked the suppressive effect of A23187 on OR activation (Figure 6 (b)). Notably, as the concentration of CCG215022 increased, the degree of its inhibition was more pronounced. In the absence of the GRK inhibitor, the suppression was 58.8% (Figure 6 (b), the orange bar), which was recovered to 78.5 and 92.8% by this inhibitor at the dose of 2.5 and 5 μ M (Figure 6 (b), the gray and black bars), respectively. On the other hand, H-89 (Figure 6(c)) and Staurosporine (Figure 6(d)) did not block the suppression of OR activation by A23187. These results suggest that GRK is at least partially involved in the A23187 (i.e., Ca^{2+} influx)-induced suppression of cAMP increase induced via ligand-stimulated OR51E1.

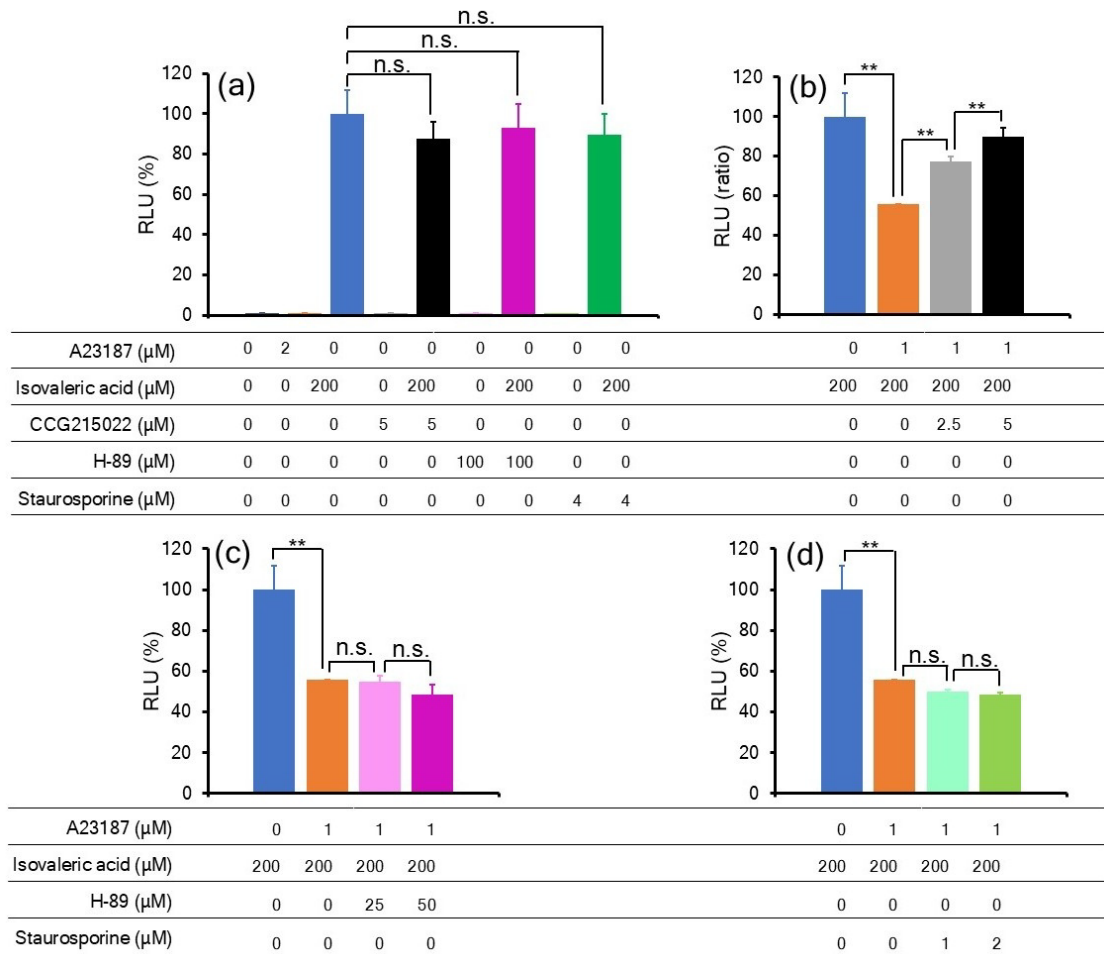


Figure 6. Effects of GRK, PKA, and PKC inhibitors on A23187-induced suppression of activated OR51E1-mediated cAMP production. HEK293T cells, cultured in a 96-well microplate, were transfected with plasmid combinations that included 50 ng of GloSensor 22F expression plasmid, 100 ng of GFP expression plasmid, 100 ng of OR51E1 expression plasmid, and 50 ng of empty vector plasmid. A23187 was applied simultaneously with isovaleric acid to HEK293T cells at the indicated doses in the table under the bar graphs in the figure. CCG215022, H-89, and Staurosporine were administered at the concentrations indicated in the tables under the bar graphs, 15 min before applying isovaleric acid and A23187. Data were obtained as described in Figure 1. Statistical analysis was performed using the Dunnett test for (a) and Tukey test for (b – d). *: $p < 0.05$; **: $p < 0.01$.

4. Discussion

In this study, we demonstrated that the activation of TRPV1 or stimulation with a calcium ionophore, both of which promote Ca^{2+} influx into HEK293T cells and suppress cAMP production via ligand-stimulated OR51E1 in HEK293T cells. Furthermore, our results suggest that Ca^{2+} influx results in GRK activation, facilitating the desensitization of activated OR51E1. We have previously reported that ORs, including OR51E1, can modulate TRPV1 activation (i.e., inducing Ca^{2+} influx) (Moriyama *et al.*, 2024ab). The effects of ORs on TRPV1 activation vary depending on TRPV1 ligands. We have demonstrated that the modulatory mechanism of ORs to TRPV1 is as follows: cAMP elevation is induced by OR activation, which subsequently activates PKA and promotes phosphorylation of TRPV1, altering TRPV1 responsiveness to TRPV1 ligands. This study demonstrated that TRPV1 and OR51E1 mutually regulate each other's activation.

Regarding the interaction between GPCRs and TRPV1, previous studies have investigated how GPCRs regulate TRPV1 function, especially in pain sensitivity regulation (Yao *et al.*, 2005). Considering the present findings on the mutual regulation between OR51E1 and TRPV1, TRPV1 may also play a role in the regulation of other GPCRs. Moreover, Ca^{2+} influx signaling appears to occur more rapidly than the cAMP production process. In our assays detecting cAMP production, maximal cAMP productions were detected around 10 min after stimulation of OR51E1 with isovaleric acid, whereas Ca influx mediated by TRPV1 was usually detected within 1 min. Considering these results, when TRPV1 and OR are activated by their respective ligands simultaneously, TRPV1 may rapidly diminish OR's signal transduction. Consequently, TRPV1's effect may dominate over that of OR in the interaction between these two receptors. Our findings in the present study were obtained through an artificial system

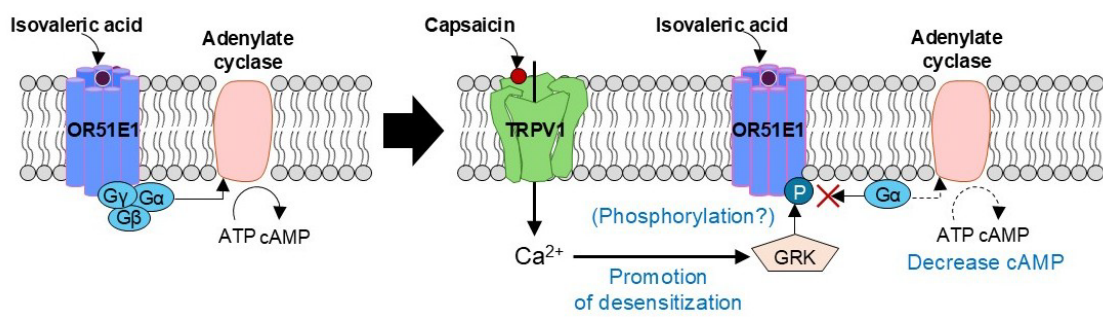
using HEK293T cells transfected with plasmids. On the other hand, ORs and TRPV1 are naturally co-expressed in cells, including OSNs or other ectopic cells, such as prostate cancer cells (Pronin *et al.*, 2021). Future studies are needed to validate the expression levels of both receptors in human OSNs or other ectopic cells and to determine if the mutual interaction between ORs and TRPV1 occurs not only in the plasmid-transfected HEK293T cells but also in these cells naturally co-expressing the two receptors.

Previous studies have shown that the GPCR desensitization process involves the phosphorylation of GPCRs by GRKs, followed by β -arrestin-mediated internalization (Preethi *et al.*, 2021). GRKs are recruited to the plasma membrane via interactions with the G $\beta\gamma$ subunits of heterotrimeric G-proteins (Pitcher *et al.*, 1992; Kameyama *et al.*, 1993), where they phosphorylate the intracellular loops and C-terminal regions of GPCRs (Eason *et al.*, 1995; Maeda *et al.*, 2003). This phosphorylation event facilitates β -arrestin binding, which subsequently blocks further G-protein coupling and promotes receptor endocytosis. It is reported that GRKs and β -arrestin 2 are abundantly expressed in the olfactory epithelium (Dawson *et al.*, 1993). Additionally, GRK3-knockout mice fail to exhibit odor-induced desensitization (Peppel *et al.*, 1997), which supports the hypothesis that GRK-mediated OR phosphorylation and desensitization occur in the olfactory system. In the present study, we utilized HEK293T cells, which are known to express high levels of GRK2 and GRK6 (Brady *et al.*, 2011). Moreover, CCG215022 predominantly inhibits GRK1, GRK2, and GRK5. Therefore, GRK2 may play an important role in the desensitization of OR51E1 in HEK293T cells under the conditions of this study. Further studies will be required to confirm which type of GRKs contribute to the desensitization and phosphorylation of ORs in HEK293T cells. In this study, we utilized OR51E1 to explore the effect of TRPV1, revealing that TRPV1 suppresses OR signal transduction

through a GRK-dependent mechanism. This mechanism appears to be consistent with the desensitization process frequently observed in other GPCRs, suggesting that similar mechanisms may apply to many ORs beyond OR51E1.

Under our experimental conditions, it is uncertain whether Ca^{2+} influx directly induces the activation of GRK. It is reported that intracellular Ca^{2+} elevation induces calmodulin activation via Ca^{2+} binding, leading to a conformational change in calmodulin, which increases its affinity for target proteins such as GRKs (Komolov *et al.*, 2021). Furthermore, GRK2/3 are known to be regulated by Ca^{2+} /calmodulin signaling; when Ca^{2+} binds to calmodulin, the resulting Ca^{2+} -calmodulin complex activates GRKs, enhancing GPCR phosphorylation and promoting desensitization (Haga *et al.*, 2002). Therefore, it is assumed that Ca^{2+} influx, triggered by either TRPV1 activation or calcium ionophore treatment, activates calmodulin, which in turn activates GRK, leading to OR phosphorylation and subsequent suppression of OR-mediated cAMP production. This assumption, coupled with the confirmation of OR51E1 phosphorylation by GRK, necessitates further verification in future studies.

In conclusion, our study demonstrates that OR and TRPV1 interaction influence their activities in both directions, rather than unidirectionally, in HEK293T cells. In the human genome, approximately 400 ORs and 27 TRP channels are identified, many of which are expressed in tissues beyond the olfactory system. Therefore, they may interact and regulate each other's activity in various tissues and cells.



Graphical abstract. TRPV1 suppresses ligand-stimulated OR51E1 signal transduction through Ca^{2+} influx and GRK activation.

Acknowledgments

We thank Dr. Kenji Tatematsu for his useful discussions.

Funding

The following entities have provided support for this work: Japan Science and Technology Agency (JST), the establishment of university fellowships toward the creation of science technology innovation, Grant Number JPMJFS2125 (to S.M.); KAKENHI (Grant-in-Aid for Challenging Research (Pioneering) from Japan Society for the Promotion of Science (JSPS) Grant Number 18H05359 (20K20370), 22K18343 (to S.K.); and Adaptable and 534 Seamless Technology Transfer Program through Target-driven 535 R&D (A-STEP) from JST Grant Number JPMJTR194C; a project JPNP 536 23200460, commissioned by the New Energy and Industrial Technology Development Organization (NEDO) (to S.K.).

Author contributions

S.M., conceptualization, methodology, validation, formal analysis, investigation, data curation, writing—original, draft preparation, writing—review and editing, and funding; S.H., conceptualization, methodology, validation, formal analysis, investigation, data curation, writing—original, draft preparation, writing—review and editing, and supervision; and S.K., investigation, writing—review & editing, resources, funding, and supervision.

Competing interests

No potential conflict of interest.

Data availability

The datasets used and/or analyzed during the current study are available from the corresponding author upon reasonable request.

5. References

- Abdel-Salam O, *et al.* Effect of capsaicin and resiniferatoxin on gastrointestinal blood flow in rats. *Eur J Pharmacol* 1996; **305** :127-36.
- Benovic JL, *et al.* Light-dependent phosphorylation of rhodopsin by β -adrenergic receptor kinase. *Nature* 1986; **321** : 869-872.
- Brady KA, *et al.* Expression of G protein-coupled receptors and related proteins in HEK293, AtT20, BV2, and N18 cell lines as revealed by microarray analysis. *BMC Genomics* 2011; **12** :14.
- Buck L, Axel R. A novel multigene family may encode odorant receptors: a molecular basis for odor recognition. *Cell* 1991; **65** :175-87.
- Bujak JK, *et al.* Inflammation, cancer and immunity-implication of TRPV1 channel. *Front Oncol* 2019; **9** :1087.
- Caterina MJ, *et al.* The capsaicin receptor: a heat-activated ion channel in the pain pathway. *Nature* 1997; **389** :816-24.
- Chen J, *et al.* Transient receptor potential (TRP) channels, promising potential diagnostic and therapeutic tools for cancer. *Biosci Trends*. 2014; **8**:1-10.
- Chijiwa T, *et al.*, Inhibition of forskolin-induced neurite outgrowth and protein phosphorylation by a newly synthesized selective inhibitor of cyclic AMP-dependent protein kinase, N-[2-(p-bromocinnamylamino)ethyl]-5-isoquinolinesulfonamide (H-89), of PC12D pheochromocytoma cells. *J Biol Chem* 1990; **265** : 5267-5272.
- Dawson TM, *et al.* β -adrenergic receptor kinase-2and β -arrestin-2as mediators of odorant-induced desensitization. *Science* 1993; **259** : 825-829.
- Eason MG, *et al.* Four consecutive serine in the third intracellular loop are the sites for β -adrenergic receptor kinase-mediated phosphorylation and desensitization of the α 2A-adrenergic receptor. *J. Biol. Chem* 1995; **270** : 4681-468.
- Fujita K, *et al.* Induction of lipid droplets in nonmacrophage cells as well as macrophages by liposomes and exosomes. *Biochem Biophys Res Commun* 2019; **510** :184-90.
- Haga T, *et al.* Regulation of G protein-coupled receptor kinase 2. *Methods Enzymol*. 2002; **343** : 559-577.
- Hardie RC, Minke B. The trp gene is essential for a light-activated Ca^{2+} channel in Drosophila photoreceptors. *Neuron* 1992 ; **8** : 643-651.
- Hinuma S, *et al.* Specific binding and endocytosis of liposomes to HEK293T cells via myrisoylated pre-S1 peptide bound to sodium taurocholate cotransporting polypeptide. *Vaccines* 2022; **10** :2050.

- Homan KT, *et al.* Crystal Structure of G Protein-coupled Receptor Kinase 5 in Complex with a Rationally Designed Inhibitor. *J Biol Chem* 2015 ; **290** : 20649-20659.
- Il Je Cho, *et al.* H89, an inhibitor of PKA and MSK, inhibits cyclic-AMP response element binding protein-mediated MAPK phosphatase-1 induction by lipopolysaccharide. *Inflamm Res* 2009; **58** :863-72.
- Jin H, *et al.* Systematic transcriptional analysis of human cell lines for gene expression landscape and tumor representation. *Nat Commun* 2023; **14** : 5417.
- Jimenez RC, *et al.* The mutational landscape of human olfactory G protein-coupled receptors. *BMC Biology* 2021; **19** : 21.
- Kameyama K, *et al.* Activation by G protein $\beta\gamma$ subunits of β -adrenergic and muscarinic receptor kinase. *J. Biol. Chem* 1993 ; **268** : 753-758.
- Komolov KE, *et al.*, Structure of a GRK5-calmodulin complex reveals molecular mechanism of GRK activation and substrate targeting. *Mol Cell*. 2021; **81** : 323–339.
- Krautwurst D, *et al.* Identification of ligands for olfactory receptors by functional expression of a receptor library. *Cell* 1998; **95** :917-26
- Kwon DH, *et al.* Heat-dependent opening of TRPV1 in the presence of capsaicin. *Nat Struct Mol Biol* 2021; **28** :554-63.
- Lin W, *et al.* Olfactory neurons expressing transient receptor potential channel M5 (TRPM5) are involved in sensing semiochemicals. *Proc Natl Acad Sci USA* 2007; **104** : 2471-6.
- Lowe G, *et al.* Adenylate cyclase mediates olfactory transduction for a wide variety of odorants. *Proc Natl Acad Sci USA* 1989; **86** : 5641-5645.
- Maßberg D, *et al.* The activation of OR51E1 causes growth suppression of human prostate cancer cells. *Oncotarget* 2016; **7** :48231-48249.
- Maeda T, *et al.* Rhodopsin phosphorylation:30years later. *Prog. Retin. Eye. Res.* 2003; **2** : 417-434.
- Mainland JD, *et al.* The missense of smell: functional variability in the human odorant receptor repertoire. *Nat Neurosci* 2014; **17** :114-20.
- Malnic B, *et al.* Combinatorial receptor codes for odors. *Cell*. 1999; **96** : 713-23.
- McNamara FN *et al.* Effects of piperine, the pungent component of black pepper, at the human vanilloid receptor (TRPV1). *Br. J. Pharmacol* 2005; **144** : 781-790.
- Mombaerts P. Genes and ligands for odorant, vomeronasal and taste receptors. *Nat Rev Neurosci* 2004; **5** :263-78.

- Moriyama S *et al.* Divergent effects of olfactory receptors on transient receptor potential vanilloid 1 activation by capsaicin and eugenol. *Biosci Biotechnol Biochem* 2024a; **88** :908-17.
- Moriyama S *et al.* Role of phosphorylation and vanilloid ligand structure in ligand-dependent differential activations of transient receptor potential vanilloid 1. *Biosci Biotechnol Biochem* 2024b; **88** : 1316-1325.
- Moriyama T *et al.* Sensitization of TRPV1 by EP1 and IP reveals peripheral nociceptive mechanism of prostaglandins. *Mol Pain* 2005; **1** :3-9.
- Nakamura T, Gold GH. A cyclic nucleotide-gated conductance in olfactory receptor cilia. *Nature* 1987; **325** : 442-444.
- Nakashimo Y *et al.* Expression of transient receptor potential channel vanilloid (TRPV) 1–4, melastin (TRPM) 5 and 8, and ankyrin (TRPA1) in the normal and methimazole-treated mouse olfactory epithelium. *Acta Otolaryngol* 2010; **130** :1278-86.
- Pace U *et al.* Odorant-sensitive adenylate cyclase may mediate olfactory reception. *Nature* 1985; **316** : 255-258.
- Peppel K, *et al.* G protein—coupled receptor kinase 3 (GRK3) gene disruption leads to loss of odorant receptor desensitization. *J. Biol. Chem.* 1997; **272** : 25425-25428.
- Persaud K, Dodd G. Analysis of discrimination mechanisms in the mammalian olfactory system using a model nose. *Nature* 1982; **299** : 352-355.
- Pronin A, Slepak V. Ectopically expressed olfactory receptors OR51E1 and OR51E2 suppress proliferation and promote cell death in a prostate cancer cell line. *J Biol Chem* 2021; **296** :100475.
- Preethi CK, *et al.* Structural Basis of Arrestin Selectivity for Active Phosphorylated G Protein-Coupled Receptors. *Int J Mol Sci* 2021; **22** : 12481.
- Pitcher JA, *et al.* Role of $\beta\gamma$ subunits of G proteins in targeting the β -adrenergic receptor kinase to membrane- bound receptors. *Science* 1992; **257** : 1264-1267.
- Pyrski M, *et al.* Trpm5 expression in the olfactory epithelium. *Mol Cell Neurosci*. 2017; **80**:75-88.
- Sakano H. Neural map formation in the mouse olfactory system. *Neuron* 2010; **67** : 530-542.
- Sakatani H, *et al.* The roles of transient receptor potential vanilloid 1 and 4 in olfactory regeneration. *Lab Invest* 2023; **103** :100051.
- Salzer I, *et al.* Nociceptor signaling through ion channel regulation via GPCRs. *Int J Mol Sci* 2019; **20** :2488.

- Schuligoi R, *et al.* Gastric acid-evoked c-fos messenger RNA expression in rat brainstem is signaled by capsaicin-resistant vagal afferents. *Gastroenterology* 1998; **115** :649-60.
- Serizawa S, *et al.* Negative feedback regulation ensures the one receptor-one olfactory neuron rule in mouse. *Science* 2003; **302** : 2088-2094.
- Shepard BD, *et al.* A cleavable N-terminal signal peptide promotes widespread olfactory receptor surface expression in HEK293T cells. *PLoS One*. 2013; **8** :e68758.
- Tamaoki T, *et al.*, Staurosporine, a potent inhibitor of phospholipid/Ca⁺⁺-dependent protein kinase. *Biochem Biophys Res Commun* 1986; **135** : 397-402.
- Verbeurgt C, *et al.* Profiling of olfactory receptor gene expression in whole human olfactory mucosa. *PLoS One*. 2014; **9** :e96333.
- Ward SM, *et al.* Distribution of the vanilloid receptor (VR1) in the gastrointestinal tract. *J Compar Neurol* 2003; **465** :121-35.
- Yang B, *et al.* Activation of vanilloid receptor 1 (VR1) by eugenol. *J Dent Res* 2003; **82** :781-5.
- Yao X, *et al.* Regulation of TRP channels by phosphorylation. *Neurosignals* 2005; **14** : 273-80.
- Yelshanskaya MV, Sobolevsky AI. Ligand-binding sites in vanilloid- subtype TRP channels. *Front Pharmacol* 2022; **13** :900623.

Chapter V Comprehensive Discussion

1. Comprehensive Discussion

This dissertation demonstrated the existence of an interaction between olfactory receptors (ORs) and the transient receptor potential vanilloid 1 (TRPV1), in which ORs and TRPV1 mutually regulate each other's activity, using a co-expression system in HEK293T cells. In this Chapter, the findings in Chapters II – IV are summarized, and some points that were not addressed in the earlier chapters are explored. In addition, perspectives grounded in the findings of these studies are considered here.

Chapter II demonstrated that activation of the cAMP signaling pathway through ORs modulates TRPV1 activation, causing intracellular Ca^{2+} influx, in response to ligand stimulation. Interestingly, OR's effects on TRPV1 altered depending on TRPV1 ligands: OR activation enhances capsaicin-induced TRPV1 activation, whereas it suppresses eugenol-induced TRPV1 activation. Eugenol is known as the main component of spices such as clove and bay leaf (laurel), and a human OR, OR10G7, has been reported as a receptor for eugenol (Saito *et al.* 2009; Mainland *et al.* 2015). While this dissertation did not examine the effects of OR10G7 on TRPV1 activation when both receptors were simultaneously stimulated with eugenol, it is anticipated that OR10G7 would exhibit similar suppressive effects on TRPV1 activation as observed with other ORs, including OR51E1 and OR51E2, which were used in the present studies.

Chapter III elucidated the process through which OR influences TRPV1 activation, focusing on its role in evoking the cAMP signaling pathway, as detailed below. Conformational changes of OR by stimulation with a ligand promote the exchange of GDP-Gs/olf to GTP-Gs/olf. Considering that Gs, rather than Golf, is predominantly

expressed in HEK293T cells (GNAS and GNAL as indicated by the Himan Gene Atlas, respectively), Gs is likely coupled to OR under the experimental conditions employed in these studies (Su *et al.* 2004). GTP-Gs released from the activated OR stimulates adenylate cyclase (AC). A detailed analysis of AC subtypes was not conducted in these studies. The AC family comprises nine membrane-bound subtypes (AC1-9) and one soluble AC (sAC), each differing in activation mechanisms and expression patterns (Cooper 2003). As HEK293T cells primarily express AC3 and AC6, these subtypes would be involved in the OR-mediated cAMP production in HEK293T cells (Soto-Velasquez *et al.* 2018). By utilizing AC inhibitors or siRNA, it could be determined which specific AC subtypes contribute to cAMP production induced by the activated OR in HEK293T cells. AC activated by GTP-Gs promotes the synthesis of cAMP from ATP, which in turn activates PKA, leading to the phosphorylation of TRPV1. ORs exhibited modulatory activity toward TRPV1 activation by both capsaicin and eugenol. Notably, the effects of ORs on TRPV1 differed depending on whether capsaicin or eugenol was used as the stimulus. These findings suggest that phosphorylation alters TRPV1, resulting in differing susceptibility to capsaicin and eugenol. However, little is known about the structural changes in TRPV1 induced by phosphorylation (Sanz-Salvador *et al.* 2012). Future research is anticipated to elucidate the differences in ligand-binding structures of TRPV1 in its phosphorylated and unphosphorylated states. Furthermore, analyses using multiple TRPV1 ligands (vanilloid compounds) in Chapter III showed that the effect of OR activation varies depending on the chemical structure of the TRPV1 ligand, resulting in either enhancement or suppression. Traditionally, the activation of TRPV1 by vanilloid compounds was thought to follow a uniform mechanism. However, our findings reveal

that these compounds can be grouped into three categories, characterized by differences in activation before and after phosphorylation.

Chapter IV revealed that TRPV1 activation suppresses cAMP production mediated by ligand-stimulated OR51E1. This suppression was due to TRPV1-mediated intracellular Ca^{2+} influx from extracellular Ca^{2+} . Furthermore, it was found that the increase in intracellular Ca^{2+} concentration activates GPCR kinases (GRKs). Based on the known activation and desensitization cycle of GPCRs, the following regulatory process of OR activation by TRPV1 can be assumed. The signal transduction pathway involving cAMP production mediated by activated OR is described above, while TRPV1 is hypothesized to regulate the following desensitization process of OR. Ca^{2+} influx induced by TRPV1 activates calmodulin, which in turn activates GRK2/3. Intracellular domains of OR are phosphorylated by activated GRK, which facilitates the binding of β -arrestin, leading to the inhibition of Gs coupling to OR and the internalization of β -arrestin/OR complex (Lefkowitz and Shenoy 2005; Figure 1).

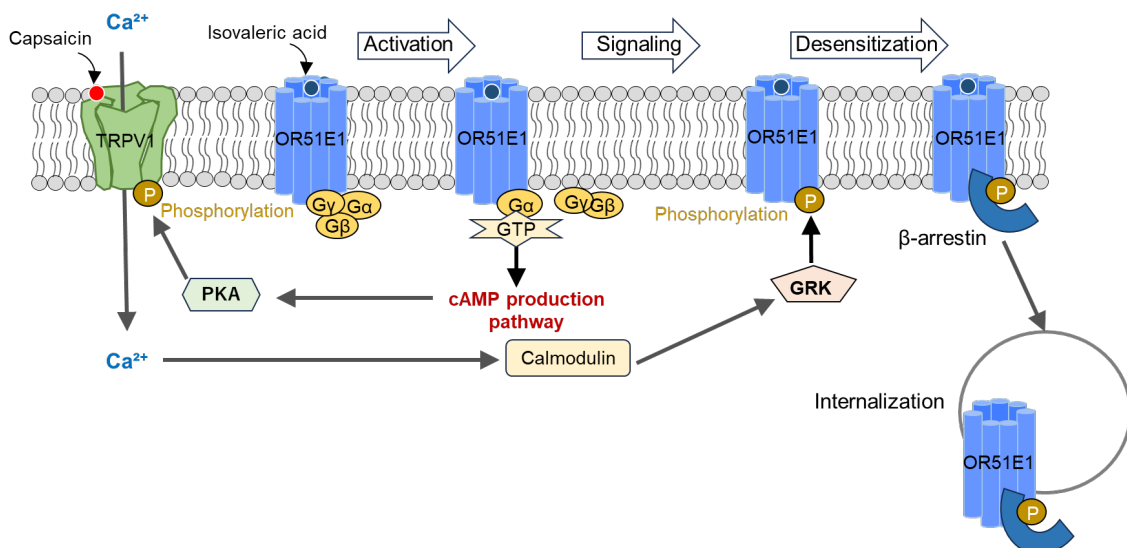


Figure 1. OR desensitization and internalization mediated by TRPV1 activation. This diagram illustrates the bidirectional interaction between TRPV1 and OR. Upon TRPV1 activation by capsaicin, Ca^{2+} influx activates calmodulin, which stimulates GRK. This kinase phosphorylates the intracellular

domains of OR, leading to β -arrestin recruitment, inhibition of G protein coupling, and receptor internalization. Meanwhile, OR activation by isovaleric acid induces cAMP production, which activates PKA and results in TRPV1 phosphorylation. .

In summary, these results demonstrate a reciprocal interaction: OR activation modulates TRPV1 sensitivity via phosphorylation, while conversely, TRPV1 activation promotes the desensitization of OR. However, these studies have yet to clarify the changes in the overall intracellular signaling that results from the integrated signal transduction of OR and TRPV1. To investigate this, the following experiments could be conducted. For instance, HEK293T cells co-expressing OR, TRPV1, and CNG channels, as well as cells expressing each molecule individually, could be prepared. Subsequently, signal transduction in these cells could be measured by assessing indicators such as calcium ion (Ca^{2+}) influx and changes in membrane potential (Figure 2). These experiments may bring valuable clues to reveal an integrated signal derived from OR and TRPV1. Additionally, as this research utilizes a heterologous expression system (HEK293T cells), further validation is required to determine if these interactions occur in OSNs and other types of cells expressing both OR and TRPV1. Utilizing animal models, complemented by behavioral assays and electrophysiological recordings, will also be crucial to determine how these interactions influence olfactory perception. TRPV1 expressions in the olfactory bulb and olfactory epithelium are confirmed based on immunohistochemistry, *in situ* hybridization, and RNA-seq (Nakashimo *et al.* 2010; Sakatani *et al.* 2023; Lin *et al.* 2007). However, TRPV1 localization within the cilia is still controversial. That is, while the expression of TRPV1 in OSNs is widely supported, a clear consensus on its presence in primary cilia has not been obtained. Therefore, re-evaluation regarding ciliary localization and function of TRPV1 would be necessary.

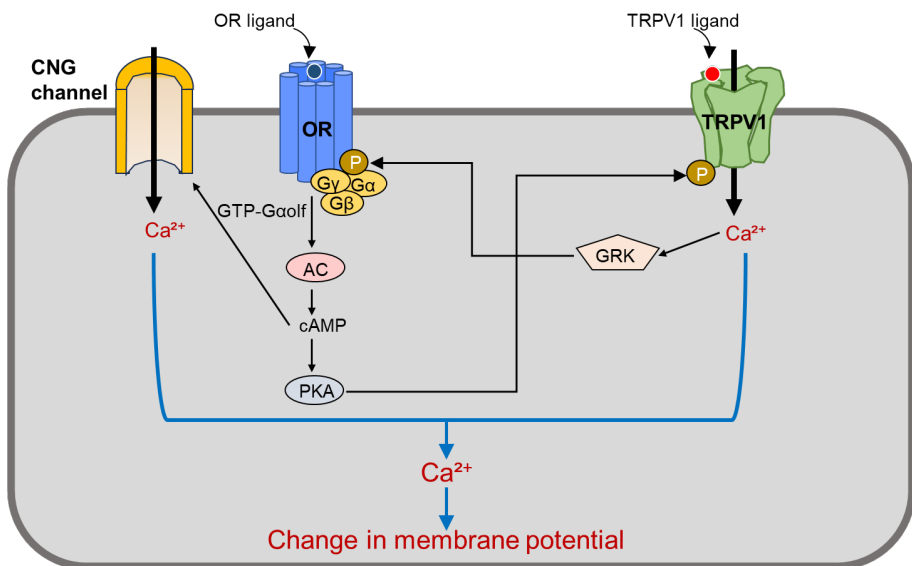


Figure 2. An experimental model to assess output of integrated OR and TRPV1 intracellular signals This model illustrates the predicted cellular response in olfactory neurons where both OR and TRPV1 are co-expressed. Upon ligand binding, OR's signaling (cAMP production) induces Ca^{2+} influx via CNG channels. On the other hand, TRPV1 activation also allows Ca^{2+} influx. During these processes, OR and TRPV1 mutually influence each other's signal transduction. The resulting intracellular events including Ca^{2+} accumulation modulate membrane potential.

From an evolutionary viewpoint, the relation between OR and TRPV1 can be speculated as follows. OR genes constitute about half of the largest and most diverse GPCR gene family, with over 400 genes in humans. This OR's diversity enables species-specific adaptation to a wide range of olfactory environments. In contrast, TRPV1, a member of the TRP channel family, is evolutionarily conserved across many vertebrates but shows species-specific differences in ligand sensitivity. For example, birds are notably insensitive to capsaicin (Jordt and Julius 2002). Although ORs and TRPV1 belong to distinct protein families, with ORs classified as class A GPCRs, both have independently evolved to detect diverse environmental chemical cues (Nei *et al.* 2008). Notably, many odorants and TRPV1 ligands, such as capsaicin and eugenol, are plant-derived compounds, suggesting that animals may have adapted by developing both receptor types to monitor overlapping ecological signals. These parallel yet distinct evolutionary

trajectories may have promoted a functional interplay between ORs and TRPV1, enabling integrated chemical sensing that links olfactory and somatosensory modalities (Mamasuew *et al.* 2010). Our findings may support this notion by demonstrating that OR activation enhances capsaicin-induced TRPV1 activation while suppressing eugenol-induced activation. Because these differential regulatory mechanisms may allow animals to recognize the ecological context of chemical stimuli with greater diversity.

In conclusion, as discussed above, some questions remain unresolved in understanding the physiological significance of the interaction between ORs and TRPV1, which future studies will need to address. Nevertheless, the findings in this dissertation provide valuable insights into the mutual regulatory system of ORs and TRPV1, which, until now, have primarily been studied independently.

2. References

- Bargmann CI. Horvitz HR. The sensory repertoire of *Caenorhabditis elegans*. *Cell*, 1997; **90**: 6: 957-969.
- Cooper DMF. Regulation and organization of adenylyl cyclases and cAMP. *Biochem J*. 2003; **375**: Pt 3: 517–529.
- Jordt SE. Julius D. Molecular basis for species-specific sensitivity to 'hot' chili peppers. *Cell*. 2002; **108**: 3: 421–430.
- Lefkowitz RJ. Shenoy SK. Transduction of receptor signals by β -arrestins. *Science*. 2005; **308**: 5721: 512–517.
- Lin W, *et al*. Olfactory neurons expressing transient receptor potential channel M5 (TRPM5) are involved in sensing semiochemicals. *Proc Natl Acad Sci USA*; 2007; **104**: 2471-2476.
- Mainland J, *et al*. Human olfactory receptor responses to odorants. *Sci Data*. 2015; **2**: 150002.
- Mamasuew K, *et al*. TRPV1 and TRPA1 channels are both expressed in olfactory sensory neurons. *Chem Senses*. 2010; **35**: 4 :279–288.
- Nakashimo Y, *et al*. Expression of transient receptor potential channel vanilloid (TRPV) 1–4, melastatin (TRPM) 5 and 8, and ankyrin (TRPA1) in the normal and methimazole-treated mouse olfactory epithelium. *Acta Otolaryngol*, 2010; **130**: 1278–1286.
- Nei M, *et al*. The evolution of animal chemosensory receptor gene repertoires: roles of chance and necessity. *Nat Rev Genet*. 2008; **9**: 12: 951–963.
- Niimura Y. Comparative evolutionary analysis of olfactory receptor gene clusters between humans and mice. *Gene*. 2005; **346**: 13–21.
- Niimura Y. Evolutionary dynamics of olfactory receptor genes in chordates: interaction between environments and genomic contents. *Hum Genomics*. 2009; **4**: 2: 107-118.
- Saito H, *et al*. Functional expression of human odorant receptors and identification of odor ligands. *Cell*, 2009; **137**: 7: 1384-1398.
- Sakatani H, *et al*. The roles of transient receptor potential vanilloid 1 and 4 in olfactory regeneration. *Lab Invest*. 2023; **103**: 100051.
- Sanz-Salvador L, *et al*. Agonist- and Ca^{2+} -dependent desensitization of TRPV1 channel targets the receptor to lysosomes for degradation. *J Biol Chem*. 2012; **287**: 23: 19462–19471.
- Soto-Velasquez M, *et al*. A Novel CRISPR/Cas9-Based Cellular Model to Explore Adenylyl Cyclase and cAMP Signaling. *Mol Pharmacol*. 2018; **94**: 3: 963–972.

- Su AI, *et al.* A gene atlas of the mouse and human protein-encoding transcriptomes. *Proc Natl Acad Sci U S A.* 2004; **101**: 16: 6062–6067.
- Takahashi K, *et al.* Mode-selective inhibitory effects of eugenol on the mouse TRPV1 channel. *Biochem Biophys Res Commun.* 2021; **556**: 156-162.

Acknowledgments

This dissertation is submitted in partial fulfillment of the requirements for the Doctor of Philosophy degree at the Graduate School of Frontier Biosciences, University of Osaka.

I would like to express my sincere gratitude to all those who have supported and guided me throughout my doctoral research. First and foremost, I would like to express my deepest gratitude to Professor Shun'ichi KURODA, Professor at the Graduate School of Frontier Biosciences and Director of at University of Osaka. for his exceptional guidance and unwavering support throughout my doctoral studies. His insightful advice and encouragement have been invaluable to my academic growth. I am also sincerely grateful to Visiting Professor Shuji HINUMA for his valuable advice on the direction of my research and experimental methodologies. His expert guidance and warm support were essential to the successful completion of this study. I would like to express my sincere appreciation to Professor Takashi Kurahashi and Associate Professor Hiroko Takeuchi for their long-standing support, thoughtful advice, and kind encouragement from my master's program through to my doctoral studies. Furthermore, I would like to thank Associate Professors Toshihide OKAJIMA, Yoh WADA, and Masaharu SOMIYA, as well as Assistant Professor Kenji TATEMATSU, for their generous support and guidance during my research activities. Their assistance has been instrumental in advancing this study.

I am profoundly grateful to my husband for his unwavering support, patience, and understanding. His assistance in managing daily life and constant encouragement enabled me to focus on my research and complete this dissertation. I also extend my heartfelt thanks to my parents for their continuous encouragement and belief in my abilities. Their support has been a constant source of motivation.

List of Publications

- Sakura MORIYAMA, Yukie TAKITA, Shuji HINUMA, and Shun'ichi KURODA, Divergent effects of olfactory receptors on transient receptor potential vanilloid 1 activation by capsaicin and eugenol, *Biosci. Biotechnol. Biochem.* 2024 ; **88** : 8: 908-917.
- Sakura MORIYAMA, Kenji TATEMATSU, Shuji HINUMA, and Shun'ichi KURODA, Role of phosphorylation and vanilloid ligand structure in ligand-dependent differential activations of transient receptor potential vanilloid 1, *Biosci. Biotechnol. Biochem.* 2024; **88**: 11: 1316-1325.
- Sakura MORIYAMA, Shuji HINUMA, and Shun'ichi KURODA, Suppressive Effect of Transient Receptor Potential Vanilloid 1 on Ligand-Induced Olfactory Receptor Signal Transduction, *Biosci. Biotechnol. Biochem., in press*, 2025.
- 森山さくら、立松健司、日沼州司、黒田俊一、ヒト嗅覚受容体セルアレイセンサーの開発と社会実装、季刊 香料、日本香料協会、2022; **296**: 9-16.
- 森山さくら、黒田俊一、ヒト嗅覚受容体発現セルアレイセンサーによる匂い情報 DX の実現、日本官能評価学会誌、2024; **28**: 11-14.
- 森山さくら、黒田俊一、ヒト嗅覚受容体センサを用いたすべての匂いをデジタルデータ化する匂い情報 DX の実現、生体ガス計測の最新動向、CMC 出版、2024 年 6 月出版（分担執筆）

International and Domestic Academic Conferences

International Conferences

- Sakura MORIYAMA, Kenji TATEMATSU, Shuji HINUMA, Shun'ichi KURODA, "Novel interaction between TRPV1 channels and olfactory receptors", The 26th SANKEN International Symposium, Ibaraki, Japan. 2023 年 1 月 11 日 (Poster)
- Sakura MORIYAMA, Shuji HINUMA, Shun'ichi KURODA, "Crosstalk between human olfactory receptors and transient receptor potential vanilloid 1", The 27th SANKEN International Symposium, Awaji, Japan. 2024 年 1 月 11 日 (Poster)
- Sakura MORIYAMA, Shuji HINUMA, Shun'ichi KURODA, "Opposite effects of olfactory receptors on transient receptor potential vanilloid 1 activation by capsaicin-type and eugenol-type ligands", 19th International Symposium on Olfaction and Taste, Reykjavík, Iceland. 2024 年 6 月 24 日 (Poster)
- Sakura MORIYAMA, Shuji HINUMA, Shun'ichi KURODA, "Divergent effects of olfactory receptor-mediated TRPV1 phosphorylation on activation by vanilloid analogs", The 28th SANKEN International Symposium, Awaji, Japan. 2025 年 1 月 10 日 (Poster)

Domestic Conferences

- 森山さくら、立松健司、日沼州司、黒田俊一、“Studies on interaction of human olfactory receptors and TRPV1 using HEK293T cells”, 第 56 回日本味と匂学会、仙台、2022 年 8 月 24 日 (Poster)
- 森山さくら、立松健司、日沼州司、黒田俊一、“Studies on interaction of human olfactory receptors and TRPV1 using HEK293T cells”, 第 78 回産研学術講演会、茨木、2022 年 11 月 25 日 (Poster)
- 森山さくら、立松健司、日沼州司、黒田俊一、“Crosstalk between human olfactory receptors and TRPV1 channels”, 第 57 回日本味と匂学会、東京、2023 年 9 月 12 日 (Poster)
- 森山さくら、日沼州司、黒田俊一、“Differential effects of human olfactory receptors and forskolin on transient receptor potential vanilloid 1 activation by capsaicin-type and eugenol-type ligands”, 日本農芸化学会 2024 年度大会、東京、2024 年 3 月 25 日 (Oral)
- 森山さくら、日沼州司、黒田俊一、“Divergent effects of olfactory receptor-mediated phosphorylation on TRPV1 activation by vanilloid analogs”, 日本農芸化学会 2025 度大会、札幌、2025 年 3 月 7 日 (Poster)
- 森山さくら、“嗅覚受容体と TRP チャネルの相互作用に基づく匂い受容機構の解明”, 京都大学「医学領域」産学連携推進機構主催第 10 回 Seeds-hub ミニセミナー、京都、2025 年 4 月 23 日 (招待講演、Oral)
- 森山さくら、“Cross-talk between olfactory receptors and TRPV1: Bridging the gap to human-like olfactory sensing”, 第 59 回日本味と匂学会、豊中、2025 年 9 月 8 日 (Young scientist symposium、Oral)
- 森山さくら、日沼州司、黒田俊一, “Functional interaction between olfactory receptors and TRPV1 in the modulation of responses”, 第 59 回日本味と匂学会、豊中、2025 年 9 月 8–10 日 (Poster)

- 森山さくら、日沼州司、黒田俊一, “Investigation of the Crosstalk between Olfactory Receptors and TRPV1 Channels”, 第 63 回日本生物物理学会年会、奈良、2025 年 9 月 24–26 日 (Oral)

Awards, Grants and Fellowships

- Sakura MORIYAMA, Shuji HINUMA, Shun'ichi KURODA, "Crosstalk between human olfactory receptors and transient receptor potential vanilloid 1", The 27th SANKEN International Symposium, Awaji, Japan. 2024 年 1 月 11 日 (BEST POSTER AWARD)
- Sakura MORIYAMA, Shuji HINUMA, Shun'ichi KURODA, " Divergent effects of olfactory receptor-mediated TRPV1 phosphorylation on activation by vanilloid analogs", The 28th SANKEN International Symposium, Awaji, Japan. 2025 年 1 月 10 日 (BEST POSTER AWARD)
- 大阪大学 超域イノベーション博士課程プログラム (博士課程教育リーディングプログラム) (2023 年 4 月 ~ 3 年間)
- 大阪大学 「社会と知の統合」を実現するイノベーション博士人材フェローシップ生 (JST 科学技術イノベーション創出に向けた大学フェローシップ創設事業) (2023 年 4 月 ~ 3 年間・JSPS DC2 採用により 2 年に短縮) , Grant Number: JPMJFS2125
- 日本学術振興会特別研究員 (DC2) (2025 年 4 月 ~ 2 年間) , Grant Number: 25KJ1737